For Reference

NOT TO BE TAKEN FROM THIS ROOM

For Reference

NOT TO BE TAKEN FROM THIS ROOM

Ex libris
universitatis
albertaensis

University of Alberta
Printing Department

Digitized by the Internet Archive
in 2019 with funding from
University of Alberta Libraries

https://archive.org/details/pipelineflowrheo00alis

Thesis
1961
#3

THE UNIVERSITY OF ALBERTA

THE PIPELINE FLOW AND RHEOLOGICAL PROPERTIES OF SULPHUR-WATER SUSPENSIONS

A THESIS
SUBMITTED TO THE FACULTY OF GRADUATE STUDIES
IN PARTIAL FULFILLMENT OF THE REQUIREMENTS FOR THE DEGREE OF
MASTER OF SCIENCE

CHEMICAL AND PETROLEUM ENGINEERING DEPARTMENT
by
ALISTAIR ALCORN

EDMONTON, ALBERTA
APRIL, 1961

ACKNOWLEDGEMENTS

The author wishes to express his appreciation of the criticism and assistance rendered by Dr. G. W. Govier under whose supervision this investigation was carried out.

Appreciation is expressed to Mr. C. R. Kirby, Mr. F. E. Butz and Mr. H. Tebelmann for their assistance with the construction of the equipment.

The sincere thanks of the author are extended to Mr. R.M. Scott for preparing the photomicrographs and to Mr. R. A. S. Brown for his care in photographing the equipment.

ABSTRACT

The rheological properties of two sulfur - water suspensions with approximately the same particle size analysis have been investigated using a modified Fann concentric cylinder viscometer. Both suspensions gave flow curves similar to those expected for pseudoplastics. The experimental data are presented as logorithmic plots of shear stress versus shear rate.

Pressure drop - flow rate data have been obtained over a range of solids concentrations for suspensions flowing through 40.17 foot and 45.35 foot lengths of 1-7/8 I.D. smooth aluminum tubing. The pressure drop data were obtained using an electrically operated differential pressure cell associated with a potentiometer.

A comparison has been made between the experimental results and the predicted values assuming the theory applicable both for Bingham-plastic behaviour and for "power-law" pseudoplastic behaviour.

As a result of these comparisons it is concluded that one of the suspensions can be treated as a Bingham-plastic in the range of the pipeline data. The properties of the other suspension are more complex, it behaves as a pseudoplastic that does not obey the power law.

TABLE OF CONTENTS

Page

Table of contents iii

List of tables v

List of illustrations vi

Introduction 1

Literature survey and theory 2

- Fluid classifications 2
- Mechanics of flow in circular pipes 6
- Determination of rheological properties using a rotational viscometer 18

Experimental equipment 22

- The pipeline unit 22

Experimental procedure 29

- Initial treatment of dry solids 29
- Operation of the pipeline 30
- Testing procedure on the samples of suspension 31

Experimental results 38

- Pipeline flow data 38
- Properties of the suspensions 48

Interpretation of the Pipeline Flow Data 60

- Interpretation assuming Bingham-plastic behavior 60
- Interpretation assuming power-law pseudoplastic behavior 68

Page

Conclusions 77

Nomenclature 79

Bibliography 82

Appendices

A. Computation of shear rate in the viscometer 84

B. Viscometer experimental data 88

C. Pipeline experimental data 92

D. Interpretation of the pipeline data assuming Bingham-plastic behavior 103

E. Interpretation of the pipeline data assuming power-law pseudoplastic behavior 109

F. Density and settling data 114

Particle size distribution data 114

G. Calibration data 118

LIST OF TABLES

		Page
Table 1A	Computation of shear rate in the viscometer	85
Table 1B	Viscometer experimental data	89
Table 1C	Pipeline experimental data	93
Table 2C	Initial interpretation of pipeline data	98
Table 1D	Interpretation assuming Bingham-plastic behaviour (laminar flow data)	104
Table 2D	Interpretation assuming Bingham-plastic behaviour (turbulent flow data)	106
Table 1E	Interpretation assuming power-law pseudoplastic behaviour	110
Table 1F	Density and settling data	115
Table 2F	Particle size distribution data	116
Table 1G	Differential pressure cell calibration data	119
Table 2G	Venturi meter calibration data (obtained using water)	121
Table 3G	Venturi meter calibration data (obtained using suspension)	124

LIST OF ILLUSTRATIONS

		Page
Figure 1	Fluid flow curves (arithmetic)	4
Figure 2	Fluid flow curves (logarithmic)	4
Figure 3	Schematic diagram of pipeline flow circuit	23
Figure 4	Differential pressure cell	26
Figure 5	Schematic diagram of the electrical circuits associated with the D.P. cell	27
Figure 6	Four-way valve arrangement	28
Figure 7	Modified Fann viscometer	33
Figure 8	Diagram of Fann viscometer	34
Figure 9	Friction factor vs. Reynolds number (Water calibration)	39
Figure 10	Friction factor vs. Modified Reynolds number (Test 1-1, 32.1 percent solids)	40
Figure 11	Friction factor vs. Modified Reynolds number (Test 1-2, 37.2 percent solids)	41
Figure 12	Friction factor vs. Modified Reynolds number (Test 1-3, 42 percent solids)	42
Figure 13	Friction factor vs. Modified Reynolds number (Test 1-4, 47.2 percent solids)	43
Figure 14	Friction factor vs. Modified Reynolds number (Test 2-1, 26.7 percent solids)	44
Figure 15	Friction factor vs. Modified Reynolds number (Test 2-2, 39.5 percent solids)	45
Figure 16	Friction factor vs. Modified Reynolds number (Test 2-3, 44.6 percent solids)	46
Figure 17	Friction factor vs. Modified Reynolds number (Test 2-4, 54.4 percent solids)	47

Figure 18	Specific gravity of suspension vs. Weight percent solids	49
Figure 19	Particle size vs. Cumulative weight percent passing	50
Figure 20A	Photomicrograph of sulphur particles in the size range 65-200 mesh	52
Figure 20B	Photomicrograph of sulphur particles in the size range smaller than 200 mesh	52
Figure 21	Initial settling rate vs. Weight percent solids	54
Figure 22	Rheological data. Shear stress vs. Shear rate (Suspension 1; weight percent solids parameter)	55
Figure 23	Rheological data. Shear stress vs. Shear rate (Suspension 2; weight percent solids parameter)	56
Figure 24	Rheological data. Shear stress vs. Shear rate (Suspension 1; weight percent solids parameter)	57
Figure 25	Rheological data. Shear stress vs. Shear rate (Suspension 2; weight percent solids parameter)	58
Figure 26	Rheological data Apparent coefficient of rigidity vs. Weight percent solids	61
Figure 27	Rheological data Apparent yield stress vs. Weight percent solids	62
Figure 28	Friction factor - Apparent Bingham Reynolds number product vs. Apparent Bingham yield number (Suspension 1)	64
Figure 29	Friction factor - Apparent Bingham Reynolds number product vs. Apparent Bingham yield number (Suspension 2)	65
Figure 30	Friction factor vs. Apparent Bingham Reynolds number (Suspension 1; apparent Bingham yield number parameter)	66
Figure 31	Friction factor vs. Apparent Bingham Reynolds number (Suspension 2; apparent Bingham yield number parameter)	67

Figure 32 Rheological data
Power-law exponent vs. Weight percent solids 70

Figure 33 Rheological data
Power-law constant vs. Weight percent solids 71

Figure 34 Friction factor vs. Power-law Reynolds number (Suspension 1) 72

Figure 35 Friction factor vs. Power-law Reynolds number (Suspension 2) 73

Figure 36 Critical friction factor vs. Power-law exponent 75

Figure 1B Correction to calibration constant vs. Dial reading 91

Figure 1G Differential pressure cell calibration 120

Figure 2G Venturi meter calibration 123

INTRODUCTION

During the last few years the natural gas industry in the Province of Alberta has developed rapidly. A by-product from this industry is sulphur and this is now being produced in large quantities. In order to avoid an accumulation of large quantities of this sulphur a method of transportation will have to be found. A convenient method of transporting this material would be by pipeline in the form of either a molten liquid or a solid-liquid suspension.

The determination of commercially useful data was not the aim of this investigation. In the initial stages it was planned to combine the obtaining of rheological and pressure drop data with an attempt to correlate the effects of particle size on the pressure drop, however, due to inadequate equipment, this was not accomplished. Instead a comparison has been made between the experimental results and values predicted by theoretical equations.

LITERATURE SURVEY AND THEORY

I Fluid Classifications.

Fluids are classified as Newtonian or non-Newtonian according to their behavior at constant temperature under imposed shearing forces in laminar flow. To illustrate this behavior suppose a fluid is confined between two plates of area A, and separated by a differential distance dr. If the lower plate is fixed, a small force F applied to the upper plate will give it a differential velocity dV in the direction of the force. A uniform velocity gradient of magnitude dV/dr is produced in the fluid since the shearing force is uniform across the distance dr.

The velocity gradient dV/dr is referred to as the "rate of shear", similarly, the shearing force per unit area, F/A, is known as the "unit shearing stress" and is denoted by T.

a) Newtonian Fluids:

By definition these fluids follow the equation

$$T = \mu \frac{dV}{dr} \quad . \; . \; . \; . \; . \; . \; . \; . \; . \; . \quad (1)$$

Thus, for laminar flow, there is a direct proportionality between shear stress and shear rate. The constant of proportionality, μ, is known as the viscosity of the fluid.

This equation is illustrated graphically in Figures 1 and 2, where shear stress is plotted against shear rate on arithmetic and logarithmic co-ordinates respectively. On arithmetic co-ordinates

the equation is represented by a straight line of slope μ passing through the origin. On logarithmic co-ordinates the curves for all Newtonian fluids have a slope of unity while the viscosity is given by the intercept at a shear rate of unity.

b) Non-Newtonian Fluids:

Non-Newtonian fluids do not obey Equation 1 and so do not possess the property of viscosity. The measure of the consistency of these fluids is known as either the "apparent viscosity" (7) or the "coefficient of rigidity" (17).

There are five general types of non-Newtonian fluid

1) Bingham Plastic
2) Pseudoplastic
3) Dilatant
4) Thixotropic
5) Rheopectic

the latter two types being more complex than the first three in that the relationship between shear stress and shear rate depends upon the duration of shear.

1) Bingham Plastic Fluids:

As shown in Figure 1 this is the non-Newtonian which differs least from a Newtonian fluid. The relation between shear stress and shear rate is still linear but it does not pass through the origin. Thus a finite shear stress Ty, known as the yield stress, is necessary to cause motion. The equation to the flow curve becomes

$$T - Ty = \eta \frac{dV}{dr} \quad . \; . \; . \; . \; . \; . \; . \; . \; . \; . \; . \; (2)$$

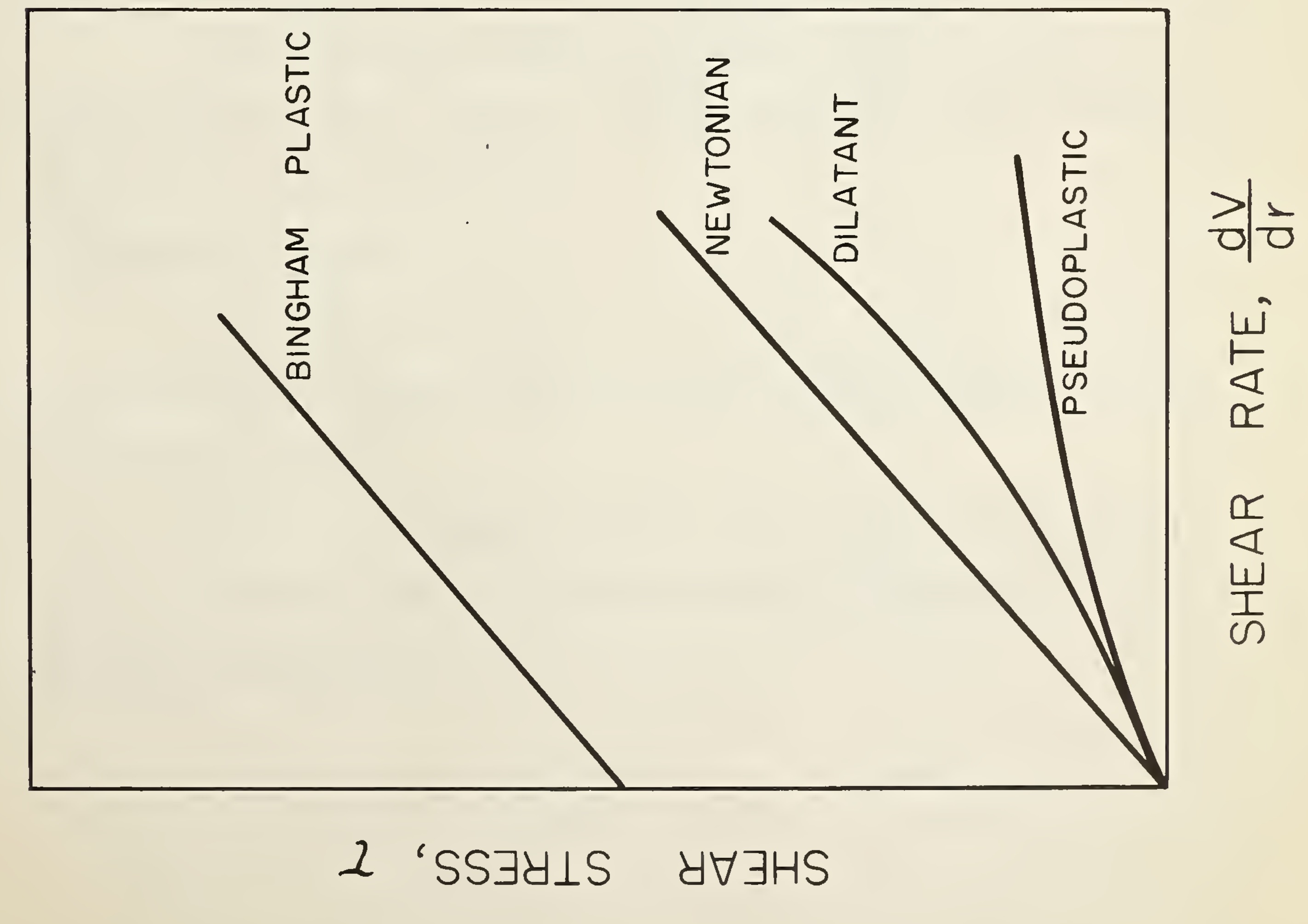

Fig. 1. Fluid Flow Curves

(Arithmetic)

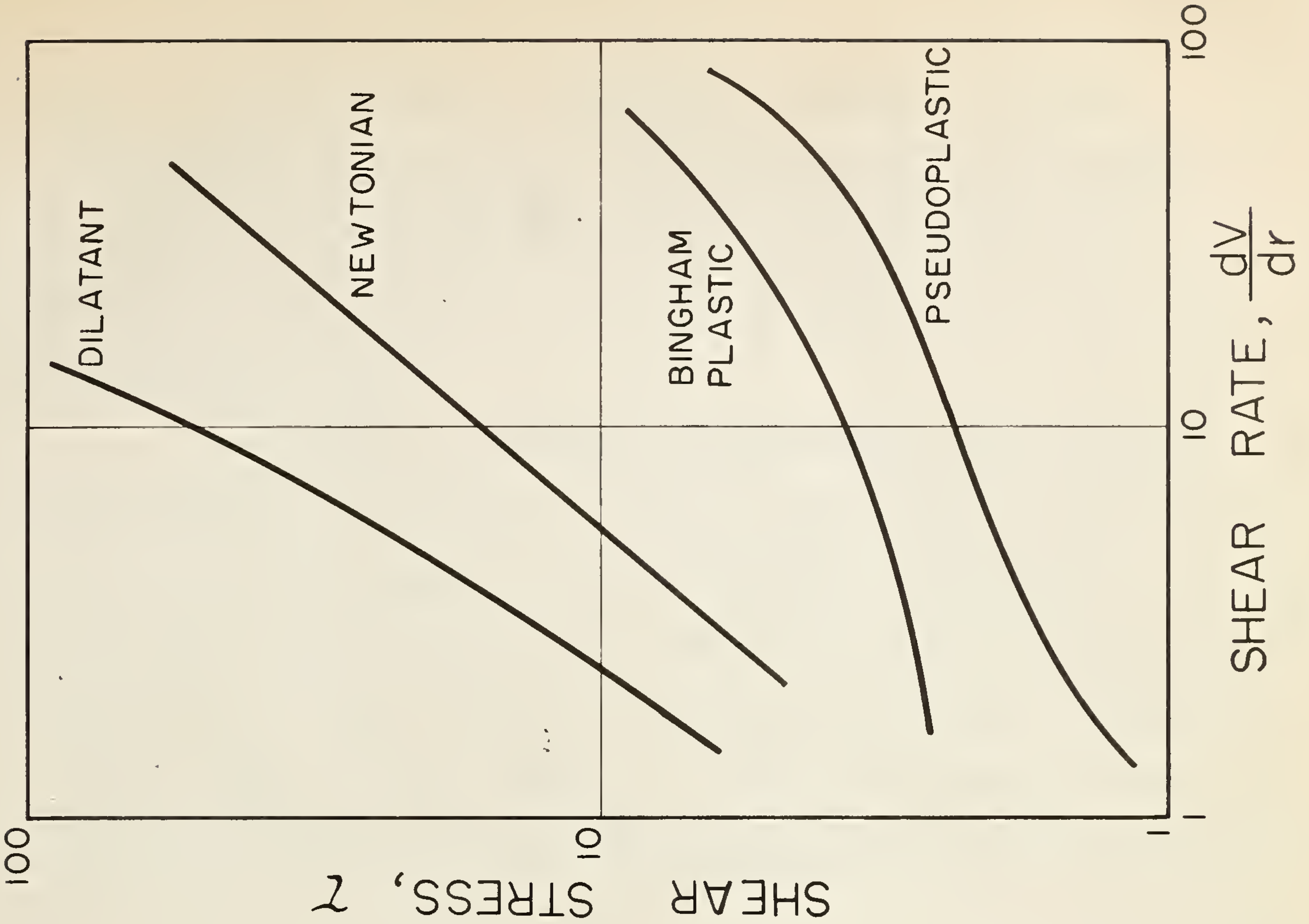

Fig. 2. Fluid Flow Curves

(Logarithmic)

where η, the "coefficient of rigidity", or "apparent viscosity", represents the slope of the flow curve. On logarithmic co-ordinates the flow curve becomes asymptotic to T_y at low shear rates, and approaches a slope of unity at very high shear rates.

2) Psuedoplastic Fluids:

On arithmetic co-ordinates a pseudoplastic fluid displays a flow curve which is concave to the rate of shear axis and passes through the origin (Figure 1). When represented on logarithmic co-ordinates (Figure 2) these fluids exhibit flow curves having slopes between zero and unity, and these are generally relatively straight over wide ranges of shear rates (16). Certain pseudoplastic fluids exhibit flow curves which can be represented by the power law function

$$T = K \left(- \frac{dV}{dr}\right)^{n} \quad . \; . \; . \; . \; . \; . \; . \; . \quad (3)$$

These materials are known as "power-law" pseudoplastics.

3) Dilatant Fluids:

Dilatant fluids display rheological behavior opposite to that of pseudoplastics (Figures 1 and 2) in that the flow curves are convex to the rate of shear axis.

4) Thixotropic Fluids:

When thixotropic fluids are sheared at a given shear rate and temperature the shear stress decreases with the duration of shear.

5) Rheopectic Fluids:

These fluids behave in the converse manner to thixotropic fluids in that the shear stress increases with the duration of shear at constant shear rate.

Examples of each of these fluids and explanations of the causes of their rheological behaviour are available (1, 10, 14, 17, 25, 26).

II Mechanics of Flow in Circular Pipes.

Relations used for the flow of fluids are developed from material balances, force balances and energy balances (24).

Applying a force balance to steady uni-dimensional flow of any fluid in a pipe yields

$$- v\,dp = \frac{V\,dV}{\alpha\,g_c} + \frac{4\,T_w\,v\,dL}{D} + \frac{g}{g_c}\,dz \quad \ldots\ldots \quad (4)$$

A non-dimensional shear stress, f, known as the friction factor, is defined by the relationship

$$f = \frac{2\,g_c\,T_w}{\rho\,V^2} \quad \ldots\ldots\ldots\ldots\ldots\ldots\ldots\ldots\ldots\ldots (5)$$

By dimensional analysis this friction factor may be shown to be a function of the relative roughness, δ/D, of the pipe surface, and the Reynolds number, $DV\rho/\mu$.

Eliminating T_w from Equations 3 and 4 gives

$$- dp = \frac{V\,dV}{\alpha\,v\,g_c} + \frac{2f\,V^2\,dL}{g_c\,D\,v} + \frac{g}{g_c}\,\frac{dz}{v} \quad \ldots\ldots \quad (6)$$

these three terms represent the loss in pressure due to acceleration, friction and change in elevation respectively, so

$$- dp_f = \frac{2\,f\,V^2\,dL}{g_c\,D\,v} \quad \ldots\ldots\ldots\ldots\ldots\ldots\ldots \quad (7)$$

this is known as the Fanning equation.

Laminar Flow in Circular Pipes.

Consider the steady laminar flow of a Newtonian fluid in a horizontal pipe of uniform diameter. The velocity at any given distance r from the axis of the pipe can be obtained by a force balance, and is given by

$$u_r = - \frac{dpf}{4 \mu \, dL} \left(\frac{D^2}{4} - r^2 \right) \quad . \; . \; . \; . \; . \; . \; . \; . \quad (8)$$

However the volumetric rate of flow through an annulus of radii r and r + dr is

$$dQ = 2\pi r \, dr \, ur \quad . \; . \; . \; . \; . \; . \; . \; . \; . \; . \quad (9)$$

eliminating u_r from Equations 8 and 9 gives

$$dQ = - \frac{dp_f}{4\mu \, dL} \left(\frac{D^2}{4} - r^2 \right) 2\pi r \, dr$$

integrating this equation between the limits $r = \frac{D}{2}$ and $r = 0$ gives

$$Q = - \frac{\pi D^4}{128 \mu} \quad \frac{dpf}{dL}$$

Thus the average velocity,

$$V = \frac{Q}{\pi D^2/4}$$

$$V = - \frac{D^2}{32 \mu} \quad \frac{dp_f}{dL}$$

$$\text{or} \quad - dp_f = \frac{32 \mu V dL}{D^2} \quad . \; . \; . \; . \; . \; . \; . \; . \quad (10)$$

This is the well known Poiseuille equation.

Now equating the pressure drop term of Equation 10 with Equation 7 gives

$$f = \frac{16}{\frac{DV\rho}{\mu}} = \frac{16}{Re} \quad \ldots\ldots\ldots\ldots\ldots \quad (11)$$

i.e. the friction factor is proportional to the Reynolds number only in laminar flow.

Turbulent Flow in Circular Pipes

Turbulent flow is a much more complex condition than laminar flow and is not as easily analyzed. However there are several empirical equations for the velocity profile which appear to fit the data over a large percent of the pipe diameter.

The simplest of these equations is (24)

$$\frac{U_{max} - u}{V_*} = A\left(\frac{r}{r_w}\right)^2 \quad \ldots\ldots\ldots\ldots\ldots \quad (12)$$

where A has a value of 7.85. It is found that this equation does not apply near the pipe wall.

The other common expression for the velocity profile is (24)

$$\frac{U_{max} - u}{V_*} = 2.5 \ln \frac{r}{r_w} \quad \ldots\ldots\ldots\ldots\ldots \quad (13)$$

this equation also does not apply very close to the pipe wall.

The Flow of non-Newtonian Fluids in Pipes

The literature relating to the flow of non-Newtonian fluids in circular pipes was reviewed by Winning (29) in his M.Sc. thesis in 1948. Ten years later, in 1958, Lindley (14) again reviewed the literature and found there had been a considerable amount of new material

published. Most notable of this was a survey by Metzner (17) on the whole field of non-Newtonian technology, giving a detailed report on the theory to that date. Since then, further work has been reported especially related to the theory of the turbulent flow of non-Newtonian fluids in pipes.

i) Bingham Plastic Fluids:

Due to the complex nature of turbulent flow an empirical approach is necessary in the development of a relationship which can be applied to turbulent as well as laminar flow. A convenient empirical approach is that of dimensional analysis. Thus, for a Newtonian fluid

$$\Delta P = \theta' \,(D, L, V, \delta, \rho, \mu, g_c) \quad \ldots\ldots\ldots \quad (14)$$

Similarly for a Bingham plastic

$$\Delta P = \theta'' \,(D, L, V, \delta, \rho, \eta, g_c, T_y) \quad \ldots\ldots\ldots \quad (15)$$

Govier and Winning (6) applied this technique to the flow of Bingham plastics in a horizontal circular pipe. They rearranged the variables to form four non-dimensional groups as the equation

$$\frac{g_c \, D \, \Delta P}{2 \, V^2 \, L \, \rho} = \theta'' \left[\frac{D \, V \, \rho}{\eta} \quad \frac{\delta}{D} \quad \frac{D \, T_y \, g_c}{V \, \eta} \right] \quad \ldots\ldots \quad (16)$$

which can be rewritten as

$$f = \theta'' \left(R_m \quad \frac{\delta}{D} \quad Y \right) \quad \ldots\ldots\ldots\ldots \quad (16a)$$

where the friction factor, $f = \dfrac{g_c \, D \, \Delta P}{2 \, V^2 \, L \, \rho}$ . . . . (17)

a modified Reynolds number, $R_m = \dfrac{D \, V \, \rho}{\eta}$ . . . . (18)

a yield number, $Y = \dfrac{D \, T_y \, g_c}{V \, \eta}$ . . . . (19)

A different approach was followed by Buckingham (3). He integrated the rheological equation

$$T - T_y = \eta \frac{dV}{dr} \qquad \ldots\ldots\ldots \qquad (2)$$

for the isothermal flow of Bingham plastics in circular pipes. The resulting equation is

$$\frac{8V}{D} = \frac{T_w \, g_c}{\eta}\left[1 - \frac{4}{3}\,\frac{T_y}{T_w} + \frac{1}{3}\left(\frac{T_y}{T_w}\right)^4\right] \qquad \ldots\ldots \qquad (20)$$

Equation 20 is usually modified in the following manner. For the shearing stress at the wall, the relationship is

$$T_w = \frac{D \, \Delta P}{4L} \qquad \ldots\ldots\ldots \qquad (21)$$

Substitution of Equation 21 in Equation 20 gives

$$\frac{8V}{D} = \frac{g_c}{\eta}\left[\frac{D \, \Delta P}{4L} - \frac{4}{3}\,T_y + \frac{1}{3}\,\frac{T_y^{\,4}}{\left(\frac{d \, \Delta P}{4L}\right)^3}\right] \qquad \ldots \qquad (22)$$

Multiplication of both sides of Equation 22 by $\eta/8V^2\rho$ and substitution of the dimensionless ratios defined by Equations 17, 18 and 19 yield the Buckingham equation in the form

$$\frac{1}{R_m} = \frac{f}{16} - \frac{Y}{6\,R_m} + \frac{1}{3}\,\frac{Y^4}{f^3\,R_m^{\,4}} \qquad \ldots\ldots \qquad (23)$$

Division of both sides of Equation 23 by f, yields

$$\frac{1}{f\,R_m} = \frac{1}{16} - \frac{1}{6}\,\frac{Y}{f\,R_m} + \frac{1}{3}\,\frac{Y^4}{(f\,R_m)^4} \qquad \ldots \qquad (24)$$

which is one of the most convenient forms of the Buckingham equation.

Equation 24 can be represented graphically in two ways, either by a logarithmic plot of the product $f\ R_m$ versus Y or by a logarithmic plot of f versus R_m with Y as a parameter. The former gives a single line curve which is asymptotic to $f\ R_m = 16$ at low values of Y, and approaches a straight line for values of Y greater than 1000. The latter yields a series of parallel lines with slopes of minus one and offset from the Poiseuille line $\left(f = \frac{16}{Re}\ ,\ Y = 0.\right)$

Govier (8) programmed Equation 24 for digital computer solution for wide ranges of values of R_m and Y and presented large scale logarithmic plots of these data as f versus R_m, and $f\ R_m$ versus Y.

A similar approach was used by Hedstrom (12). He presented his results as a plot of f versus R_m but used a different non-dimensional quantity $Y\ R_m$, as parameter. This parameter has been called the Hedstrom number. Perkins and Glick (19) later rearranged Equation 20 in terms of this non-dimensional group to obtain

$$\frac{1}{R_m} = \frac{f}{16} - \frac{H}{6\ R_m^2} + \frac{H^4}{3\ f\ R_m^8} \quad \ldots\ldots\ldots\ldots\ldots \quad (25)$$

where $H = R_m\ Y = \frac{T_y\ D^2\ g_c\ \rho}{\eta^2}$

In turbulent flow Equation 24 no longer applies and the importance of Y is diminished. If a logarithmic plot (f versus R_m) is made of turbulent data it is found to fall close to the Von Karman-Nikuradse line with $R_m = D\ V\ \rho/\eta$ replacing $D\ V\ \rho/\mu$ as the Reynolds number.

ii) General Discussion Applicable to all Fluids:

Most development related to the pipeline flow of pseudoplastic materials stem from relationships developed by Rabinowitsch (20) and Mooney (18). The latter showed that the relationship between the shear stress at the wall of the pipe, $\frac{D\,\Delta P}{4L}$, and the term $\frac{8V}{D}$ were independent of the diameter of the pipe in laminar flow.

Alves, Boucher and Pigford (1) made use of this relationship between $\frac{D\Delta P}{4L}$ and $\frac{8V}{D}$ in correlating data on non-Newtonian suspensions and solutions. For laminar flow they suggested that a comparison of pipeline and rotational viscometer data could be made on the basis of comparing the rate of shear and the shear stress at the pipe wall with the rate of shear and the shear stress at the inner cylinder wall of the viscometer. They also recommended a design procedure for turbulent flow which was based upon experimentally determined viscosities.

Several other relationships and procedures have been proposed as useful in the prediction of pressure drop data:

1) An empirical power-law function

$$T = K\left(-\frac{dV}{dr}\right)^n \quad \dots\dots\dots\dots \quad (3)$$

The uses of this function are dealt with in the next section.

2) The Powell-Eyring equation

$$T = -\mu\frac{dV}{dr} + \frac{1}{B}\sinh^{-1}\left(\frac{dV/dr}{c}\right) \quad \dots\dots\dots \quad (26)$$

has been used by investigators at the University of Utah. Christiansen, Ryan and Stevens (4) have integrated this equation numerically and have presented the resulting relationships as functions of non-dimensional parameters. However it is applicable only for laminar flow.

3) For turbulent flow an apparent viscosity at infinite shear has been used (28) to calculate a modified Reynolds number and hence to obtain a friction factor from the conventional friction factor versus Reynolds number plot.

iii) Power-Law Fluids:

The starting point for the theory on power-law fluids is an equation developed by Rabinowitsch (20) and Mooney (18) for the shear rate at the wall of a tube. The equation is

$$\left(-\frac{dV}{dr}\right)_w = \frac{3}{4}\left(\frac{8V}{D}\right) + \frac{1}{4}\ \frac{D\,\Delta P}{4L}\ \frac{d(8V/D)}{d(D\Delta P/4L)} \quad . \ . \ . \ . \ . \ . \qquad (27)$$

Equation 27 was rearranged by Metzner and Reed (16) to give

$$\left(-\frac{dV}{dr}\right)_w = \frac{3n' + 1}{4n'}\left(\frac{8V}{D}\right) \quad . \ . \ . \ . \ . \ . \ . \ . \ . \ . \ . \qquad (28)$$

$$\text{where} \quad n' = \frac{d\left(\ln \dfrac{D\,\Delta P}{4L}\right)}{d\left(\ln \dfrac{8V}{D}\right)} \quad . \ . \ . \ . \ . \ . \ . \ . \ . \ . \qquad (29)$$

which is the slope of a logarithmic plot of $\frac{D\,\Delta P}{4L}$ versus $\frac{8V}{D}$. It follows that

$$\frac{D\,\Delta P}{4L} = T_w = K'\left(\frac{8V}{D}\right)^{n'} \quad . \ . \ . \ . \ . \ . \ . \ . \qquad (30)$$

If n' is a constant then this equation is rigorously true; if n' is not a constant but varies with T_W then Equation 30 represents the tangent to the curve at any chosen value of $\frac{D\,\Delta P}{4L}$.

The similarity between Equations 3 and 30 is obvious; however Equation 30 has the advantage that it does not have to be integrated in order to relate pressure drop to flow rate. Metzner and Reed (16) have shown that, for fluids that obey the power-law (Equation 3)

$$n' = n \quad \ldots\ldots\ldots \quad (31)$$

$$\text{and} \quad K' = K\left(\frac{3n' + 1}{4n'}\right)^{n'} \quad \ldots\ldots\ldots \quad (32)$$

if the shear stress - shear rate data has been obtained from a rotational viscometer. These equations may be used with Equation 30 to draw a curve of $\frac{D\,\Delta P}{4L}$ versus $\frac{8V}{D}$.

The parameters n and n' characterize the extent of non-Newtonian behaviour. When they equal unity, the fluid is Newtonian; values of n and n' less than unity indicate pseudoplastic or Bingham-plastic behaviour, and values greater than unity indicate dilatant behaviour. The use of exponents such as n and n' has also been proposed by Weltmann (27).

Regrouping Equation 5 as

$$f = \frac{D\,\Delta P}{4L} \Big/ \frac{\rho\, V^2}{2g_c} \quad \ldots\ldots\ldots \quad (33)$$

and solving for a generalized or power-law Reynolds number using Equations 11, 30 and 33 yields

$$Re' = \frac{D^{n'} V^{2-n'} \rho}{\gamma} \quad . . . . \quad (34)$$

$$\text{where} \quad \gamma = g_c K' 8^{n'-1} \quad . . . . \quad (35)$$

The denominator γ can be obtained from rotational viscometer data, for power-law fluids, by using Equations 31, 32 and 35.

For Newtonian fluids, $n' = 1$, $K' = \mu/g_c$ and Equation 34 reduces to

$$Re' = Re = \frac{D V \rho}{\mu}$$

As the equation $f = \frac{16}{Re}$ has been used in the derivation of Equation 34 it follows that a power-law fluid, in laminar flow, should give data that falls on a line given by $f = \frac{16}{Re'}$, when plotted as friction factor versus power law Reynolds number. Metzner (17) has reviewed a large amount of published data for the laminar flow of power-law solutions and suspensions and has obtained good agreement with the equation $f = \frac{16}{Re'}$.

A convenient approach to the development of a relationship for "power-law" pseudoplastics is dimensional analysis. Thus

$$\Delta P = \theta''' (D. v. \rho. K. L. n') \quad . . . . \quad (35A)$$

Rearrangement of these variables yields three dimensionless groups as the equation

$$f \, Re' = 2 \left[\frac{2 \, (3n' + 1)}{n'} \right]^{n'} \quad . . . . \quad (35B)$$

which should be applicable to laminar and turbulent flow.

Ryan and Johnson (22) have suggested a local stability parameter

$$Z = \frac{r_w \ \rho \ u}{T_w} \ \frac{du}{dy} \quad \ldots\ldots\ldots \quad (36)$$

as the starting point for the estimation of the pressure drop in the transition from laminar to turbulent flow. This parameter is applicable to Newtonian or non-Newtonian flow. Application of Equation 36 requires knowledge of the laminar velocity profile, which can be derived from the rheological law for the fluid of interest.

For a Newtonian fluid

$$Z_{max} = \left(\frac{4}{27}\right)^{1/2} \frac{D \ V \ \rho}{\mu} \quad \text{at} \quad \frac{r}{r_w} = \left(\frac{1}{3}\right)^{1/2}$$

and as the critical value of the Reynolds number is 2100 then

$$\left(Z_{max}\right)_c = \left(\frac{4}{27}\right)^{1/2} 2100 = 808 \quad \ldots\ldots\ldots \quad (37)$$

Ryan and Johnson believe that 808 is the critical value of the parameter irrespective of the rheological behaviour of the fluid.

For a power-law fluid

$$Z_{max} = \frac{r_w^2 \ \rho \ W^2}{T_w} \ \phi\ (n) \quad \ldots\ldots\ldots \quad (38)$$

$$\text{at} \quad \frac{r}{r_w} = \left(\frac{1}{n+2}\right)^{n/n + 1}$$

$$\text{where} \quad \phi\ (n) = \left(\frac{3n+1}{n}\right)^2 \left(\frac{1}{n+2}\right)^{\frac{n+2}{n+1}} \quad \ldots\ldots\ldots \quad (39)$$

By definition the friction factor is given by the expression

$$f = \frac{2\ T_w}{r_w^2\ \rho\ W^2} \quad . \ . \ . \ . \ . \ . \ . \ . \ . \ . \quad (5)$$

Combining Equations 5 and 38 and setting $(Z_{max})_c = 808$ gives

$$f_c = \frac{\phi\ (n)}{404} \quad . \ . \ . \ . \ . \ . \ . \ . \ . \ . \quad (40)$$

Experimental data may be used to check the accuracy of this equation by plotting f_c versus n .

Dodge and Metzner (5) have performed a theoretical analysis for the turbulent flow of power-law fluids in smooth tubes. The following relationship was proposed between the pressure drop and the mean flow rate,

$$\left(\frac{1}{f}\right)^{1/2} = A_{1n}\ \log\left(Re'\ (f)^{1-\frac{n'}{2}}\right) + C_{n'} \quad . \ . \ . \ . \ . \quad (41)$$

$$\text{where} \quad C_{n'} = A_{1n}\ \log\left[\frac{1}{8}\left(\frac{6n' + 2}{n'}\right)^{n'}\right] + C_n$$

the constants A_{1n} and $C_{n'}$ were found experimentally and Equation 41 finally arranged in the form

$$\left(\frac{1}{f}\right)^{1/2} = \frac{4\ 0}{(n')^{0.75}}\ \log\left(Re'\ (f)^{1-\frac{n'}{2}}\right) - \frac{0\ 4}{(n')^{1.2}} \quad (42)$$

Equation 42 is solved graphically and presented in the form friction factor versus power-law Reynolds number, $\frac{D^{n'}\ V^{2-n'}\ \rho}{\gamma}$. In this plot theoretical lines obtained for different values of the exponent

n' fall parallel to the Karman-Nikuradse line (n' = 1). For values of n' greater than unity the lines are above the n' = 1 line while for values of n' less than unity they are below.

A similar method of presentation has been used by Shaver and Merrill (23). For experimental, turbulent data a plot was made of friction factor versus power-law Reynolds number; this yielded a family of lines for values of n' between 0.53 and unity. These lines were not parallel, as proposed by Dodge and Metzner (5), but had increasing slopes for decreasing values of n', the limiting case being 45° or an extension of the Poiseuille line.

III Determination of Rheological Properties Using a Rotational Viscometer.

A rotational viscometer consists of an inner and outer cylinder so arranged that the fluid to be tested fills the annular space between the cylinders. One of the cylinders may be rotated, causing a torque on the other cylinder which can be measured and taken as an indication of the consistency of the fluid.

For a Newtonian fluid the relationship between the speed of the rotor and the rate of shear at the wall of the stator may be determined mathematically from the Reiner-Riwlin (21) equation

$$\left(\frac{dV}{dr}\right)_r = \frac{4\pi R_1^2 R_2^2}{r^2\left(R_2^2 - R_1^2\right)} N \quad . \; . \; . \; . \; . \; . \; . \; . \; . \quad (43)$$

where $\left(\frac{dV}{dr}\right)_r$ = rate of shear at r, sec^{-1}, when $R_1 < r < R_2$.

N = rotor speed, revolutions per second

R_1 = inner radius of the annulus

R_2 = outer radius of the annulus

If the outer cylinder is rotated, the rate of shear at the wall of the inner cylinder is required, so substituting R_1 for r

$$\left(\frac{dV}{dr}\right)_{R_1} = \frac{4\pi R_2^2}{R_2^2 - R_1^2} N = \frac{4\pi}{1 - 1/S^2} N \quad . \quad . \quad . \qquad (44)$$

where $S = \dfrac{R_2}{R_1}$

A linear relationship exists between the torque on the inner cylinder, and the shear stress at the wall of this cylinder. This relationship is

$$T_{R_1} = K_1 \theta \quad . \ . \ . \ . \ . \ . \ . \ . \ . \ . \qquad (45)$$

the constant K_1 is obtained by calibration of the instrument with a Newtonian fluid of known viscosity at a given temperature.

Maintenance of laminar flow in the annulus is essential. As a criterion for the onset of turbulent flow Merrill (15), quoting Barr (2), suggested

$$\frac{2\pi R_2 (R_2 - R_1) \rho N}{\eta} = 592 \quad . \ . \ . \ . \ . \qquad (46)$$

where $\dfrac{2\,\pi\,R_2\,(R_2 - R_1)\,\rho\,N}{\eta}$ is the modified Reynolds number of Barr.

Krieger and Maron (13) proposed a more general equation, the validity of which was independent of the shear stress - shear rate relationship for the fluid. Hence an expression for the rate of shear at the stator wall can be obtained. This equation applied to the wall of the inner cylinder is

$$\left(\frac{dV}{dr}\right)_{R_1} = \frac{4\,\pi\,N}{1 - 1/S^2}\left[1 + k_1\left(\frac{1}{n''} - 1\right) + k_2\left(\left[\frac{1}{n''} - 1\right]^2 + \frac{d\left[\frac{1}{n''} - 1\right]}{d\,\ln t}\right)\right] \qquad (47)$$

$$\text{where}\quad k_1 = \frac{S^2 - 1}{2S^2}\left(1 + \frac{2}{3}\ln S\right) \quad \ldots\ldots\ldots \quad (48)$$

$$k_2 = \frac{S^2 - 1}{6S^2}\ln S \quad \ldots\ldots\ldots\ldots \quad (49)$$

n'' = slope of the logarithmic plot of torque versus rotational speed.

Often the last term of Equation 47 is relatively small so that the equation can be reduced to

$$\left(\frac{dV}{dr}\right)_{R_1} = \frac{4\,\pi\,N}{1 - 1/S^2}\left[1 + k_1\left(\frac{1}{n''} - 1\right) + k_2\left(\frac{1}{n''} - 1\right)^2\right] \quad \ldots \quad (50)$$

Equation 50 can be applied to either a Newtonian or a non-Newtonian fluid.

A paper published recently by Govier (9) discusses the application of these rheological equations to data obtained for

Bingham - and pseudoplastics from a concentric cylinder viscometer. The interpretation of the resulting shear stress - shear rate curves for prediction of pressure drops in pipeline flow is discussed using some of the theory dealt with in section II.

EXPERIMENTAL EQUIPMENT

The Pipeline Unit

A diagram of the flow circuit is shown in Figure 3. The flow circuit consisted of a supply tank, a pump and motor, the two test pipelines, a venturi meter, and a weight tank on scales.

I Supply Tank:

An 18 cubic foot capacity tank was used to store the suspension, this was connected directly to the pump by a length of 2-1/2 inch diameter pipe. To ensure uniform mixing of the suspension two Greey "Lightning" mixers, one with a paddle type impeller and the other with a propellor type impeller, were used.

II Pump and Motor:

The pump used was a "Moyno" positive displacement unit operating at 770 R.P.M. to give 35 g.p.m. against a maximum pressure of 75 psi. The drive unit was a 5 HP., three phase, 220 volt motor.

The two basic pumping elements of a "Moyno" pump are a helical rotor and a double thread, rubber lined, helical stator. The two helical surfaces mesh together to push the liquid ahead with uniform motion.

III Pipeline Test Sections:

The discharge from the pump was designed to deliver suspension either to the pipeline or return it to the supply tank. Both this return and the discharge from the pipeline entered the supply tank tangentially

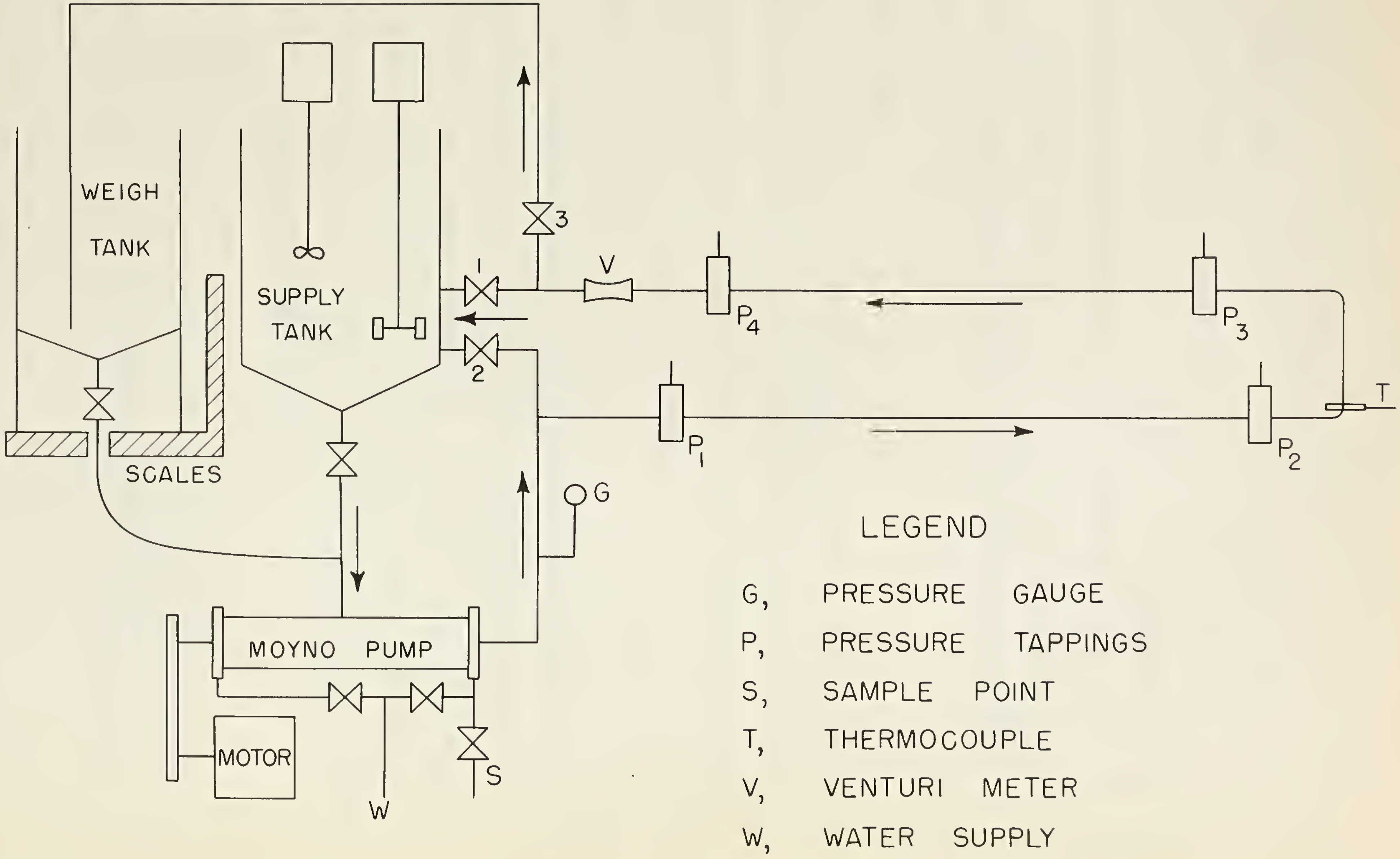

Fig. 3. Schematic Diagram of Pipeline Flow Circuit

and well below the surface of the suspension.

Two lengths of 1-7/8 I.D. aluminum tube were installed parallel to one another and connected in series by a 180° bend. An iron-constantan thermocouple was inserted into the pipeline at the bend to measure the temperature of the flowing fluid.

The pressure tappings on the section upstream of the bend were spaced 45.35 feet apart and those on the downstream section spaced 40.17 feet apart.

IV Venturi Meter:

The venturi meter was specially machined from a cylinder of aluminum to give a pressure drop of about 15 psi at the maximum flow rate, and was positioned at the end of the downstream section just before the line entered the supply tank.

V Weighing Tank:

The weighing tank was mounted on a set of Fairbanks scales with a capacity of 500 lbs. These scales were fitted with a weigh arm graduated in half pounds. Emptying of the tank was effected by direct pumping into the supply tank. The line connecting the tank with the pump was initially a jointed metal hose, however this corroded badly and was replaced by a rubber hose.

VI Sample Cock:

The sample cock S (Figure 3) was placed on the discharge side of the pump where a representative sample of flowing material

could be obtained.

VII Pressure Measuring System:

A Statham electrical differential pressure (DP) cell (Figure 4), having a working range of ± 15 psid was used to measure the pressure drop across each of the test sections and across the venturi meter. Figure 5 is a schematic illustration of the electrical circuits associated with this DP cell. In Figure 5 the left hand side represents the excitation circuit which was made up of an 18 volt DC source, a variable resistance and a voltmeter. The right hand side of this Figure represents the output circuit which was made up of a 'backed-up' potentiometer and a recording potentiometer.

In order to transmit the pressure to the DP cell hydraulic connecting lines were installed. These lines joined the pressure tappings to one of two four-way valves (Figure 6), depending on whether it was an upstream or downstream pressure measurement. A single line connected each valve to the appropriate side of the DP cell.

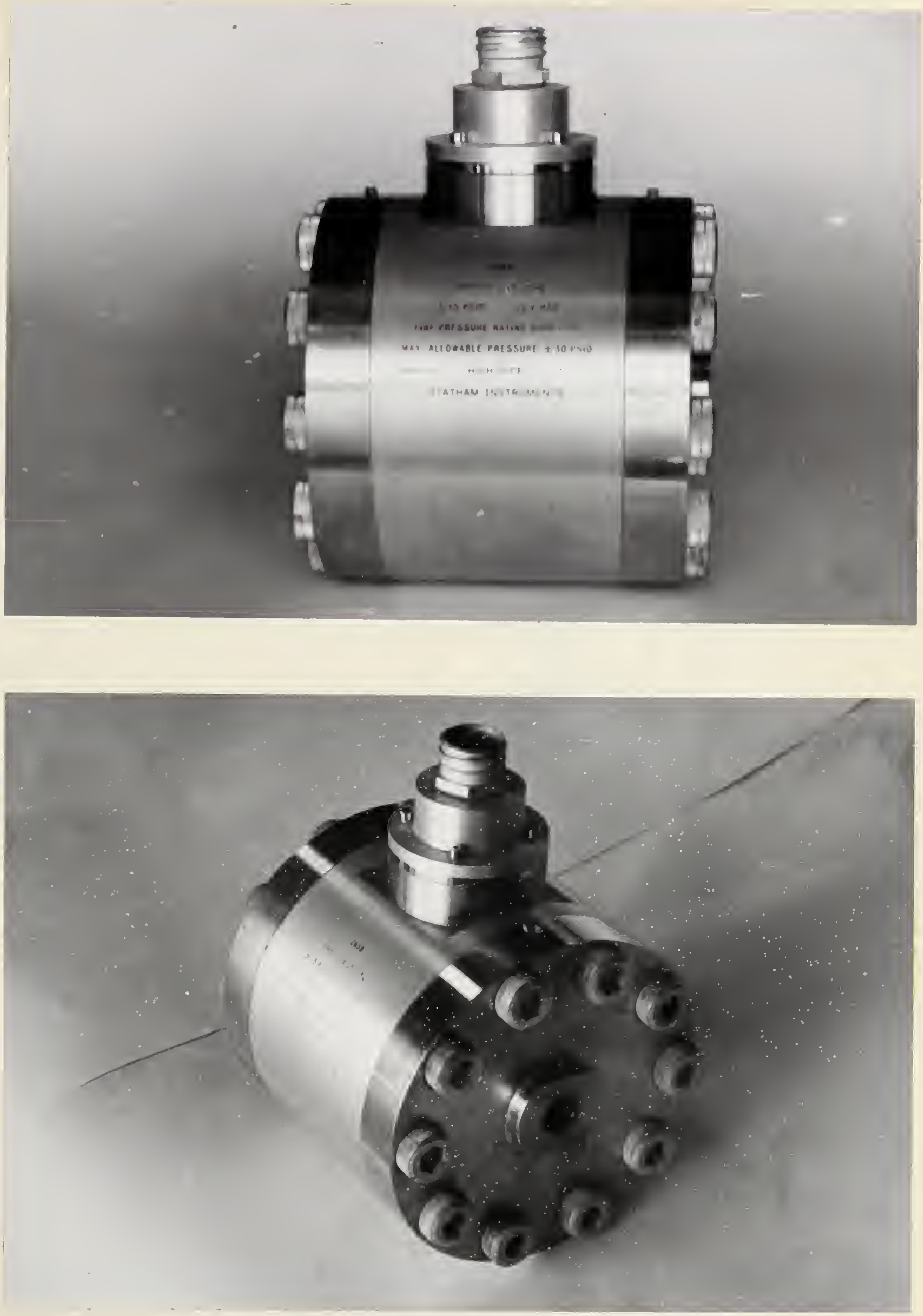

Fig. 4. Differential Pressure Cell

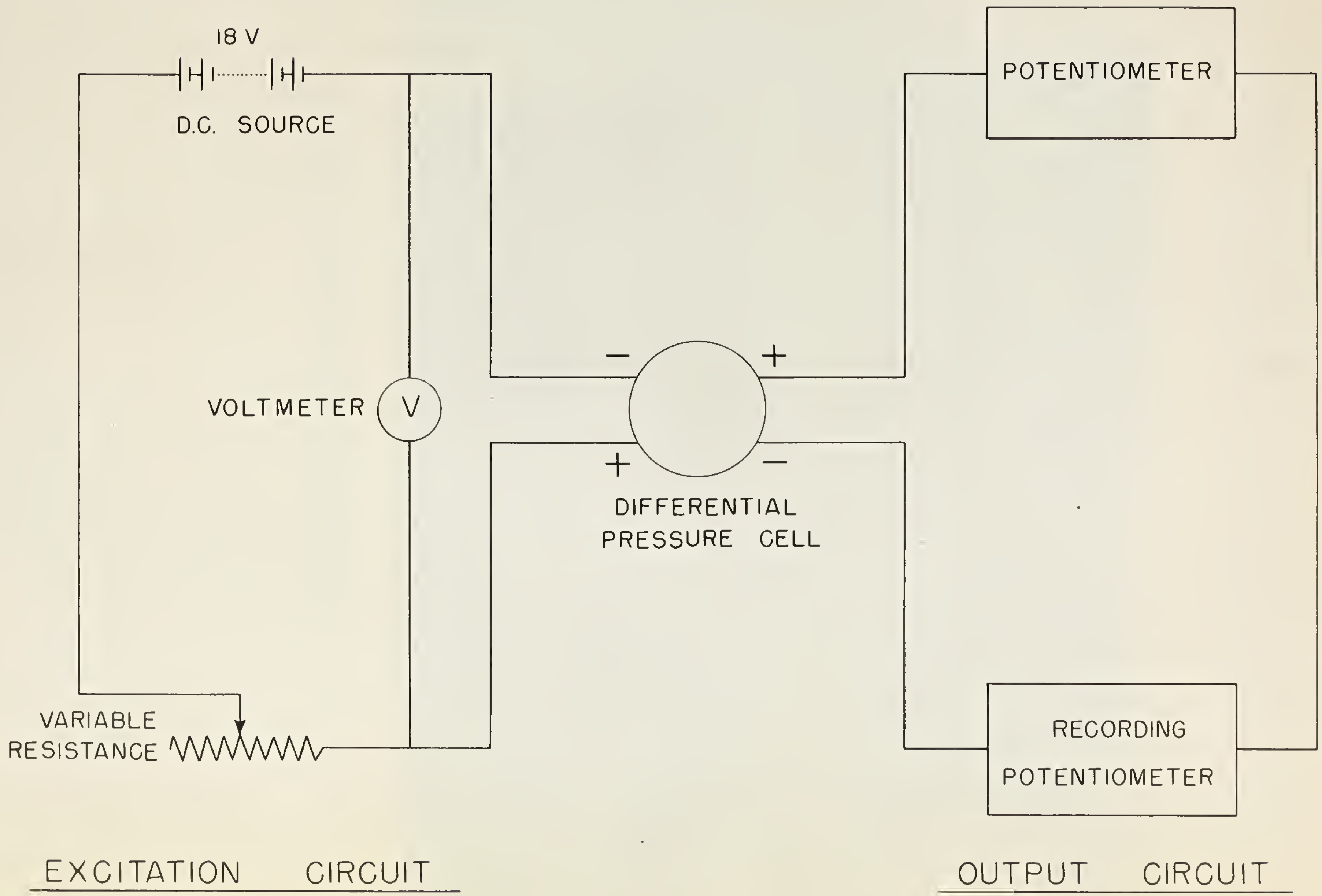

Fig. 5. Schematic Diagram of the Electrical Circuits Associated with the DP Cell

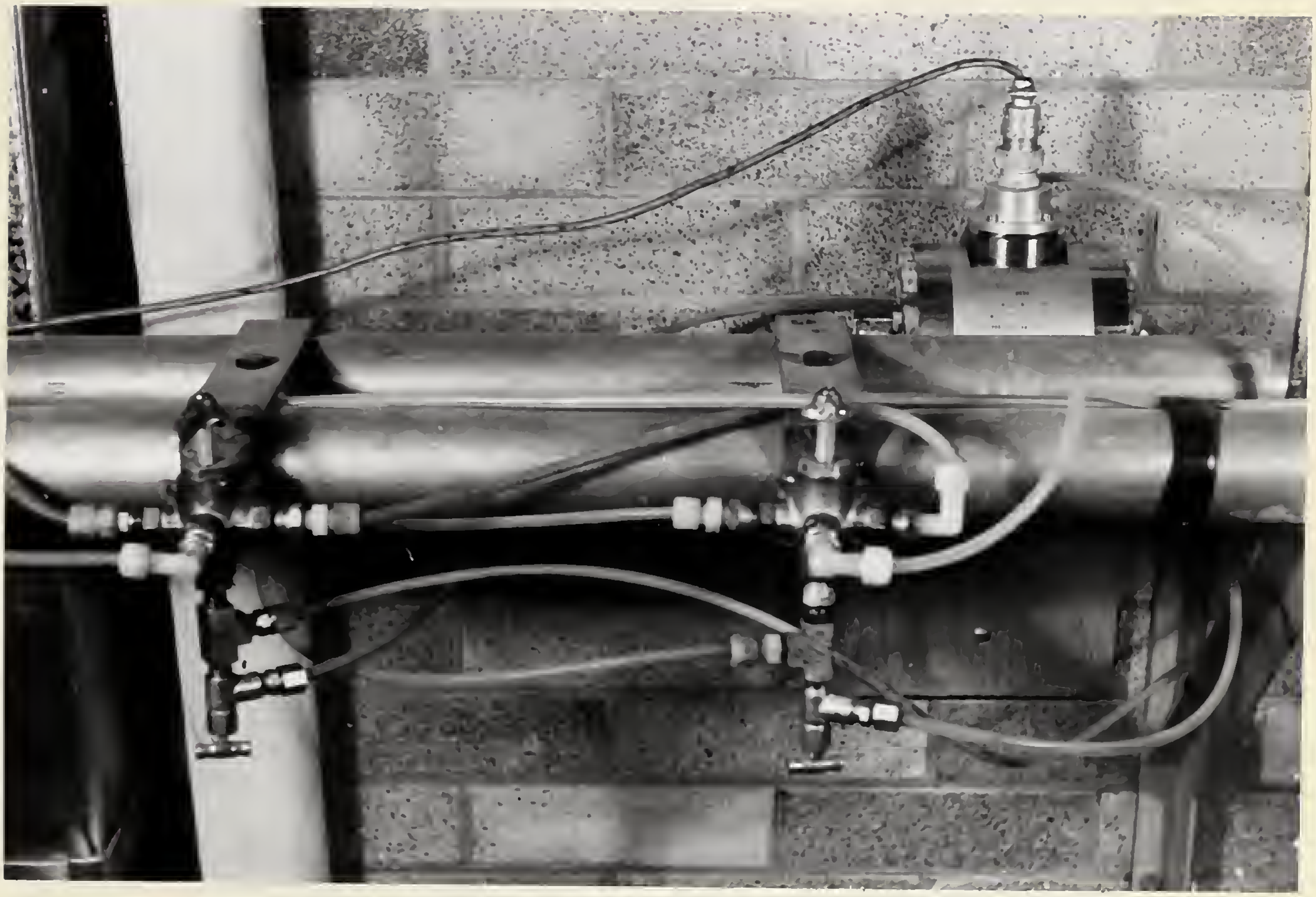

Fig. 6. Four-way Valve Arrangement

EXPERIMENTAL PROCEDURE

A. Initial Treatment of the Dry Solids.

Six tons of coarse lump sulphur were obtained from Shell Oil Co. of Canada Ltd., Calgary. A sieve size analysis carried out on a representative sample of this material showed it to contain particles varying from 2 inches in diameter to less than 37 microns (400 mesh). The larger lumps were removed by passing all the material over an 8 mesh "Dillon" vibrating screen. This large material was then crushed, using a heavy roller, and rescreened.

During subsequent screening an attempt was made to obtain a good separation of the material into definite size ranges. The size ranges sought had the following Tyler mesh values: 8-10, 10-14, 14-20, 20-28, 28-35, 35-48, 48-65, 65-100 and less than 100. Due to the limitations of the screening equipment however, these size groups were not obtained.

Two suspensions were used in this investigation. The first was composed of material obtained by the above screening, in the size range 48-100 mesh, supplemented by larger material in the range 8-48 mesh. Due to inefficient screening and lengthy periods of pumping this suspension (No. 1) had the size analysis shown in Figure 19 when satisfactory data were obtained. Suspension "No. 2" was made up of a certain weight of suspension 1 and 350 lbs. of sulphur flour. The size analysis for this is also shown in Figure 19.

B. Operation of the Pipeline.

The procedure adhered to from start-up of the pilot pipeline was as follows:

1. The "Lightning" mixers were switched on and the suspension agitated until a uniform concentration had been attained.

2. The pump was switched on and the suspension circulated through the pipeline.

3. Standardization of both the potentiometers was effected and the D.C. voltage applied to the DP cell.

4. Water from the main source was flushed through the hydraulic lead lines and the DP cell to remove air bubbles and any suspension present in the pressure tappings.

5. The four-way valves were manipulated so that the pressure drop over the venturi meter could be measured. This pressure drop caused the DP cell to produce a given voltage, which was partially balanced by imposing a reverse E.M.F. from the standard potentiometer. The residual voltage was then measured by the recording potentiometer.

6. Manipulation of the four-way valves enabled the pressure drops over both of the test sections to be measured as described under section 5.

7. The flow conditions in the pipeline were changed by the adjustment of valves 1 and 2 (Figure 3) and the procedure for obtaining the pressure drops (sections 5 and 6) repeated. Conditions for a number of flow rates were measured in this manner.

When a complete series of pressure drop measurements had been made three samples were taken. These were

a) A calibrated, two gallon bucket which gave a bulk density test. This sample was returned to the supply tank.

b) Four 1 litre Erlermeyer flasks which were stoppered and kept for subsequent rheological, percent solids and size distribution tests.

c) A litre graduated cylinder from which settling data was obtained.

C. Testing Procedure on the Samples of Suspension.

Subsequent tests were carried out on the suspensions to determine the following properties:

i) density
ii) initial settling rate
iii) weight percent solids
iv) rheology
v) particle size distribution
vi) particle shape.

These tests are described below

i) Density:

The bucket containing sample (a) was weighed and, as the volume was known, the density could be obtained directly.

ii) Initial Settling Rate:

A stopwatch was used to determine the rate of fall of the

clear water suspension interface in a litre graduated cylinder (sample c).

iii) Weight Percent Solids:

One of the samples collected in a litre Erlermeyer flask was transferred to a beaker of known weight and weighed. The sample was placed in a drying oven and left until no further loss in weight was observed. The weight of the beaker and dry sample was then taken.

iv) Rheological Properties:

A concentric cylinder rotational viscometer was used to determine the rheological properties of the sulphur-water suspensions. The particular model used, illustrated in Figures 7 and 8, was the "Fann V-G Meter" (Model 35) manufactured by the Fann Instrument Corporation, Houston, Texas.

Fluid is contained in the annular space between two coaxial cylinders. The annular space is filled to a predetermined height with the fluid to be tested. The outer cylinder, or rotor, suspended in a precision bearing, is driven at a constant rotational speed and the torque, arising from the viscous drag of the fluid, is exerted on the inner cylinder, or bob. The torque is rapidly balanced by a helically wound spring. The deflection of the spring, which is proportional to the torque, is read on a calibrated dial through an optical reticule.

In this viscometric method the flow data are analysed in terms of the fundamental relationship between shear rate, proportional

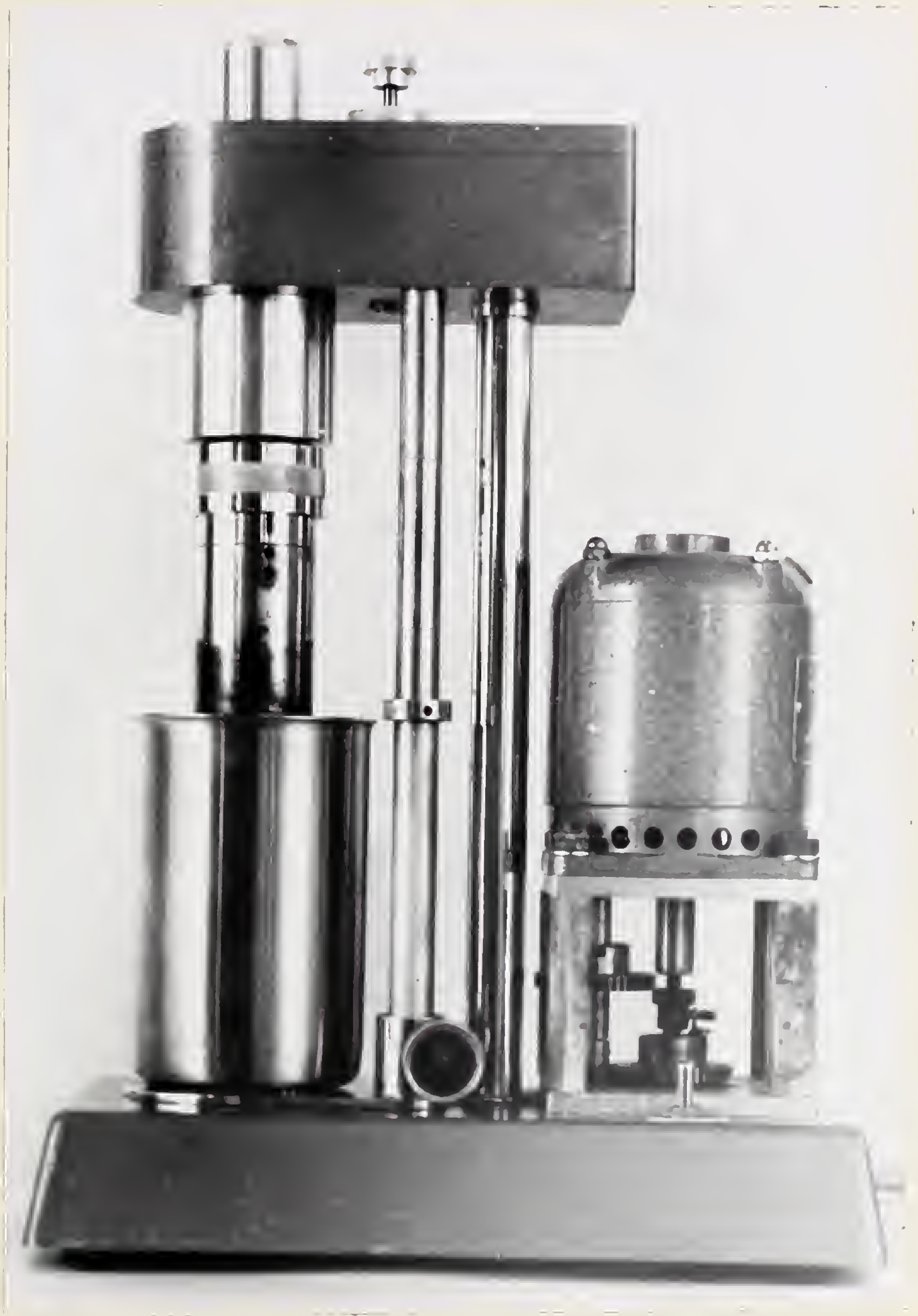

Fig. 7. Modified Fann Viscometer

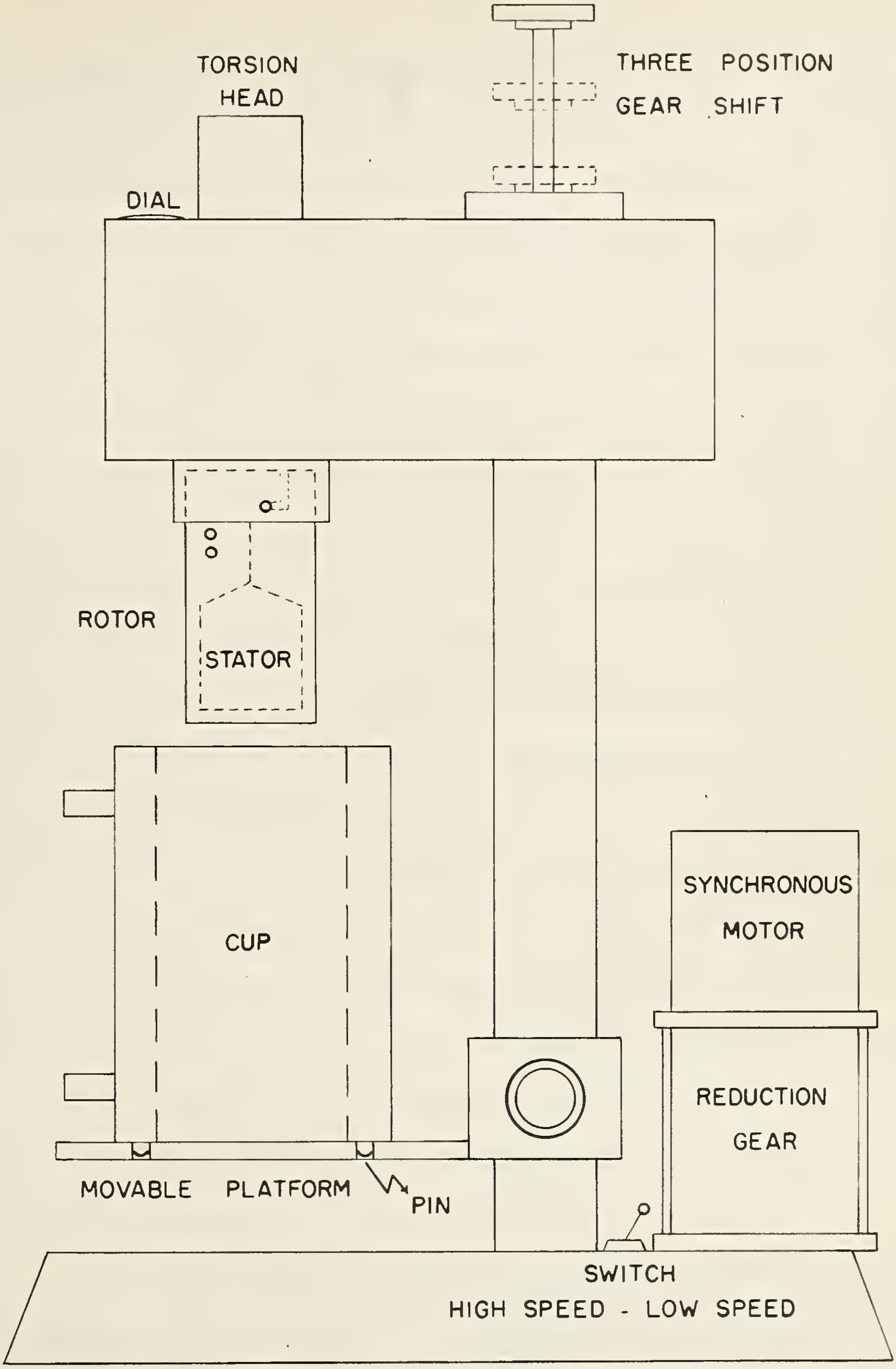

Fig. 8. Diagram of Fann viscometer

to rotor speed, and shear stress, proportional to the dial reading. The cylindrical rotor and bob design permits calculation of the shear rate corresponding to each rotational speed. The shear stress is only obtainable by calibration of the instrument with a Newtonian fluid of known viscosity. Careful calibration of the instrument was carried out separately by Lindley (14) and by Hahn (11), the calibration factor found by these workers being used in this investigation. This calibration factor was checked using one standard oil. Hahn also found that, at low values of dial reading, a correction had to be applied to this calibration. The correction curve is included in Appendix B.

The Fann viscometer is a commercial instrument; it is reasonably accurate and simple to operate. Rotor speed changes for 3, 6, 100, 200, 300 and 600 R.P.M. are effected smoothly and rapidly without stopping rotation. This is achieved by the use of a three position gear shift in conjunction with a two position switch controlling the motor speed. The rotor is driven by a 115 volt 50 cycle dual speed synchronous motor. In the standard model the sample being tested is placed in a stainless steel cup, the base of which is equipped with pins to locate and to lock to a platform. This platform can be moved vertically on sliders. The rotor and bob may be detached from the main body of the instrument for cleaning.

One modification was made to the standard model in order to allow further rheological data to be obtained. This modification was

the interposing of a 9:1 reduction gear between the synchronous motor and the body of the instrument. This resulted in the instrument being capable of producing twelve different shear rates ranging from approximately 1000 reciprocal seconds to 1/2 reciprocal second.

A sample of the suspension was placed in a 600 ml. beaker and stirred vigorously using an electric mixer. The beaker was placed upon the movable platform of the viscometer and the platform raised until the rotor and enclosed stator were submerged to the depth indicated by a mark etched on the rotor. The motor was started and a torque, arising from the viscous drag of the fluid on the bob, was balanced by the helically wound suspension spring. After the instrument was started the dial reading was observed to rise to a maximum. This maximum dial reading and the rotor speed were noted. The motor was stopped, the sample lowered and the rotor removed. Careful cleaning of both the rotor and the stator was effected and the instrument reassembled. This procedure was repeated three times for each rotor speed, an average value of the three deflections being recorded and used to calculate the shear stress.

The number of shear stress determinations carried out on a given suspension was dependent upon the magnitude of the dial reading at low shear rates. Consequently for suspensions having low percent solids content the only meaningful data were obtained at shear rates in the range from 200-1000 reciprocal seconds, whereas, at high percent solids concentrations, readings could be obtained in the range from 5-1000 reciprocal seconds.

All the rheological data given in Appendix B were determined as described above.

v) Particle Size Distribution:

A sample of the suspension was weighed then wet sieved, using water, through the following Tyler standard mesh sieves: 20, 28, 35, 48, 65, 100, 150, 200, 230, 270, 325 and 400, all of known weight. The sieves and samples were dried and then shaken on an electric shaker to ensure a complete separation. Each sample was then weighed while still on the sieve. The weight of particles less than 400 mesh was obtained by difference.

vi) Particle Shape:

Two photomicrographs were obtained using a Reichart Metallograph. One was at 70 magnifications and was of particles in the size range 210-74 microns, the other was at 140 magnifications and was of particles in the size range smaller than 74 microns.

EXPERIMENTAL RESULTS

The experimental results are presented under two headings:

I Pipeline Flow Data

II Properties of the Suspensions

I Pipeline Flow Data

The results of the preliminary test on the single phase flow of water are presented (Figure 9) in the form of the conventional plot of friction factor versus Reynolds number. The experimental data show good agreement in the turbulent region with the Karman-Nikuradse line. Because of the good agreement, it is concluded that the calibrations of the venturi meter and the DP cell were accurate, and that the auxiliary equipment was functioning properly. The data for this test are tabulated in Appendix C, Table 1C.

The results of the pipeline flow tests, using sulphur - water suspensions 1 and 2, are presented in Figures 10 to 17. These are plots of friction factor versus a modified Reynolds number (Re_W). This modified Reynolds number is based upon the density of the flowing fluid and the viscosity of water at the pipeline conditions. The numerical data are tabulated in Appendix C. Tables 1C and 2C.

Each of these curves show two distinct portions:

1. At high Reynolds numbers the curve is approximately parallel to but displacedupwards from the Karman-Nikuradse line for single phase fluids. It is apparent that, for both suspensions, the

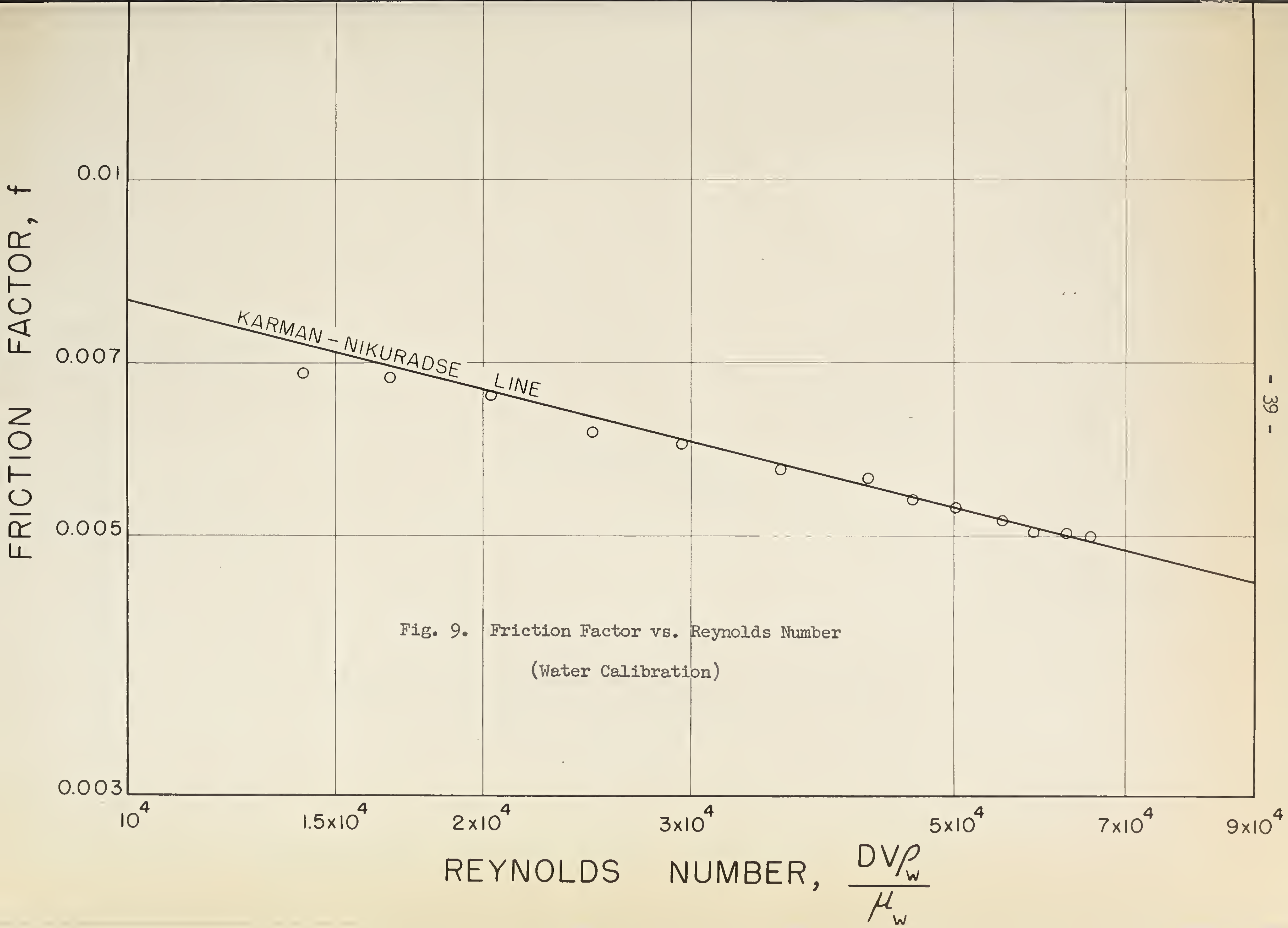

Fig. 9. Friction Factor vs. Reynolds Number

(Water Calibration)

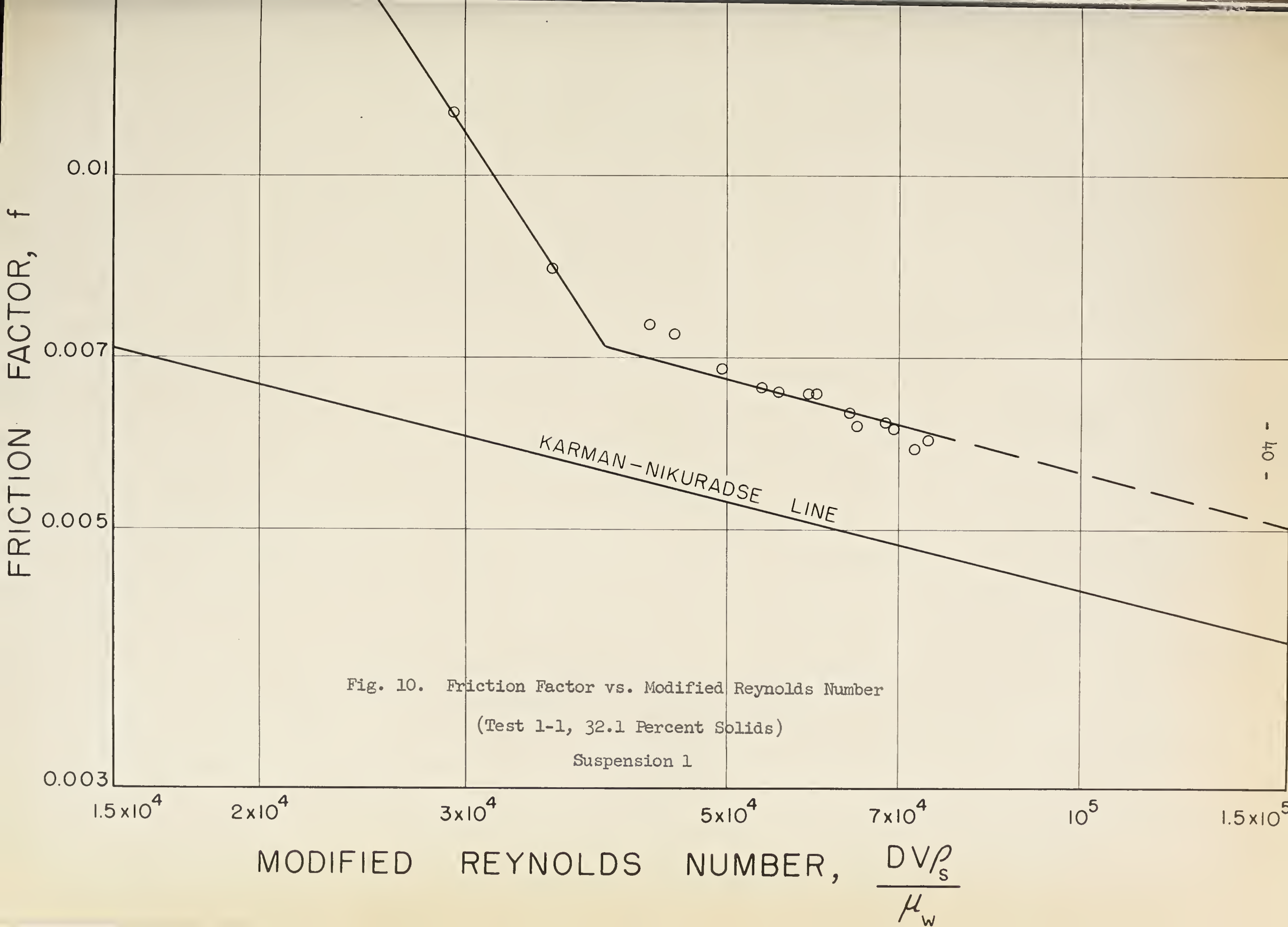

Fig. 10. Friction Factor vs. Modified Reynolds Number

(Test 1-1, 32.1 Percent Solids)

Suspension 1

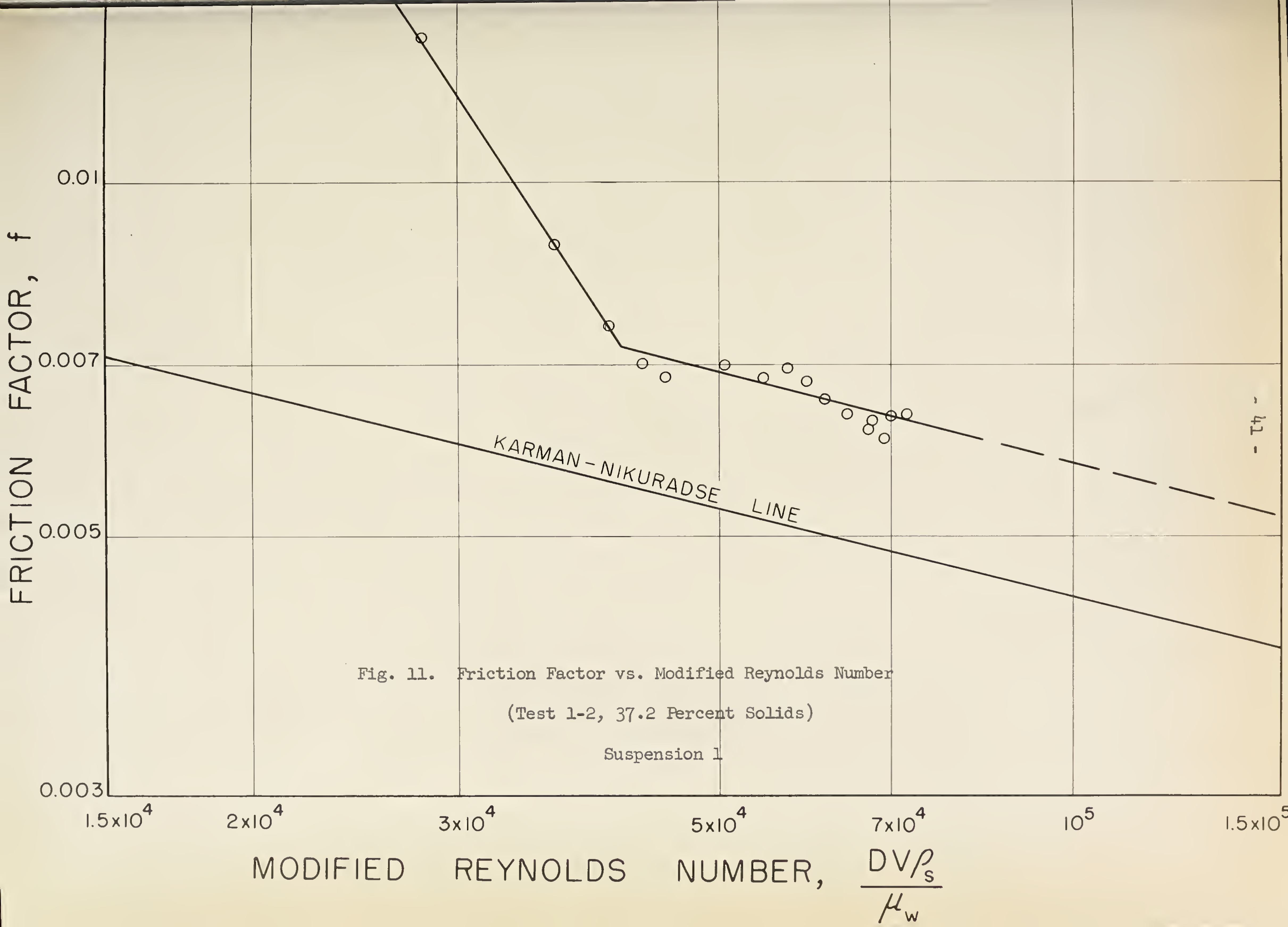

Fig. 11. Friction Factor vs. Modified Reynolds Number

(Test 1-2, 37.2 Percent Solids)

Suspension 1

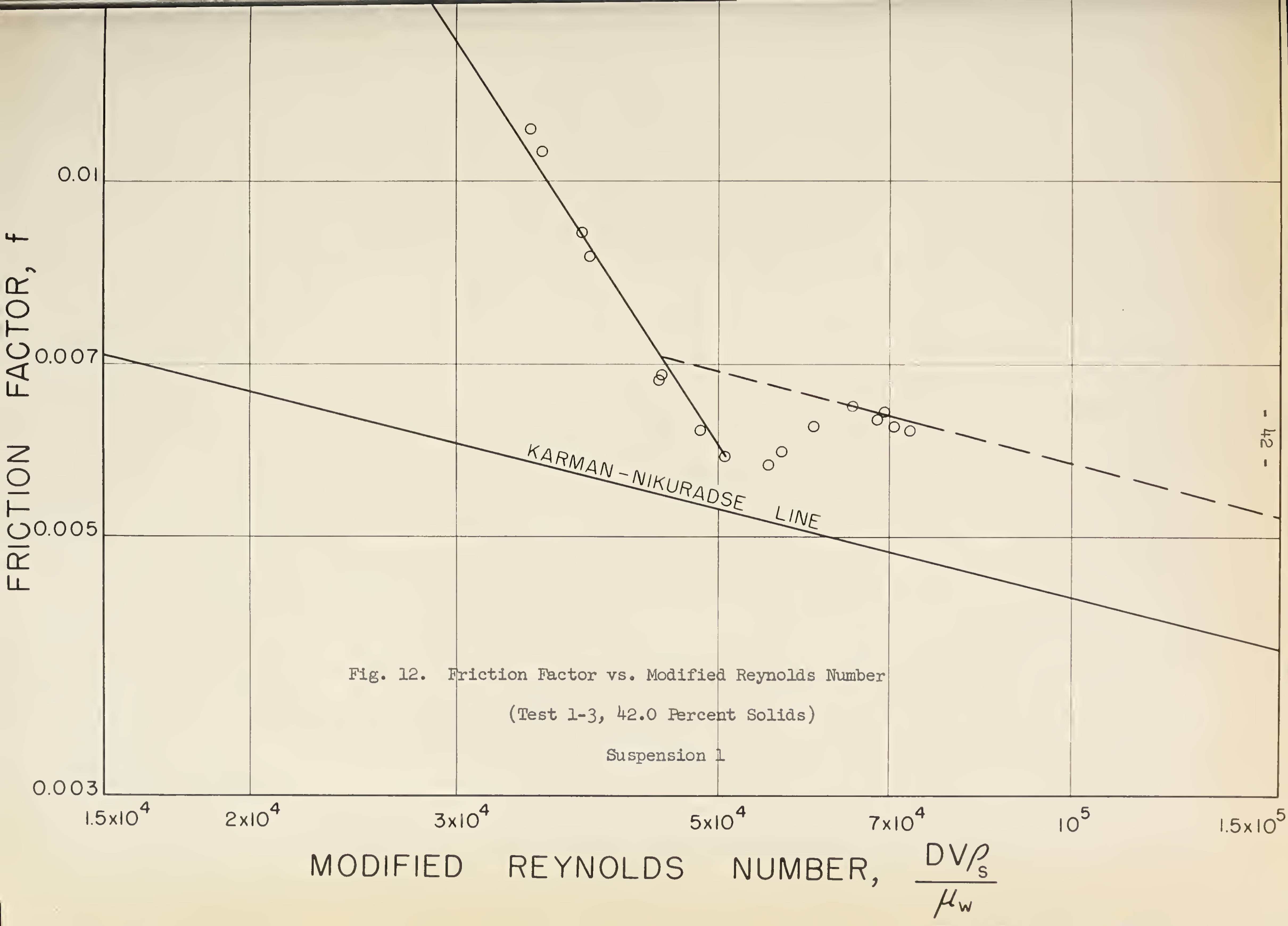

Fig. 12. Friction Factor vs. Modified Reynolds Number

(Test 1-3, 42.0 Percent Solids)

Suspension 1

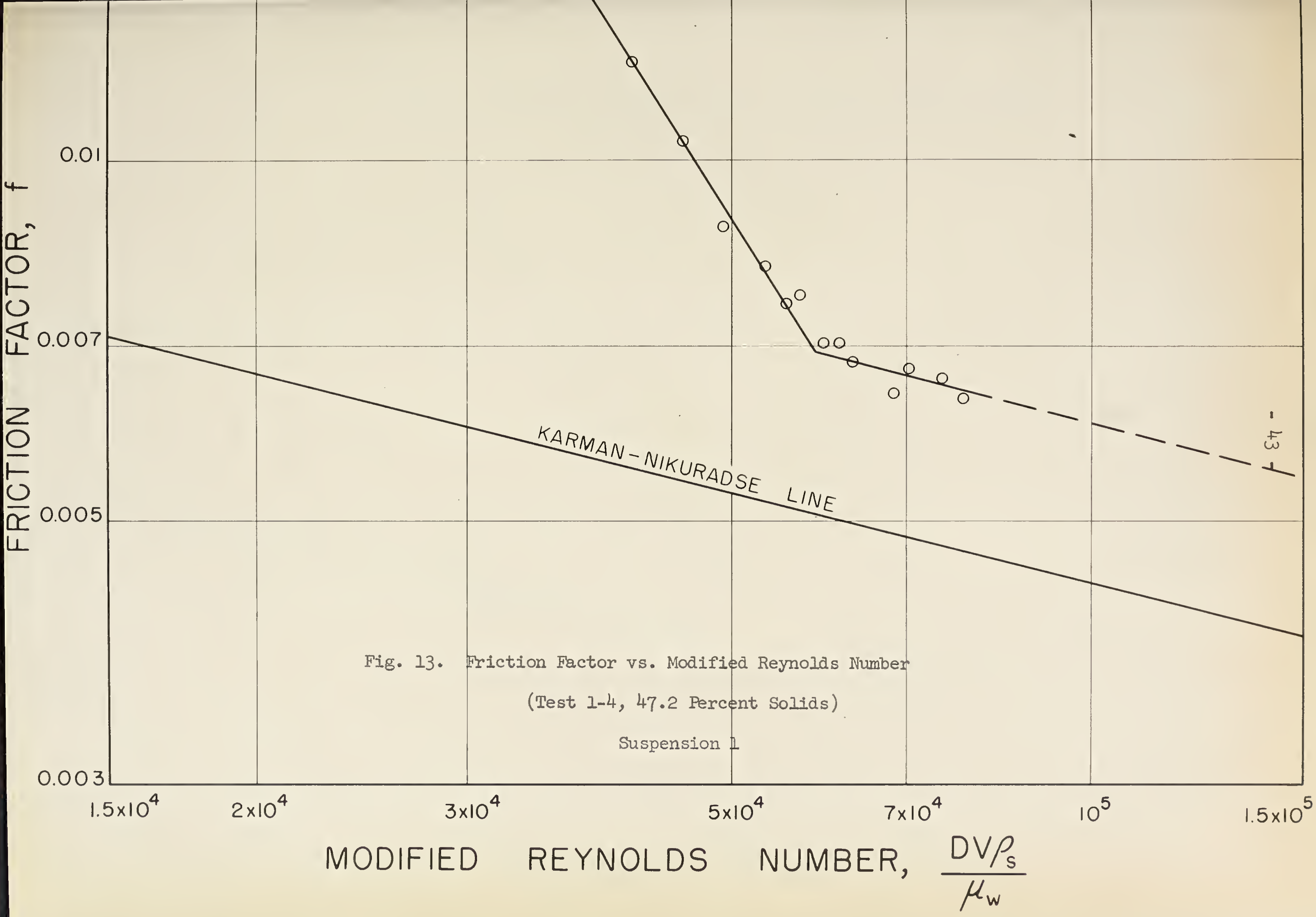

Fig. 13. Friction Factor vs. Modified Reynolds Number

(Test 1-4, 47.2 Percent Solids)

Suspension 1

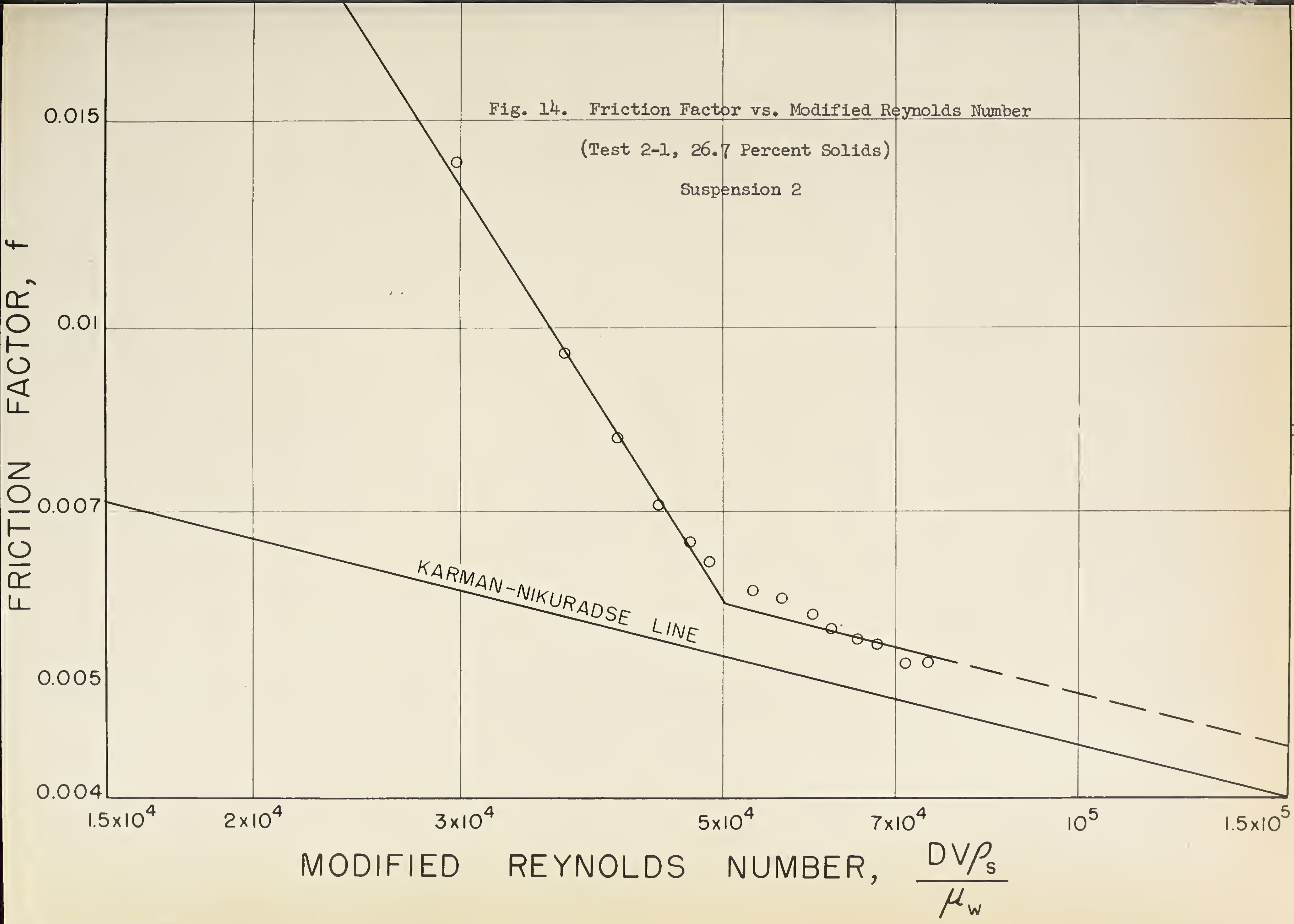

Fig. 14. Friction Factor vs. Modified Reynolds Number

(Test 2-1, 26.7 Percent Solids)

Suspension 2

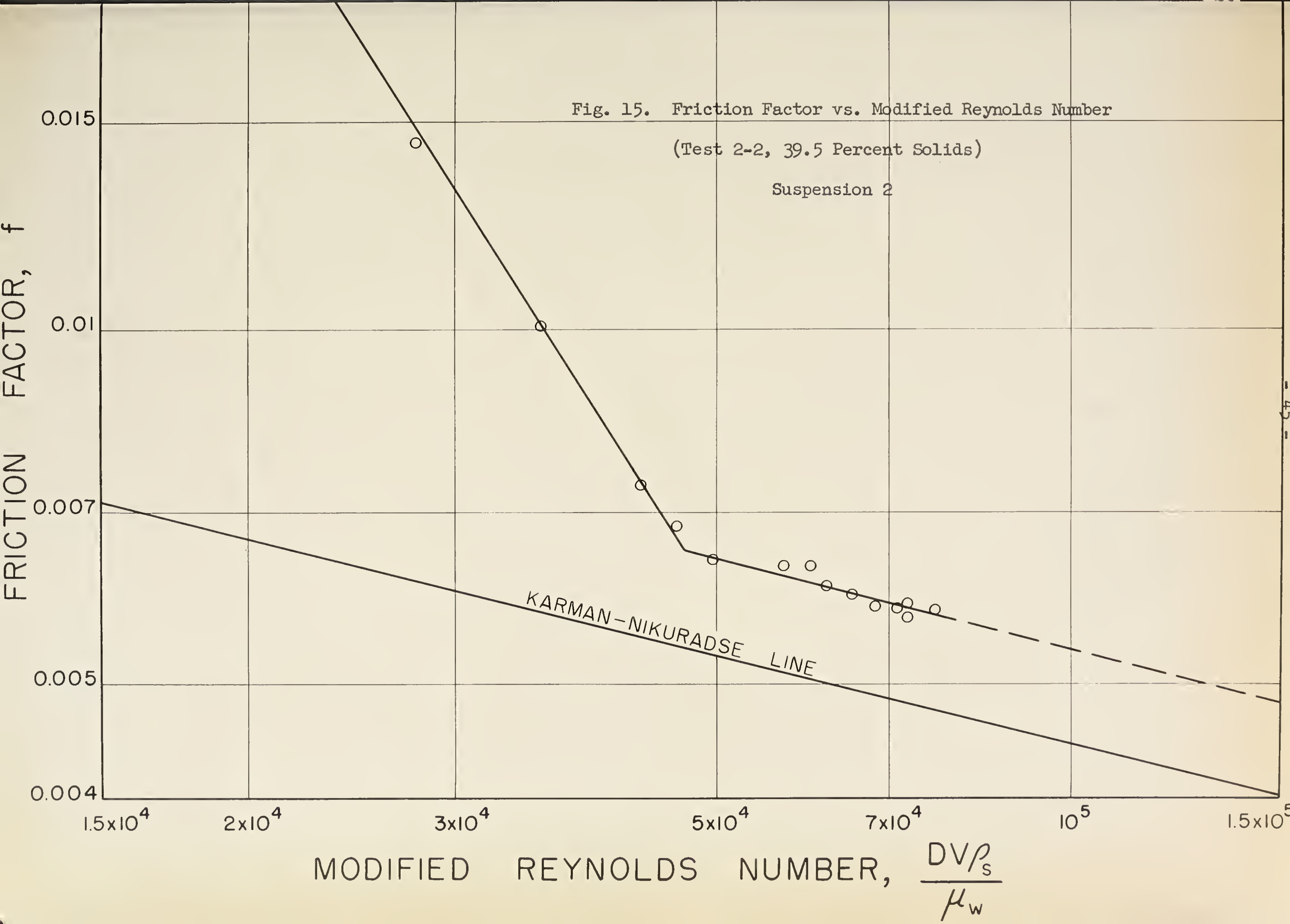

Fig. 15. Friction Factor vs. Modified Reynolds Number

(Test 2-2, 39.5 Percent Solids)

Suspension 2

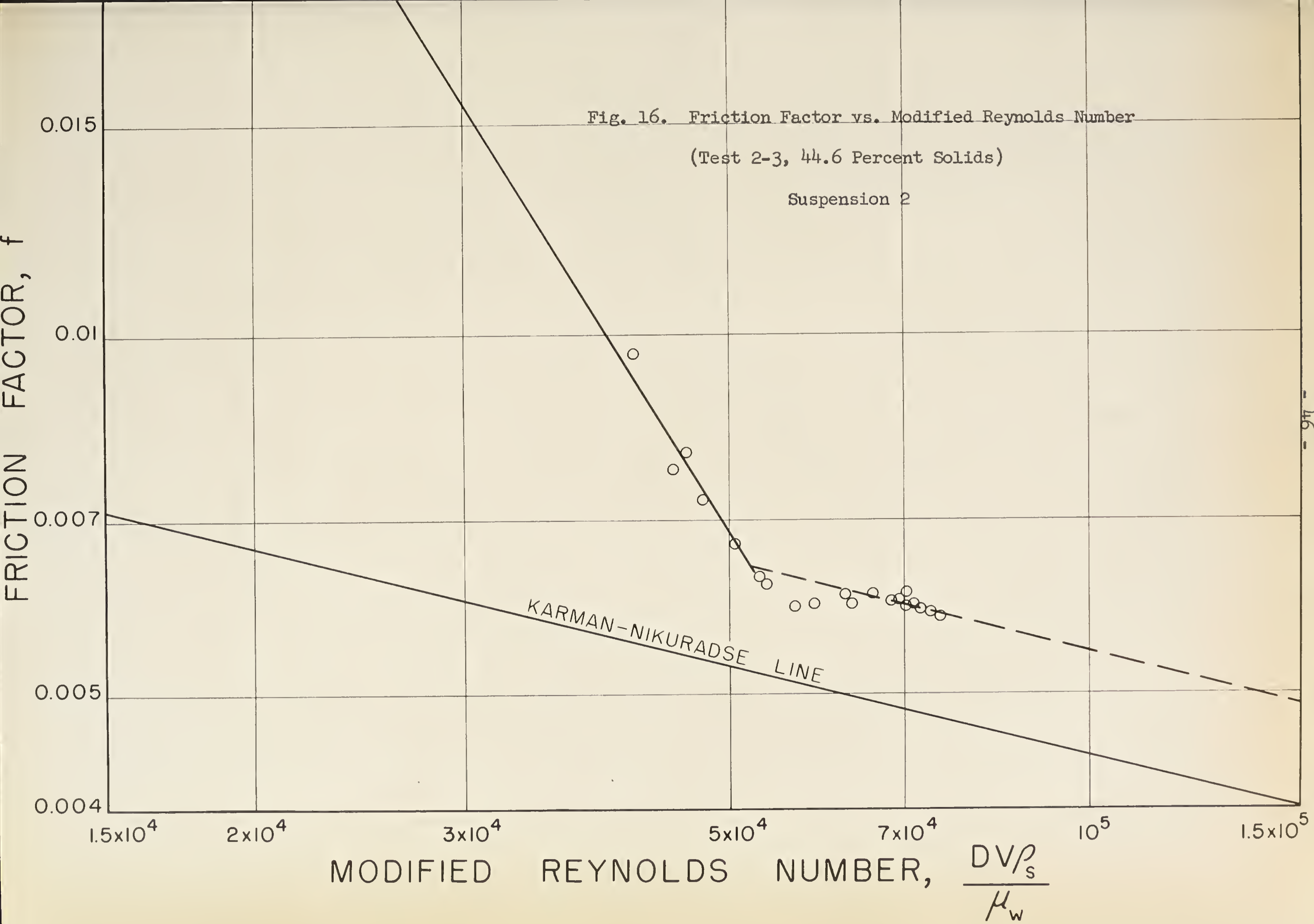

Fig. 16. Friction Factor vs. Modified Reynolds Number

(Test 2-3, 44.6 Percent Solids)

Suspension 2

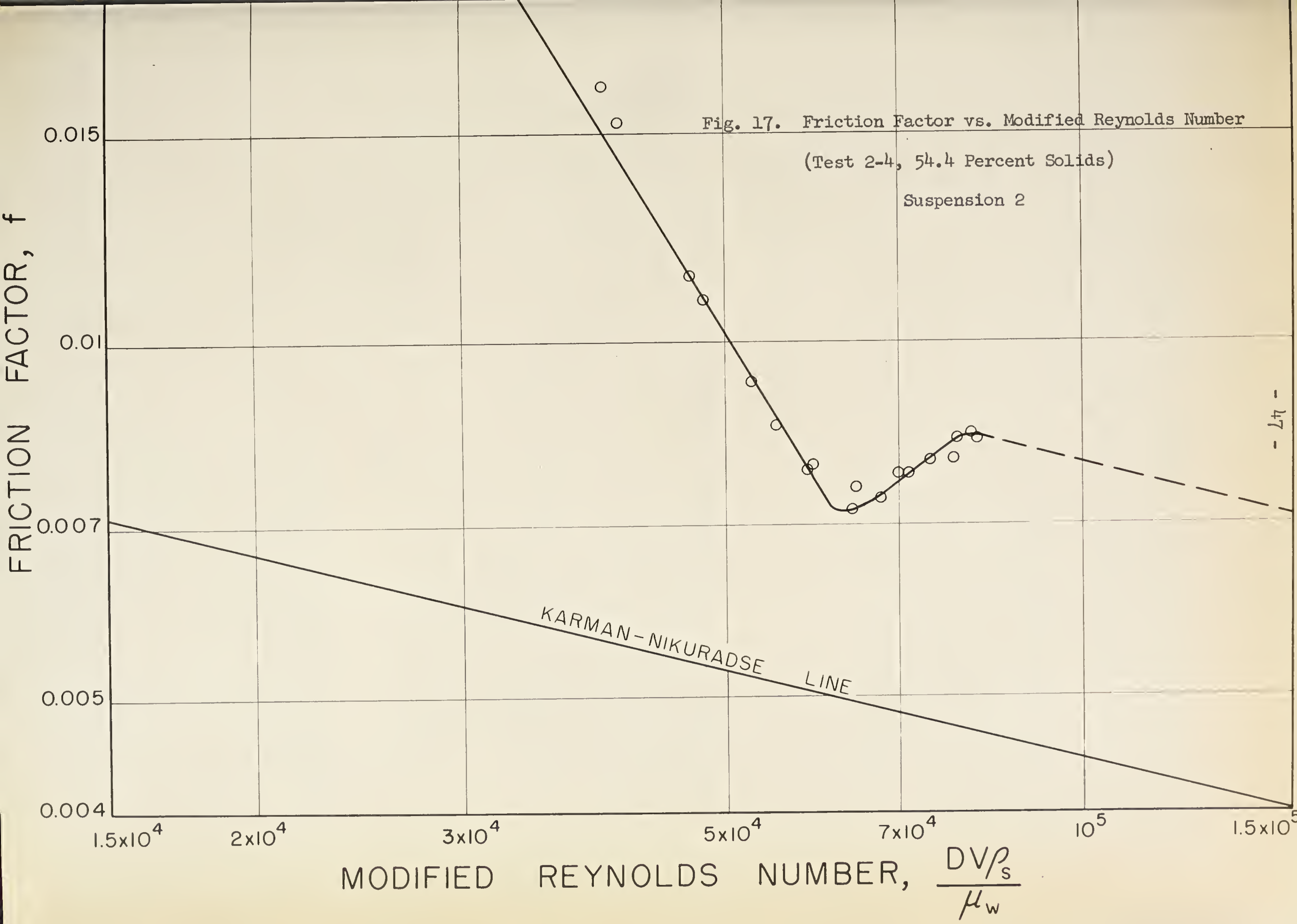

Fig. 17. Friction Factor vs. Modified Reynolds Number

(Test 2-4, 54.4 Percent Solids)

Suspension 2

separation between the experimental and theoretical curves increases with increasing percent solids.

2. At lower Reynolds numbers the data fall on lines which lie at an angle of approximately 60° to the abscissa. For suspension 1 these lines are approximately parallel and move closer to the Poiseuille line as the percent solids decreases. For suspension 2 there is a definite tendency for the slopes to become less as the percent solids decreases.

II Properties of the Suspensions

a) Density:

The results of the density determinations on the suspensions are given in Appendix F, Table 1F. These data are plotted in Figure 18 as specific gravity versus weight percent sulphur, a comparison being made with values calculated assuming a specific gravity of 2.05 for sulphur, zero solubility and additive volumes. There is satisfactory agreement between the experimental and calculated data. The small displacement could be due to air entrained, the presence of solid impurities in the suspension or a discrepancy in the value assumed for the specific gravity of the sulphur.

b) Particle Size Distribution:

Figure 19 is a plot, on logarithmic - probability co-ordinates, of particle size versus percent solids passing a given micron size.

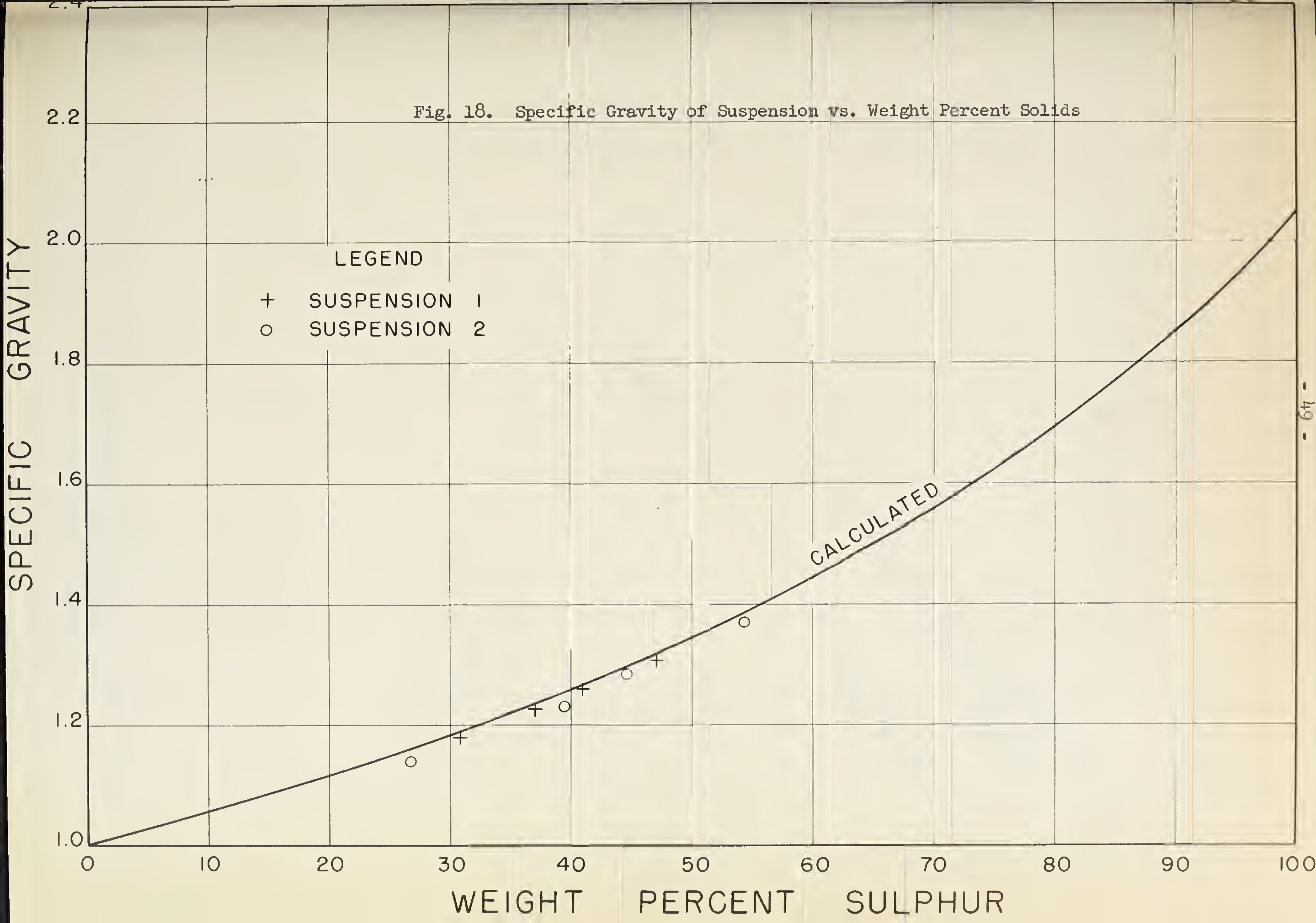
Fig. 18. Specific Gravity of Suspension vs. Weight Percent Solids

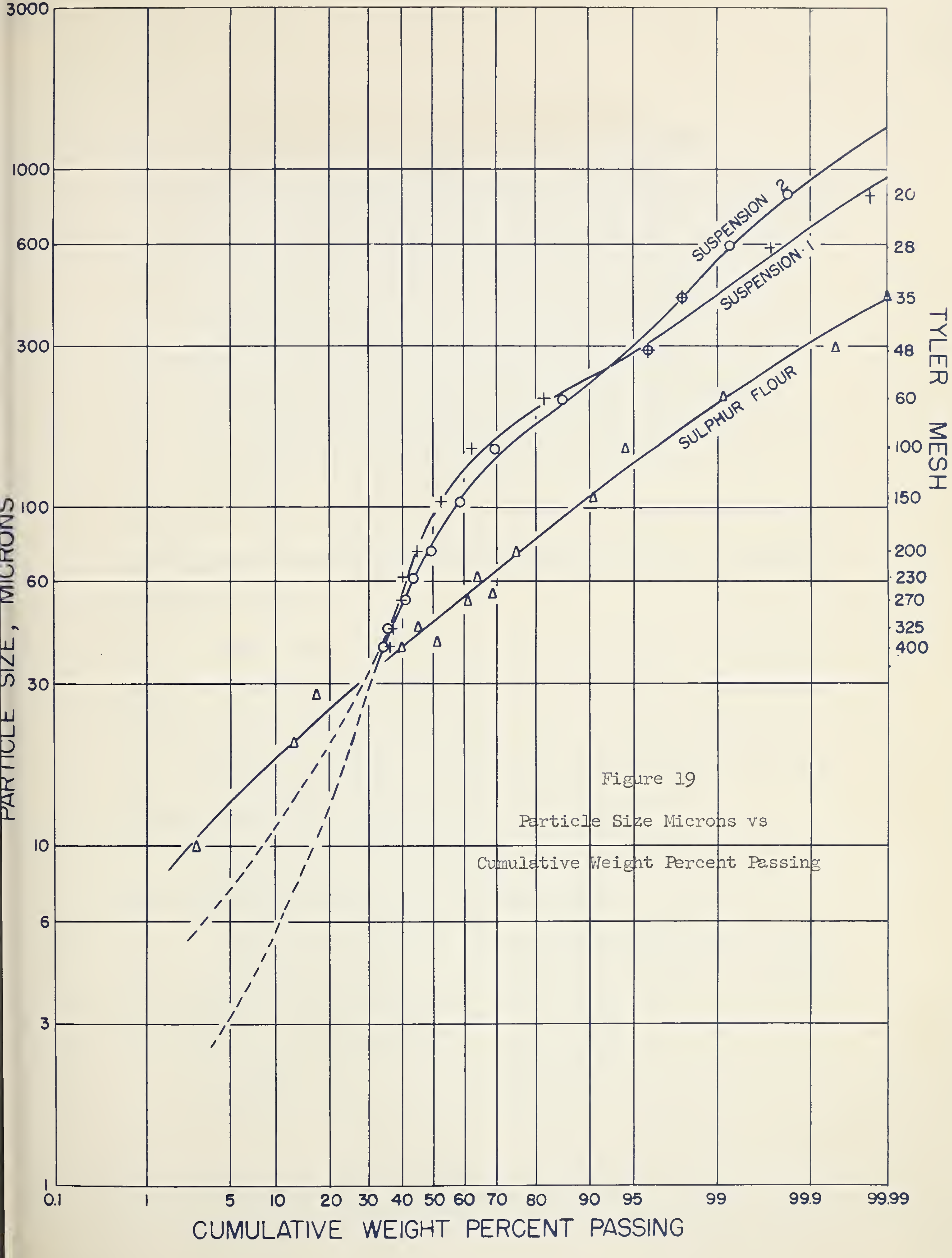

Figure 19

Particle Size Microns vs

Cumulative Weight Percent Passing

Curves are presented for the two suspensions on which flow tests were made and for the sulphur flour used as an ingredient in Suspension 2. Unfortunately the size analyses of the suspensions were terminated at 400 mesh and the samples were destroyed before it was realized that size analysis to smaller diameters was important. The curves, representing the size analyses below 400 mesh (37 microns) are estimated but are thought to be realistic. The size distribution curves are of abnormal shape reflecting the synthesis of the mixture and the degradation by attrition. Suspension 2 is coarser than suspension 1 in the first 40 percent fraction, slightly finer in the next 50 percent fraction and coarser in the last 10 percent fraction.

c) Particle Shape:

Figure 20A is a photomicrograph of particles in the size range 65 to 200 mesh for suspension 2, the separation being obtained by wet sieving a sample of suspension. The uniformity in the size of the particles is apparent, this is an indication that the sieving procedures employed were efficient.

Figure 20B is the photomicrograph of particles in the size range less than 200 mesh, also for suspension 2.

All particles appear to have a fairly uniform shape being rounded with few sharp edges. This rounding of the edges is probably due to attrition during pumping.

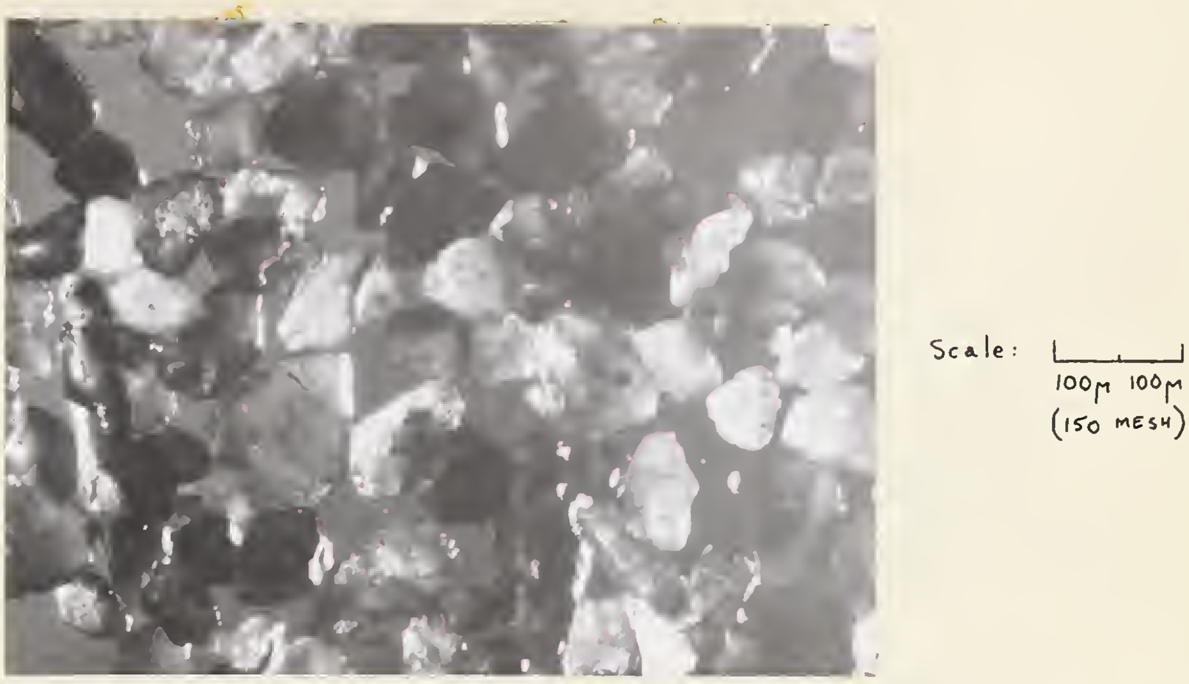

Fig. 20A. Photomicrograph of Sulphur Particles in Size Range 65-200 Mesh (x 70 Magnifications)

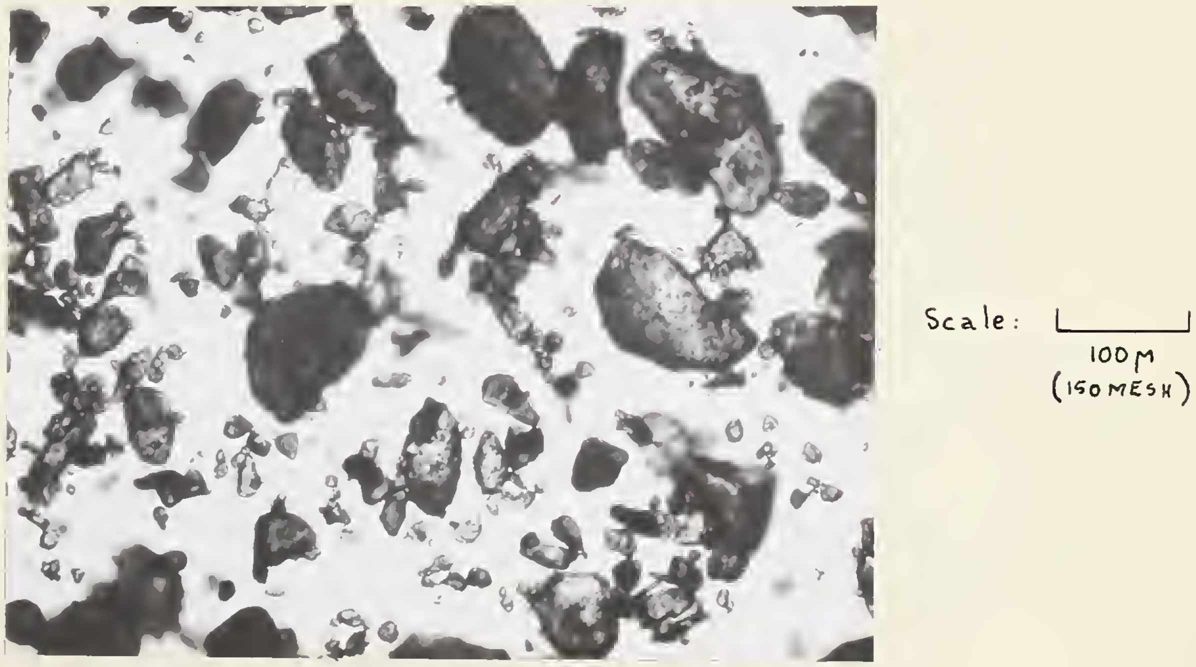

Fig. 20B. Photomicrograph of Sulphur Particles in Size Range Smaller Than 200 Mesh (x 140 Magnifications)

d) Initial Settling Rates:

The initial settling rates of the two suspensions were obtained by extrapolating the observed settling rate data to zero time. Figure 21 shows this extrapolated initial settling rate plotted against weight percent solids. The data are shown extrapolated to zero percent solids, the free falling velocity of the largest particle is the value used, this was obtained from the Stokes equation.

Settling rates for suspension 1 are much less than for suspension 2 at the same weight percent solids. This agrees with the size analyses which show that suspension 1 contains more fine particles than suspension 2. Thus suspension 1 would be expected to have a higher apparent viscosity. The initial settling rates are tabulated in Appendix F, Table 1F.

e) Rheological Properties:

The experimental data from the viscometer tests are tabulated in Appendix B, Table 1B. Initially these data were plotted as dial reading versus revolutions per second. The Krieger-Maron equation (Equation 50) was used to determine the shear rates, the value of the slope (n") being found from a smoothed plot of n" versus revolutions per second. The values of the terms in Equation 50 and the final shear rates at the wall of the stator are tabulated in Appendix A, Table 1A. The shear stress was obtained from Equation 45 using the value of the

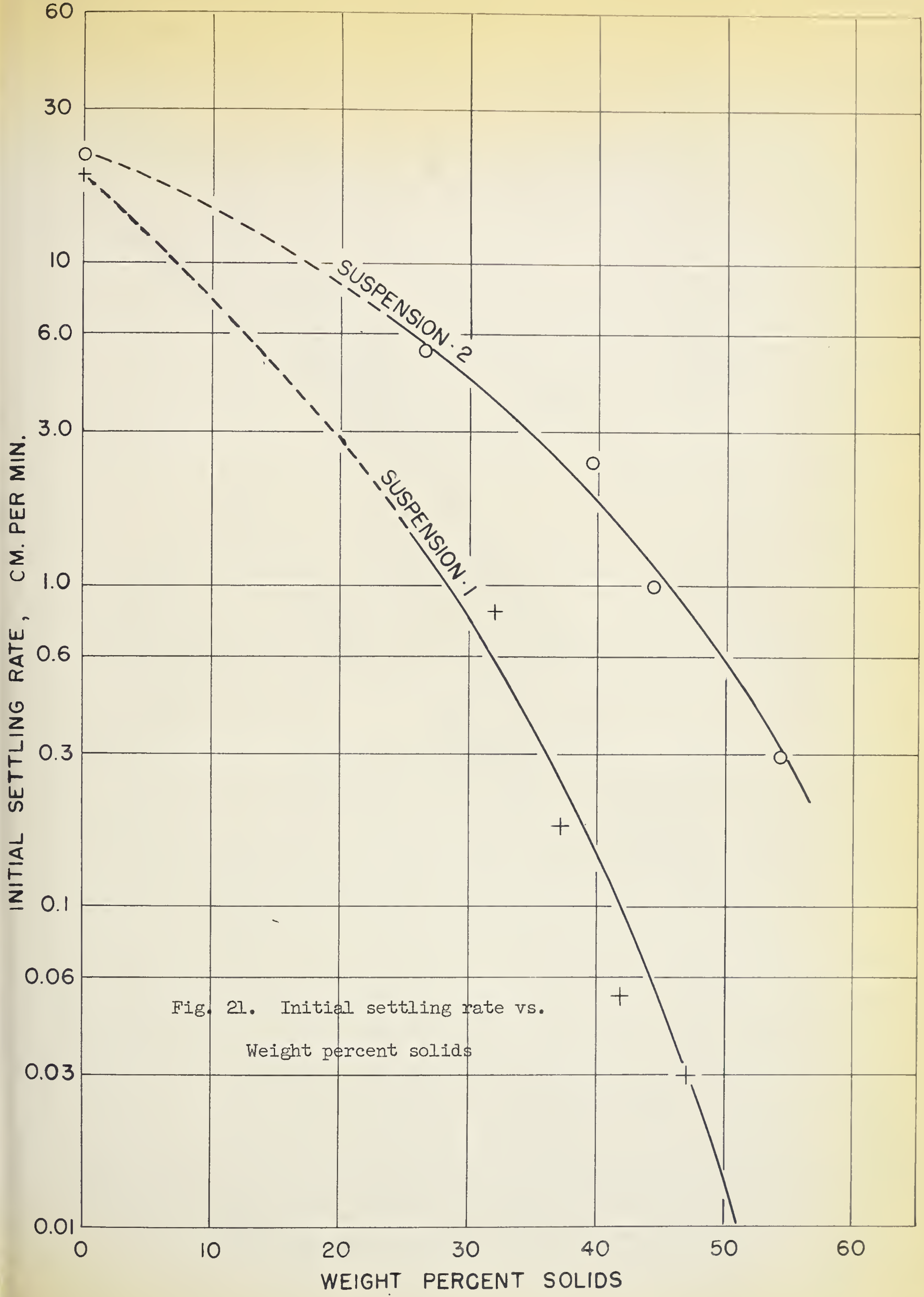

Fig. 21. Initial settling rate vs. Weight percent solids

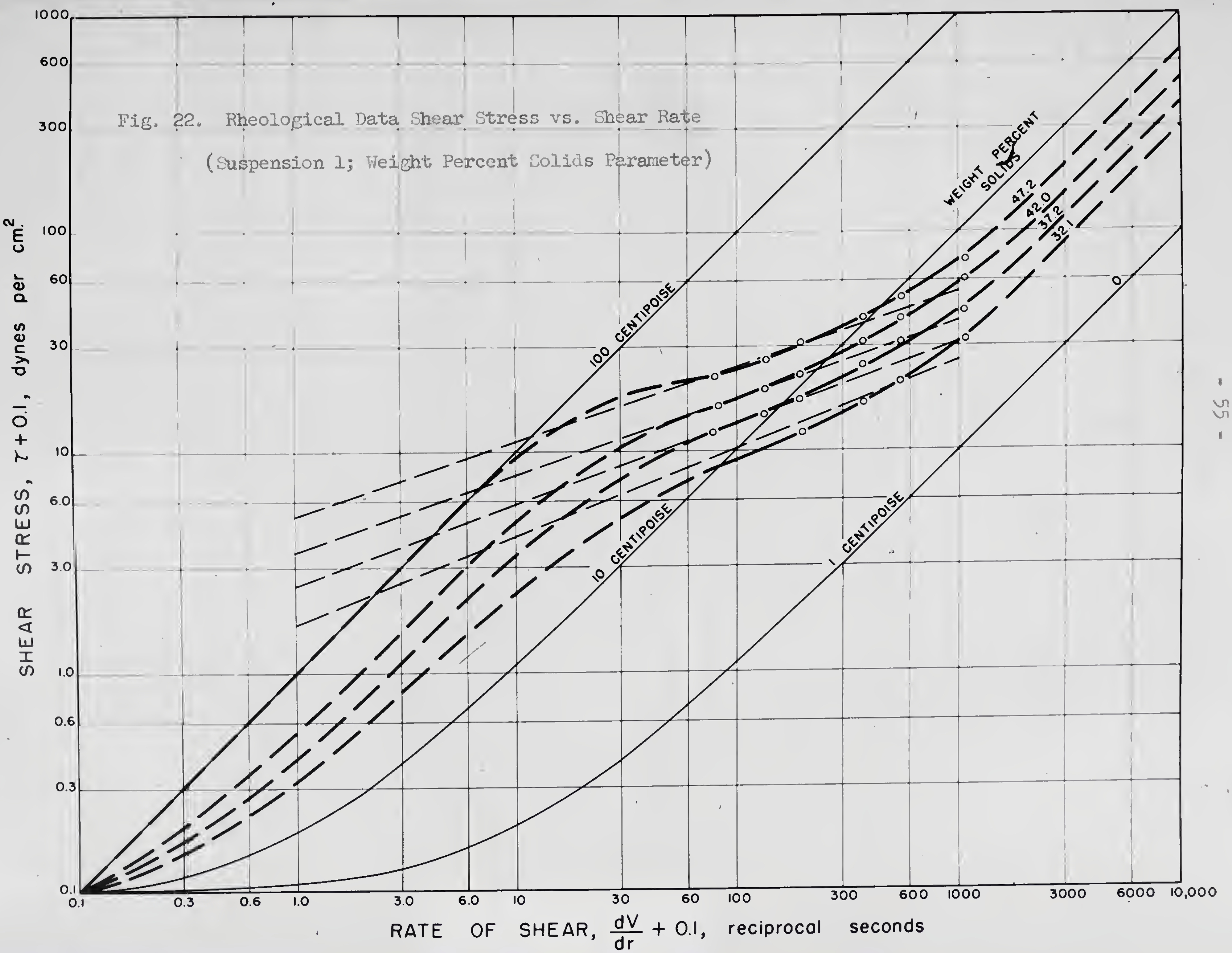

Fig. 22. Rheological Data Shear Stress vs. Shear Rate

(Suspension 1; Weight Percent Solids Parameter)

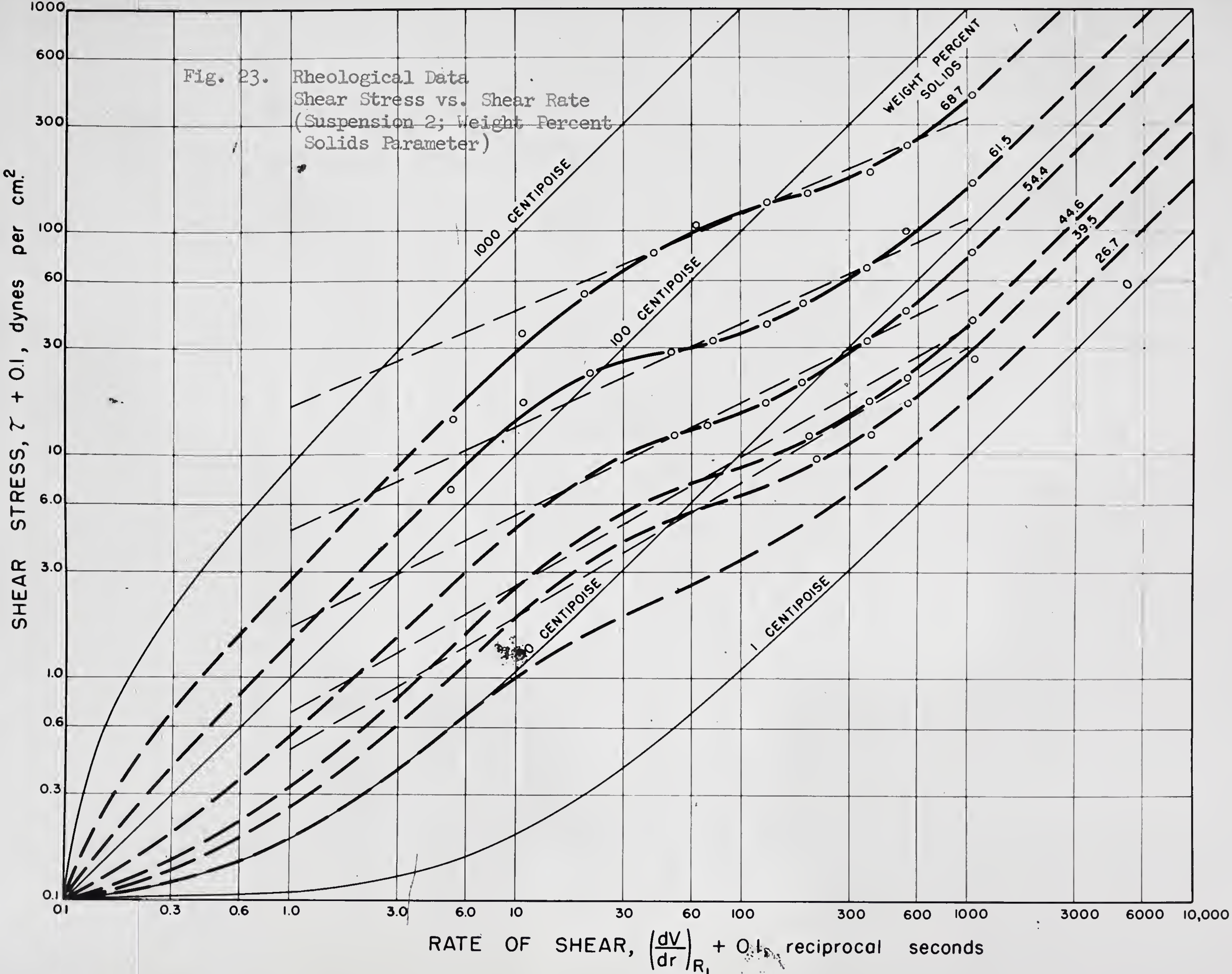

Fig. 23. Rheological Data
Shear Stress vs. Shear Rate
(Suspension 2; Weight Percent
Solids Parameter)

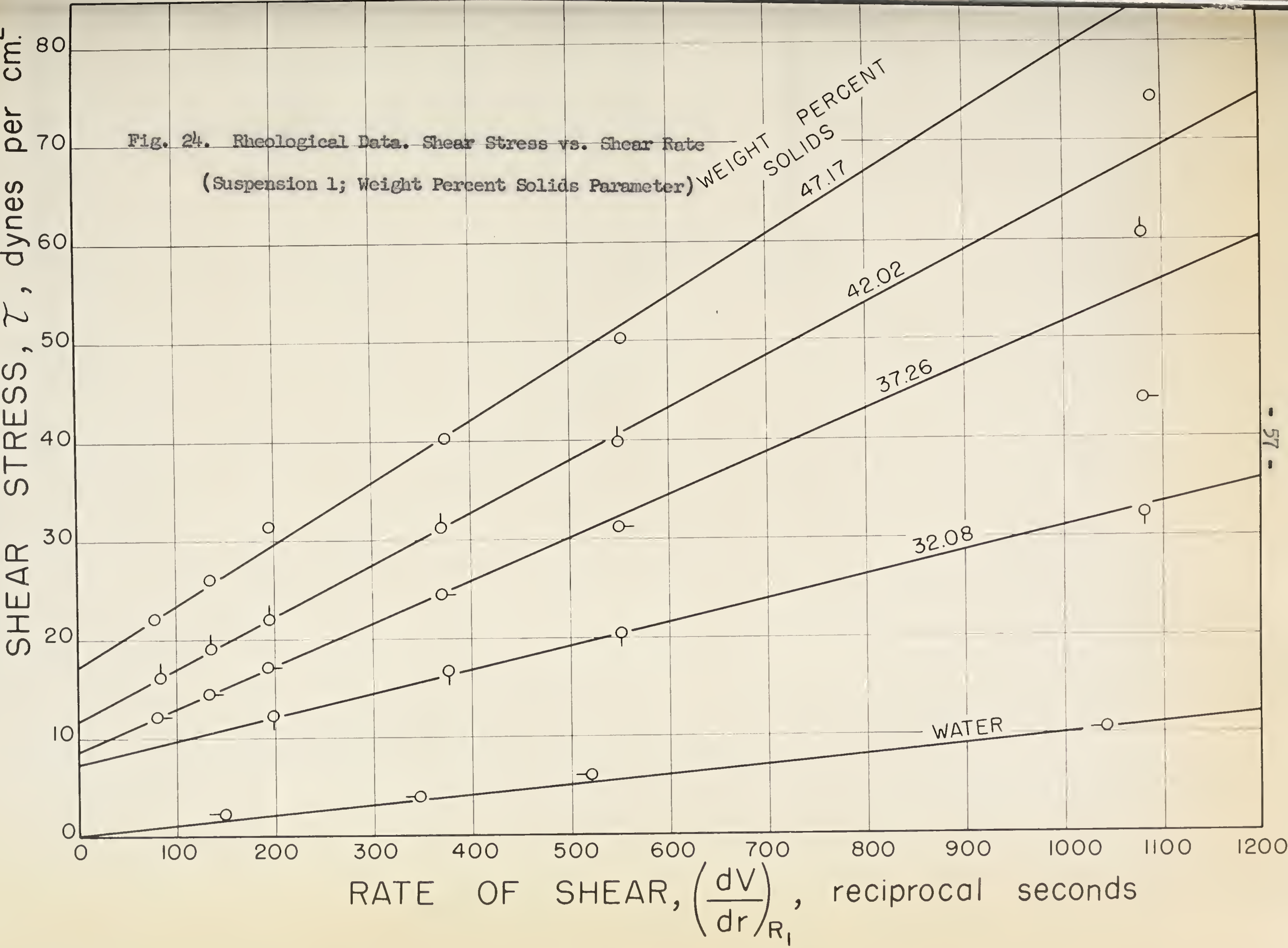

Fig. 24. Rheological Data. Shear Stress vs. Shear Rate

(Suspension 1; Weight Percent Solids Parameter)

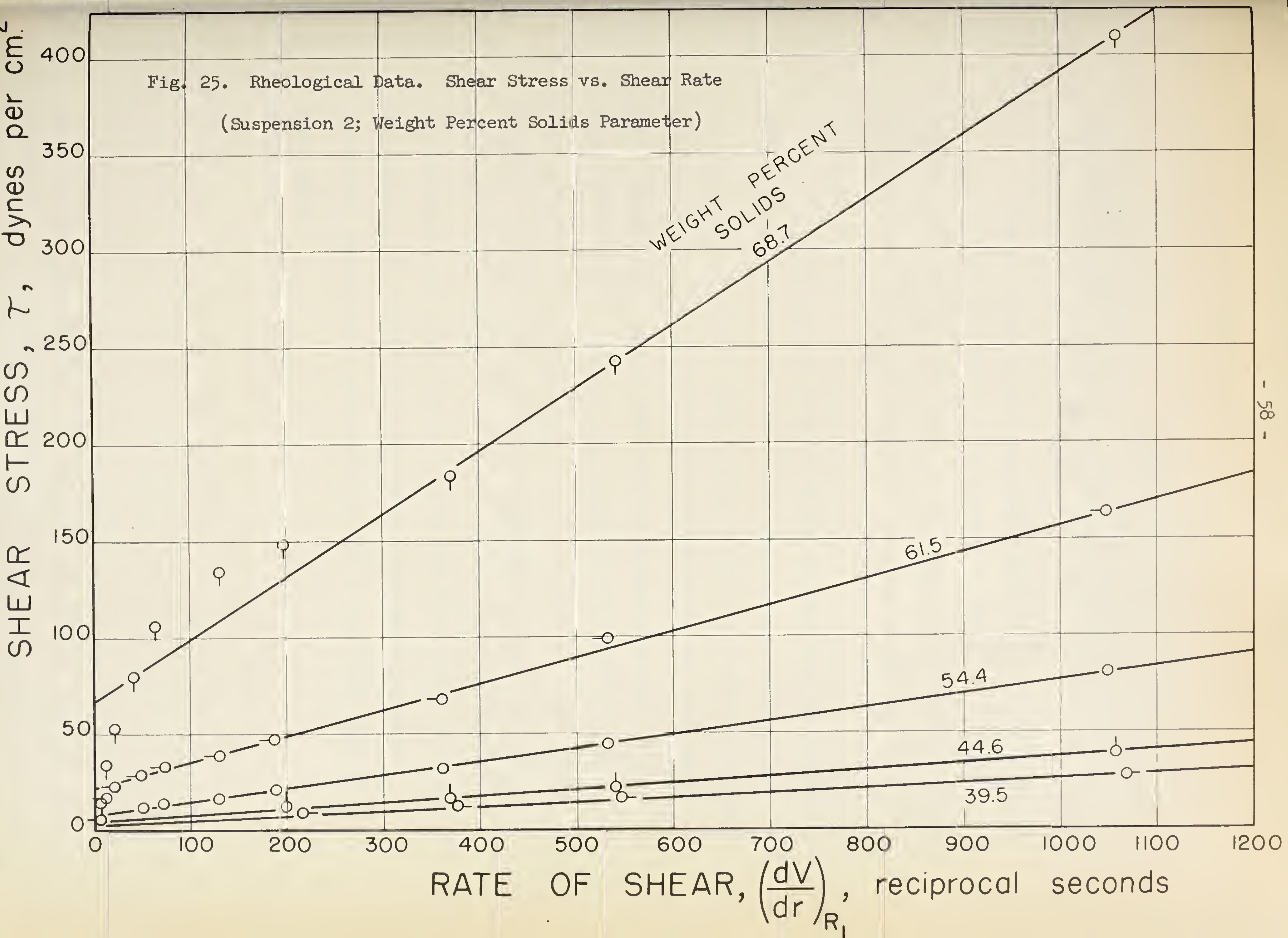

Fig. 25. Rheological Data. Shear Stress vs. Shear Rate

(Suspension 2; Weight Percent Solids Parameter)

calibration constant determined by Lindley (14) and Hahn (11), and the adjustments to this found by Hahn.

Figures 22 and 23 are logarithmic plots of shear stress versus shear rate for the data tabulated in Appendix B, Table 1B. A small constant has been added to the ordinates and abscissa so that the lines can be extrapolated to zero. Figures 24 and 25 are arithmetic plots of the same data.

The data indicate (Figures 22 and 23) that both the suspensions had complex rheological behavior. Shear stresses were obtained for several shear rates in the range between 70 and 1100 reciprocal seconds. No indication of yield stresses were obtained during the tests which suggested that the materials were not true Bingham-plastics. Figures 24 and 25, however, do suggest near Bingham-plastic behavior. Thus two interpretations are reasonable, first that of near Bingham-plastic behavior, and second that of complex pseudoplastic behavior. The heavy dashed lines on Figures 22 and 23 indicate the pseudoplastic interpretation with extrapolation to lower and higher rates of shear. Also shown on the figures are light dashed lines which represent "power-law" pseudoplastic interpretation over a restricted range of shear rates.

INTERPRETATION OF THE PIPELINE FLOW DATA

I Interpretation Assuming Bingham-Plastic Behavior

For interpretation of the flow data by the nearest equivalent Bingham-plastic two physical properties were obtained from the rheological data. These two properties were the apparent coefficient of rigidity (η_a) and the apparent yield stress ($^{T}y_{a}$).

Figure 26 is a semi-logarithmic plot of apparent coefficient of rigidity, in centipoise, versus weight percent solids. The curves are extrapolated to zero percent solids as the viscosity of water is known accurately at 70°F. The coefficients of rigidity, at different percent solids, were obtained by extrapolation of the rheological curves to straight lines at shear rates greater than 1200 reciprocal seconds.

In the determination of $^{T}y_{a}$ the shear stress was obtained for two values of shear rate at each percent solids concentration. $^{T}y_{a}$ was found by substitution of these values of shear stress and shear rate in Equation 2. This resulted inpairs of points, these are shown joined by dotted lines in Figure 27 which is a semi-logarithmic plot of apparent yield stress versus weight percent solids. The extrapolation to zero percent solids is again indicated as the yield stress of water is zero.

Using the values of η_a and $^{T}y_{a}$ taken from Figures 26 and 27 the values of the dimensionless ratios R_{m_a} (Equation 18) and Y_a (Equation 19), the apparent Bingham Reynolds number and the apparent

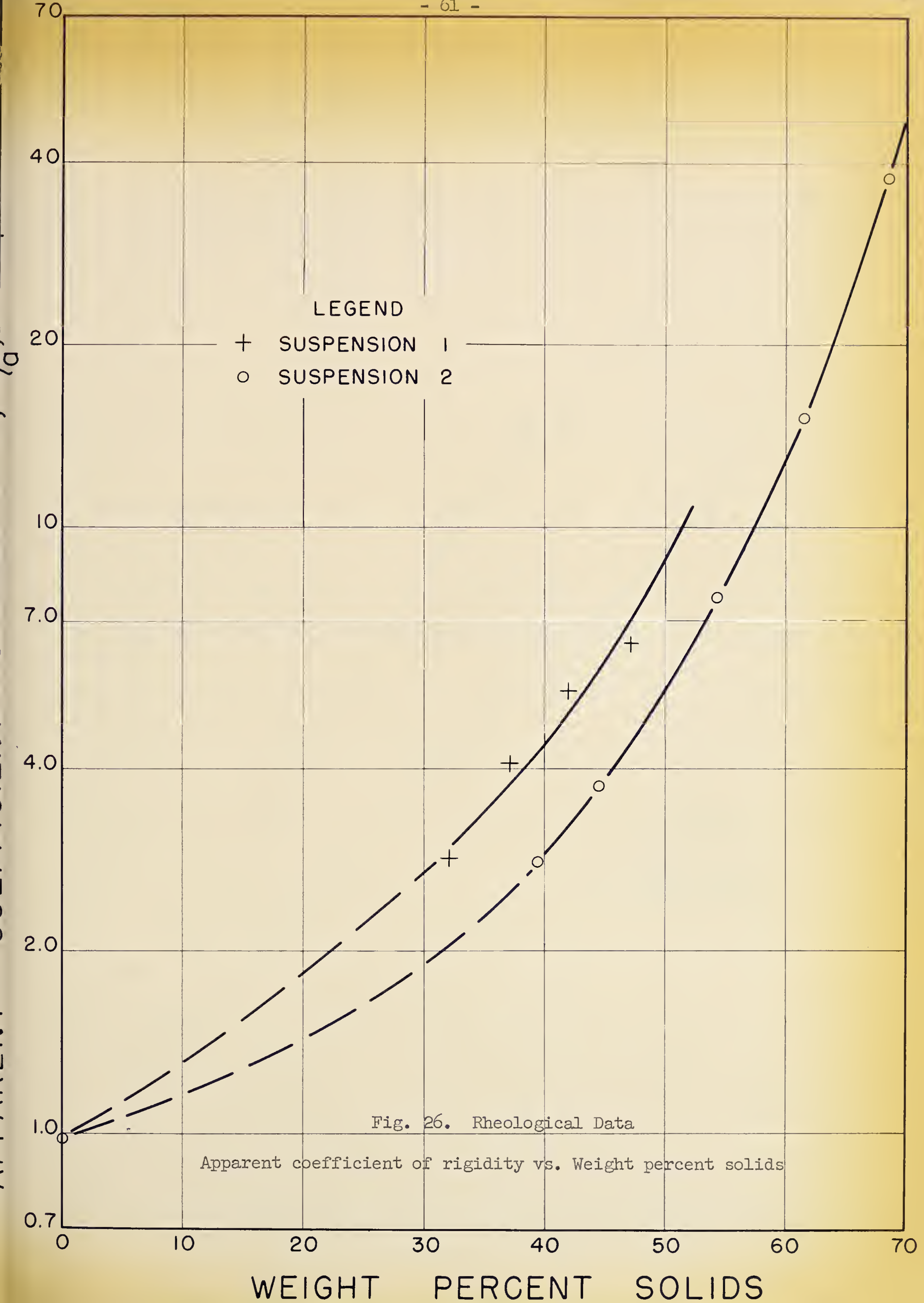

Fig. 26. Rheological Data

Apparent coefficient of rigidity vs. Weight percent solids

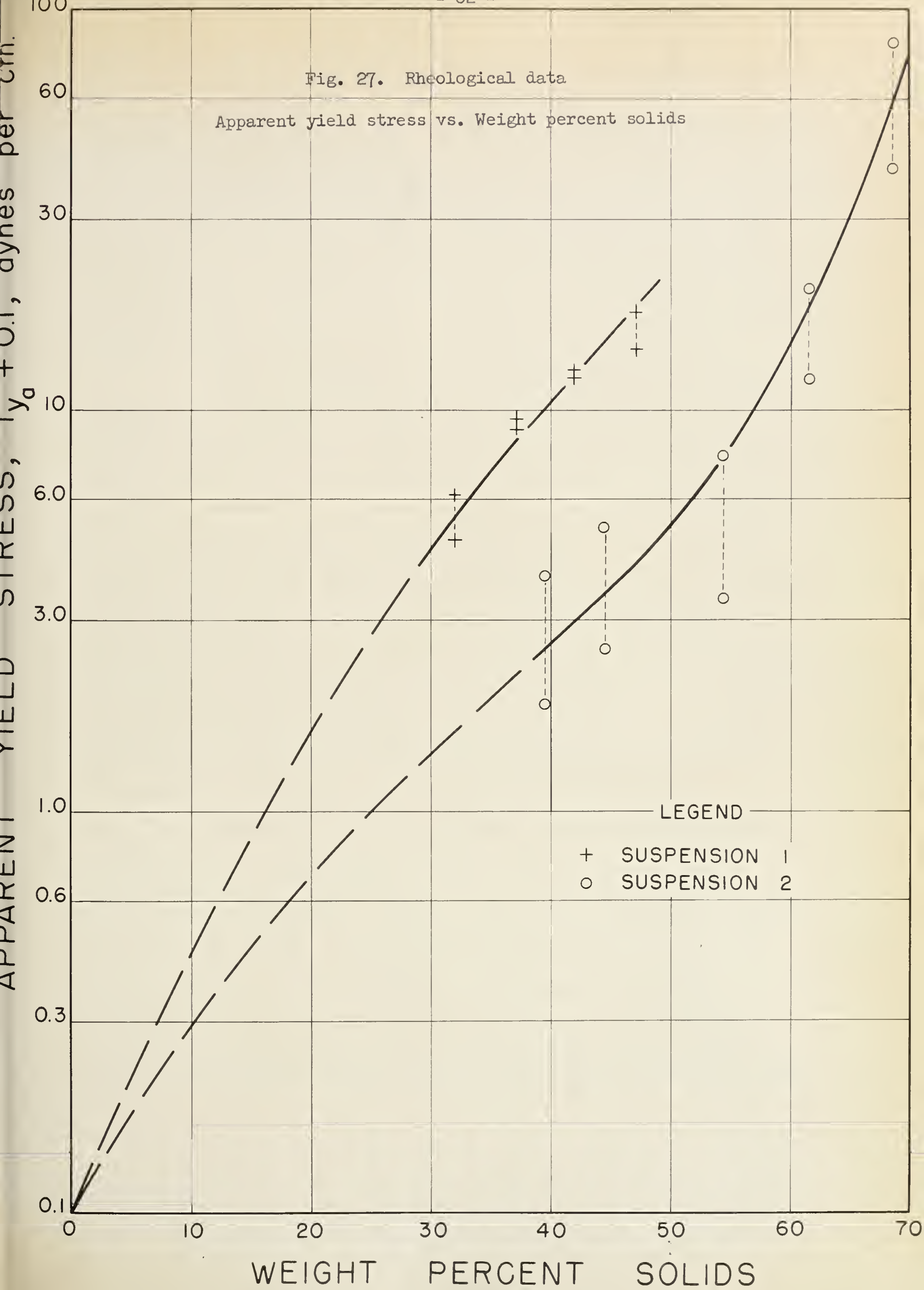

Fig. 27. Rheological data

Apparent yield stress vs. Weight percent solids

Bingham yield number respectively, could be calculated for experimental data at different percent solids. Figures 28 and 29 are logarithmic plots of the product fR_{m_a} versus Y_a for laminar flow data obtained for suspension 1 and suspension 2 respectively. The solid line in each figure indicates the form of the curve required by Equation 24.

Figure 28 indicates that, by approximating the rheological behavior of suspension 1 to that of an equivalent Bingham-plastic, near agreement is obtained between the experimental and theoretical values of fR_m and Y. A similar approximation applied to suspension 2 does not give such near agreement (Figure 29). The difference in these results can be attributed to the different rheological properties of the suspensions; this difference has been discussed previously. The data for both suspensions are displaced upwards from the theoretical line indicating that neither are true Bingham-plastics. It should be noted that the higher the percent solids concentration the better is the agreement between the experimental and theoretical data.

Figures 30 and 31 are logarithmic plots of friction factor versus apparent Bingham Reynolds number with the apparent Bingham yield number as parameter. In these figures both laminar and turbulent flow data are plotted. The comparison between the laminar flow data and Equation 24 is made by imposing lines representing values of Y equal to 0, 10, 20, 30 and 40 on the plot showing the experimental data. It is suggested that it would be permissible to extend the curve

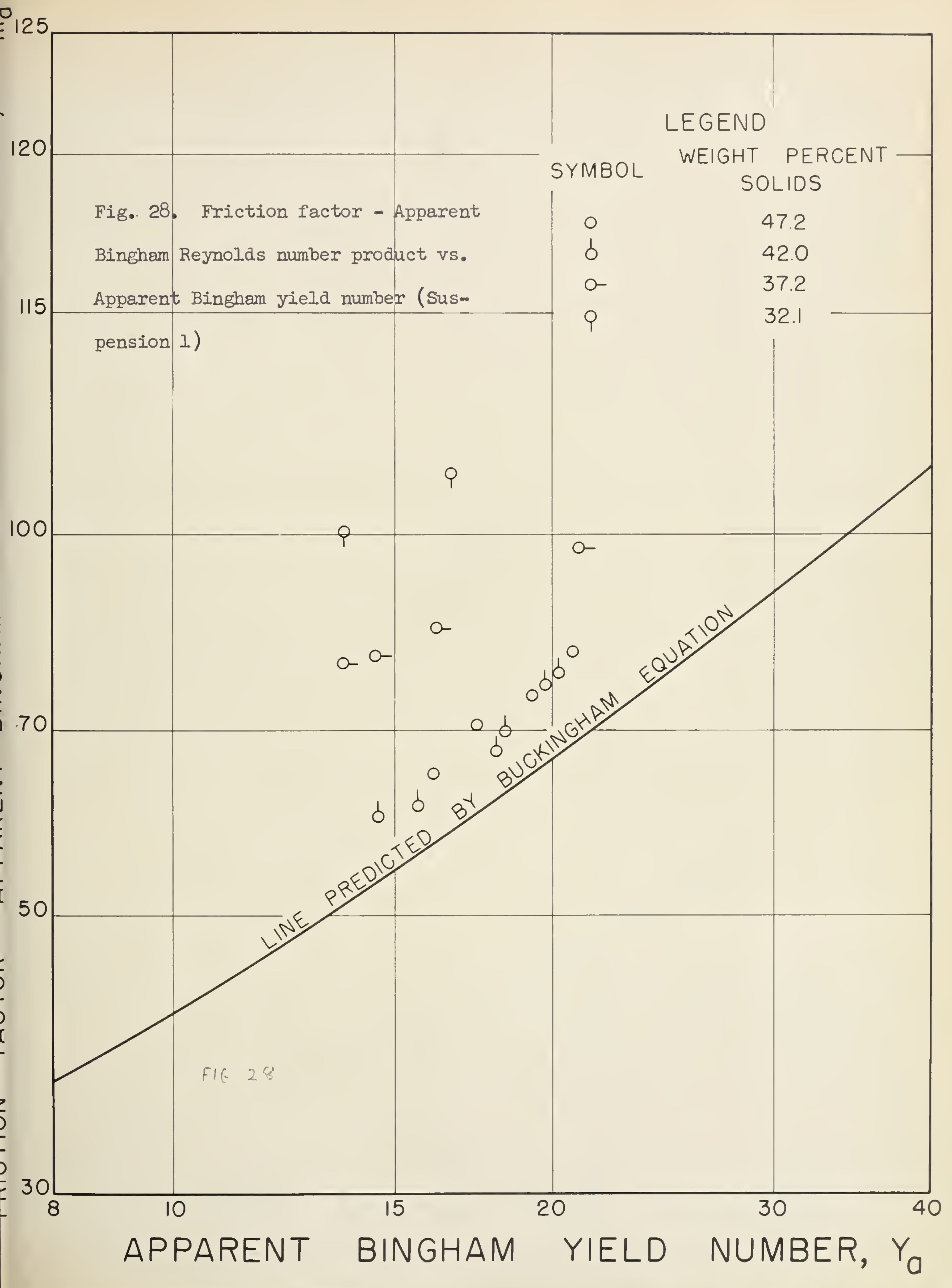

Fig. 28. Friction factor - Apparent Bingham Reynolds number product vs. Apparent Bingham yield number (Suspension 1)

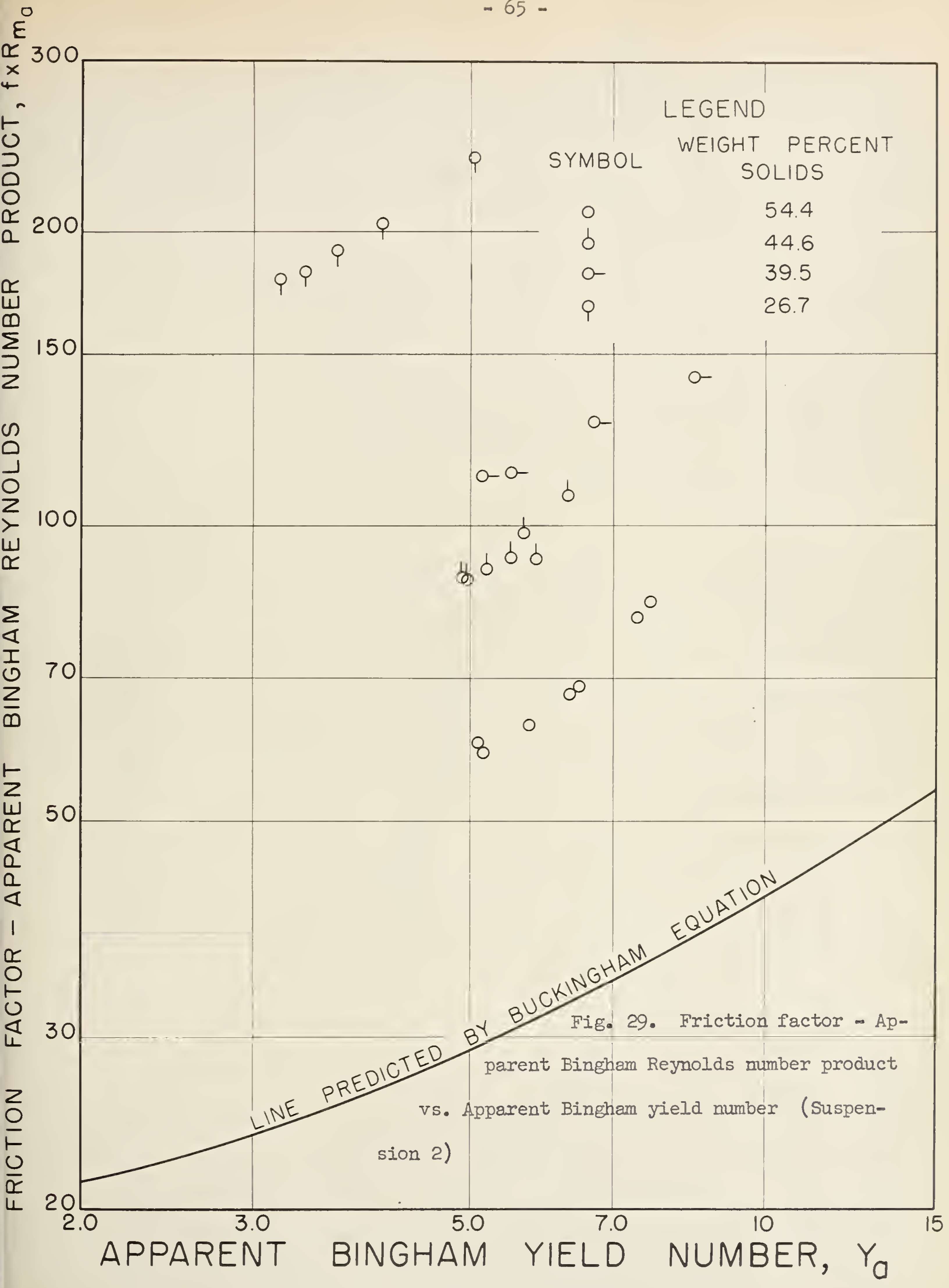

Fig. 29. Friction factor - Apparent Bingham Reynolds number product vs. Apparent Bingham yield number (Suspension 2)

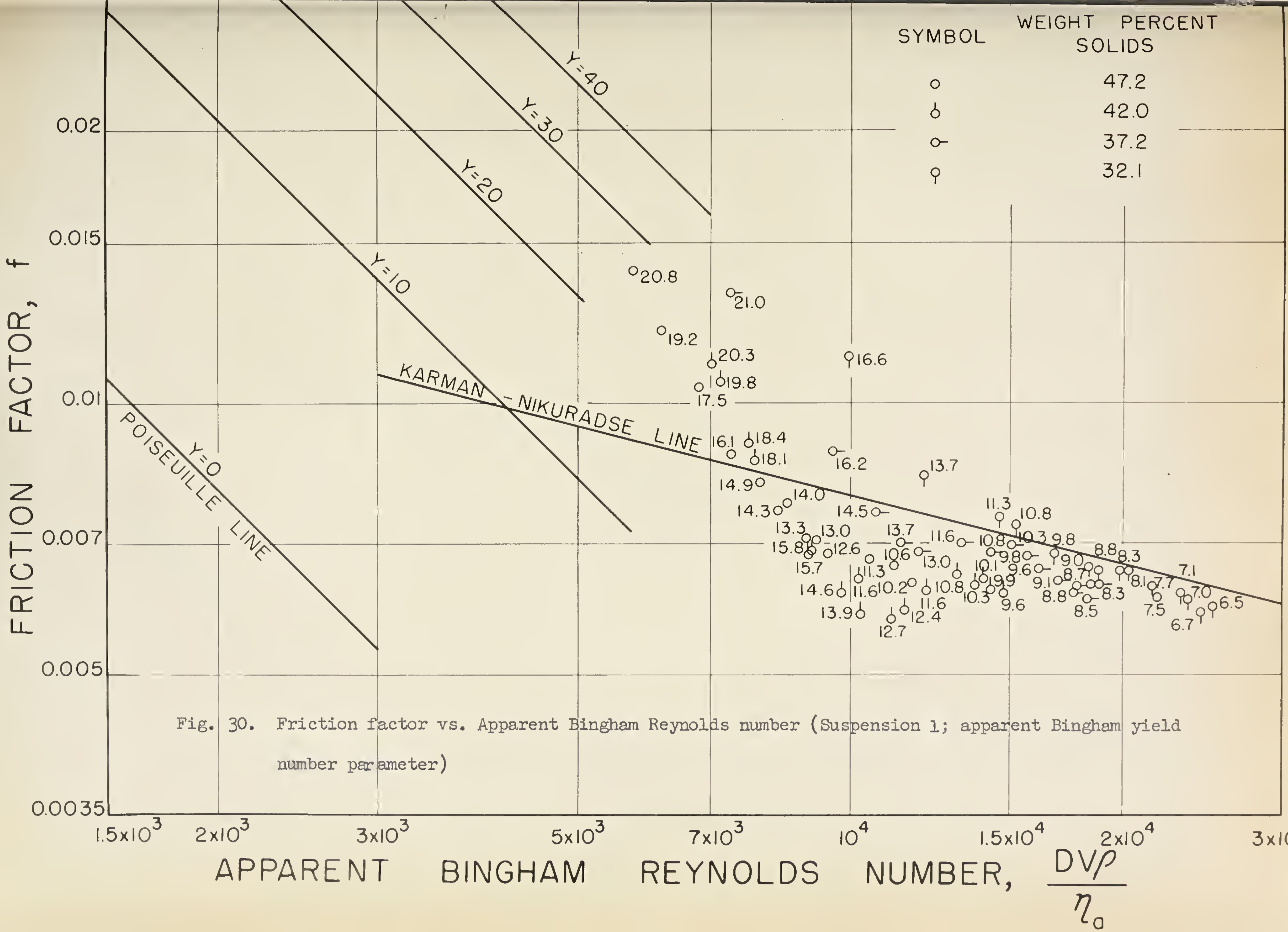

Fig. 30. Friction factor vs. Apparent Bingham Reynolds number (Suspension 1; apparent Bingham yield number parameter)

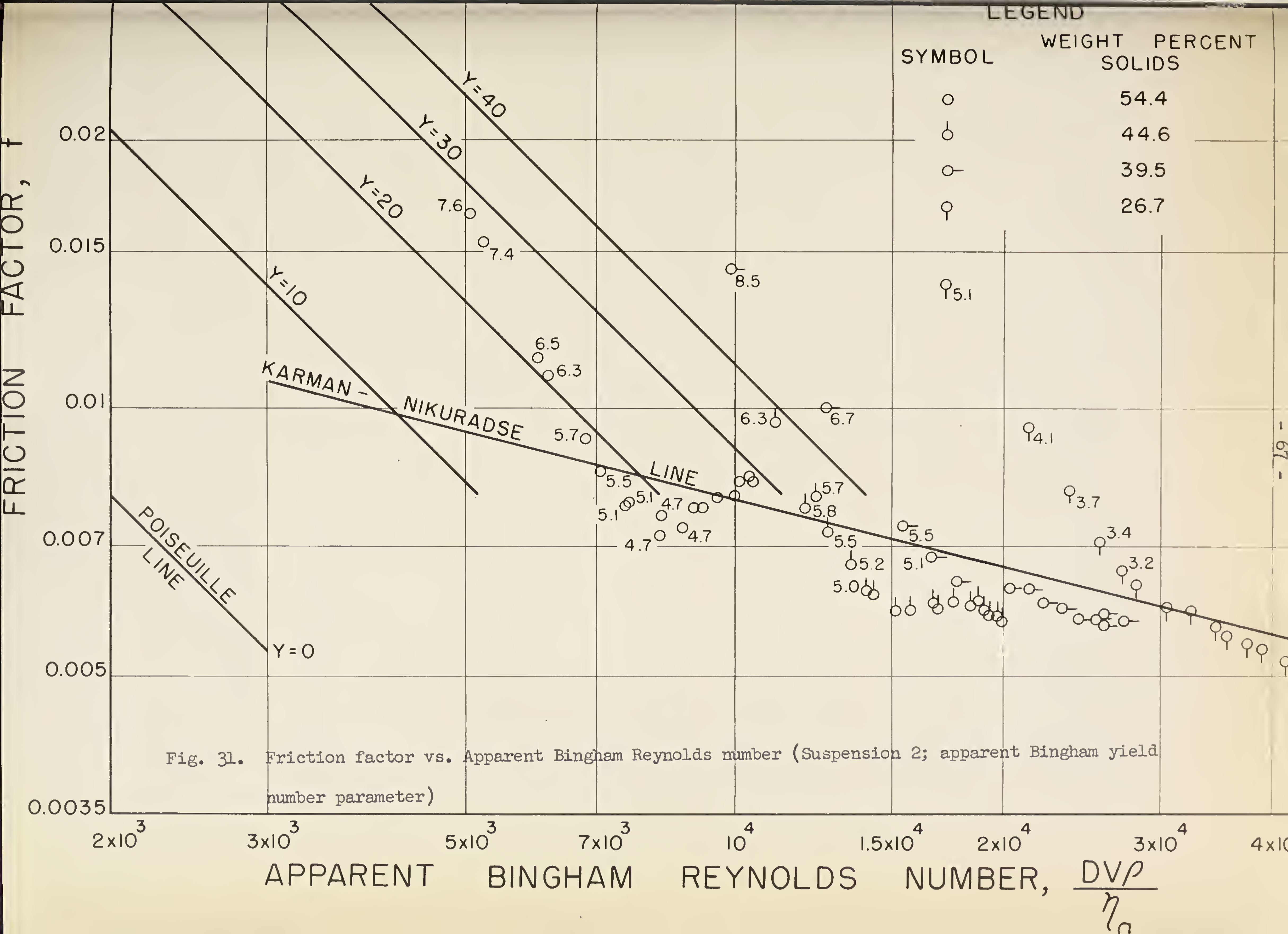

Fig. 31. Friction factor vs. Apparent Bingham Reynolds number (Suspension 2; apparent Bingham yield number parameter)

for Y = 10 as a loop to pass through the points labelled in Figure 30. The turbulent flow data are compared with the Karman-Nikuradse line.

The comparison between the experimental and theoretical data for the laminar flow region again indicates that suspension 1 behaves more nearly as a Bingham-plastic than does suspension 2. The experimental, turbulent flow data for both suspensions compares well with the Karman - Nikuradse line.

II Interpretation Assuming Power-Law Pseudoplastic Behavior

In this interpretation a logarithmic plot of friction factor versus power law Reynolds number is used to compare the experimental data with theoretical predictions.

The power-law Reynolds number, as defined by Equation 34 is,

$$Re' = \frac{D^{n'} V^{2-n'} \rho}{\gamma} \quad \ldots\ldots\ldots\ldots\ldots (34)$$

where

$$\gamma = g_c K' \, 8^{n'-1} \quad \ldots\ldots\ldots\ldots\ldots (35)$$

and

$$K' = K \left(\frac{3n' + 1}{4n'}\right)^{n'} \quad \ldots\ldots\ldots\ldots\ldots (32)$$

The values of K and n' are determined from the rheological data, plotted in Figures 22 and 23, in the following manner

a) The maximum wall shear stress is determined from the pressure drop data.

b) The range of shear stresses affecting the flow is taken to be between the limits of this maximum shear stress and 25%

[illegible]

[illegible]

[illegible]

[illegible] . . . . [illegible]

[illegible] . . . . [illegible]

[illegible] . . . . [illegible]

[illegible]

of this shear stress.

c) A straight line is drawn through the rheological curve between these limits.

d) The slope of this line is n', and K is given by the intercept at a shear rate of unity.

The lines used in the interpretation are shown lightly dashed in Figures 22 and 23, and the values of n' and K are plotted against weight percent solids in Figures 32 and 33. The smoothed values of n' and K are used to determine K' from Equation 32 and γ from Equation 35.

Figures 34 and 35 are logarithmic plots of friction factor versus the power-law Reynolds number obtained from Equation 34. The laminar flow data are compared with the power-law equivalent of the Poiseuille line ($f = {}^{16}/_{Re'}$) proposed by Metzner (17). The turbulent data is compared with the lines, proposed by Dodge and Metzner (5), representing the theoretical position of data for n' equal to 1.0, 0.6 and 0.3. The poiseuille line and the lines representing these values of n' are shown on Figures 34 and 35.

The laminar flow data for suspension 1 (Figure 34) are displaced upwards from the Poiseuille line. They lie parallel to this line and have only a small variation over the whole range of solids concentrations. The turbulent flow data are also displaced upwards from the lines predicted by Dodge and Metzner (5) but the

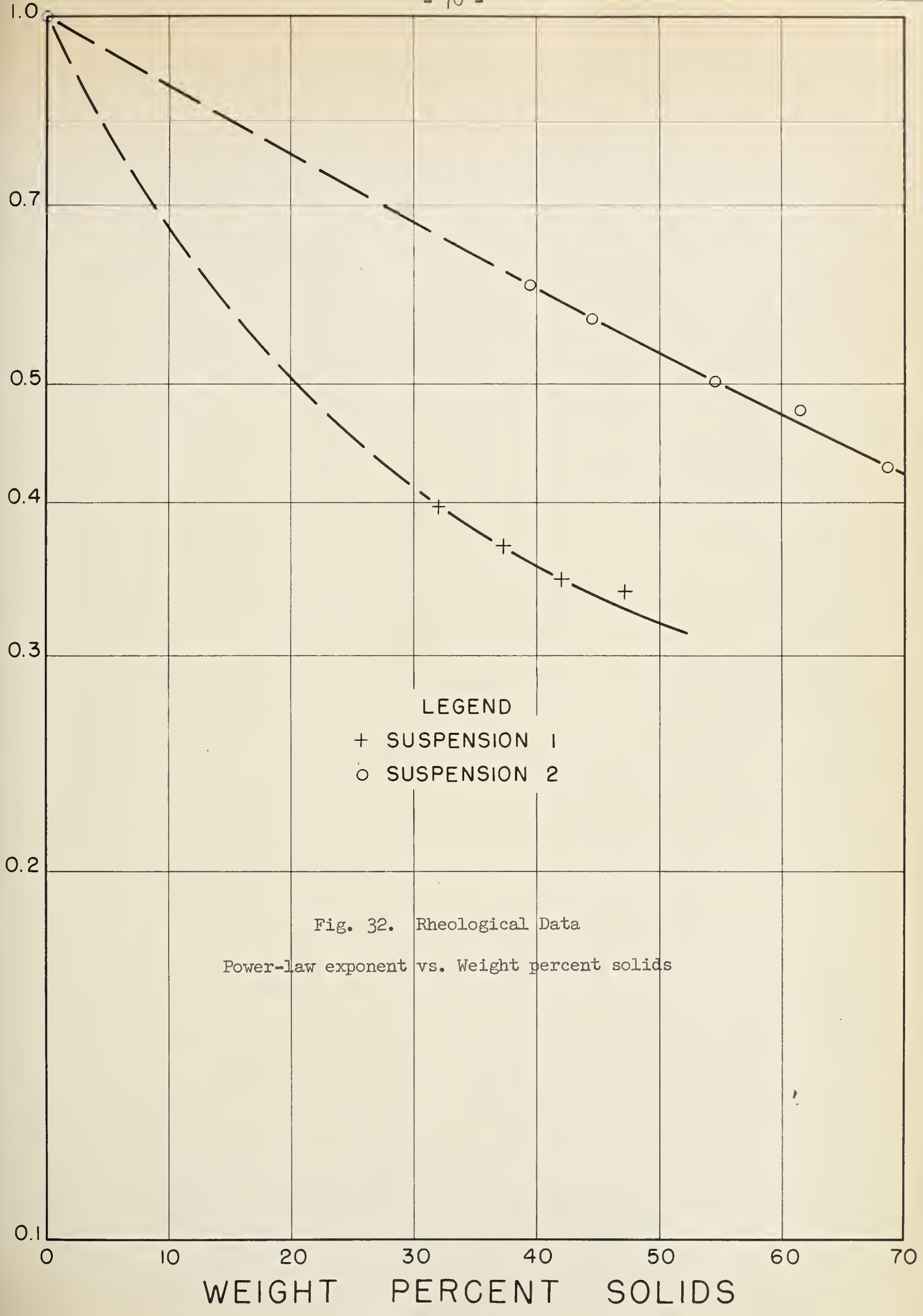

Fig. 32. Rheological Data

Power-law exponent vs. Weight percent solids

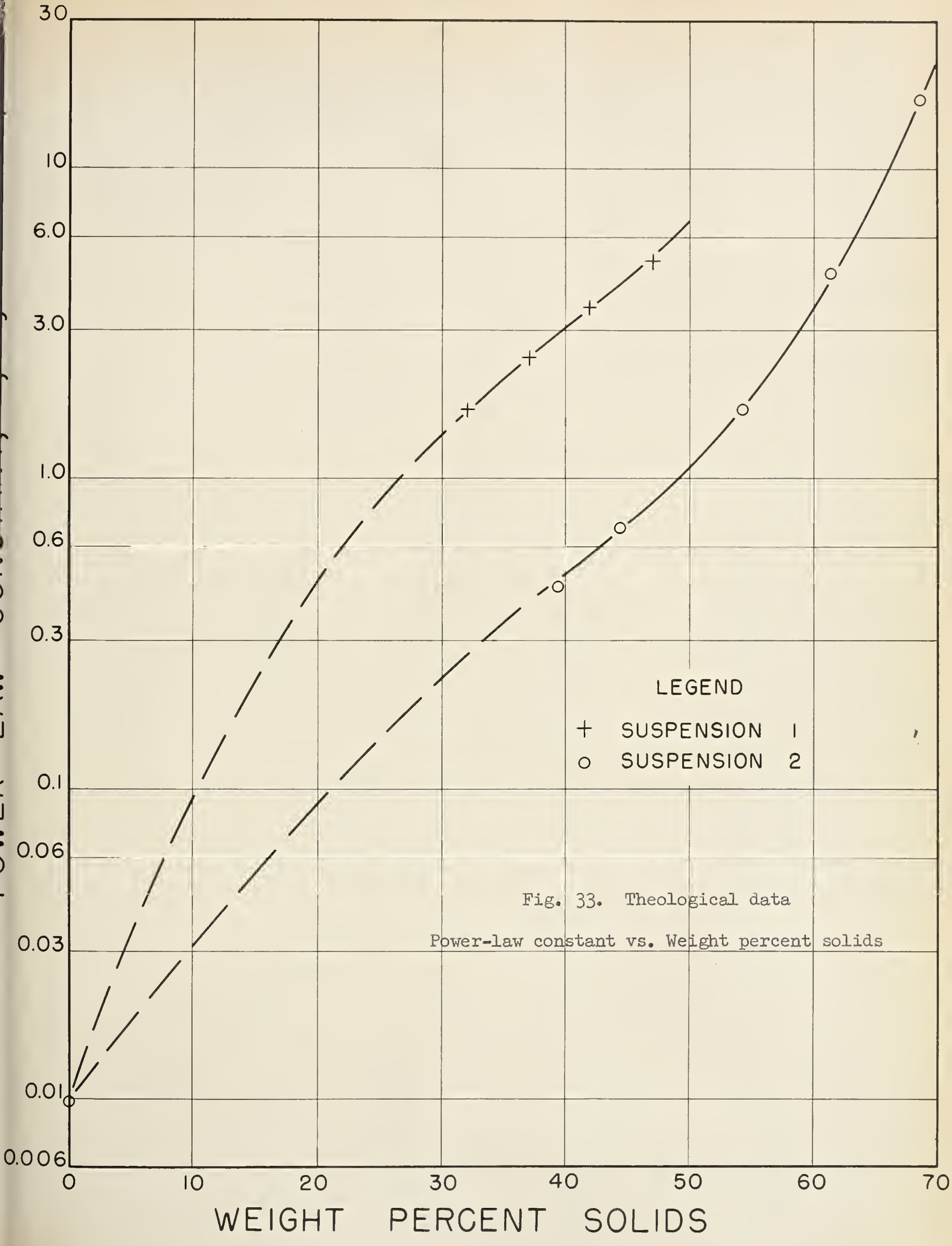

Fig. 33. Theological data

Power-law constant vs. Weight percent solids

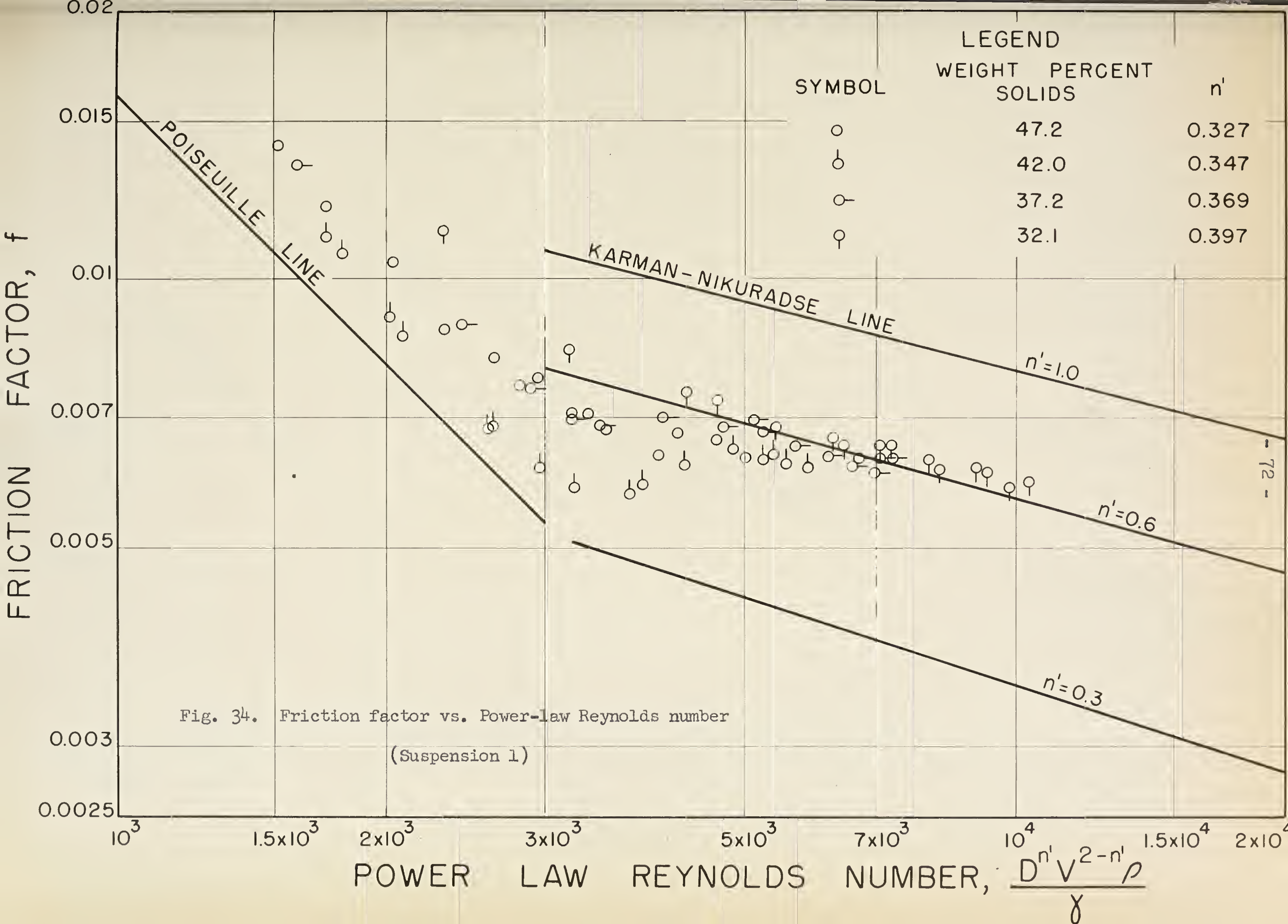

Fig. 34. Friction factor vs. Power-law Reynolds number

(Suspension 1)

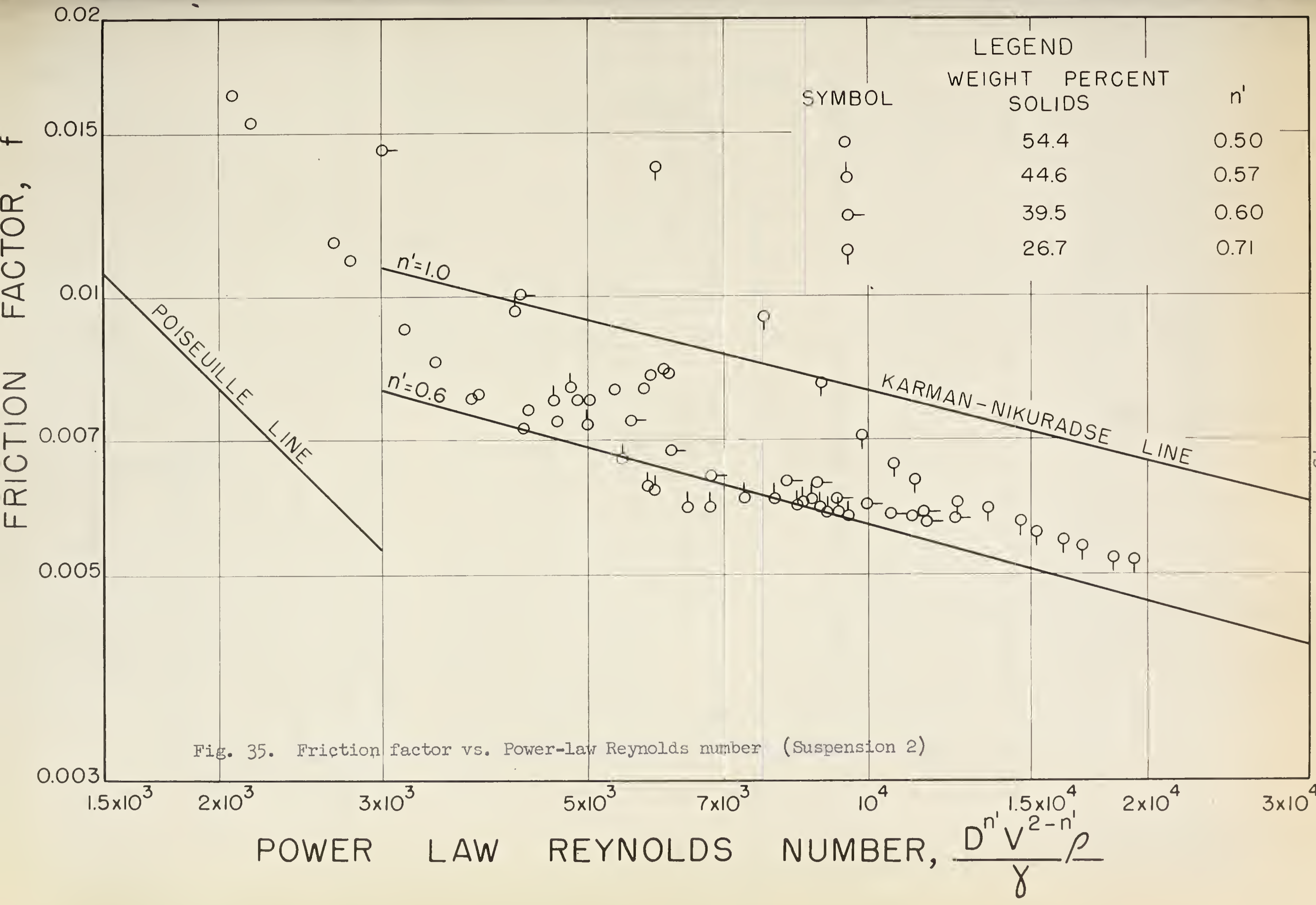

Fig. 35. Friction factor vs. Power-law Reynolds number (Suspension 2)

data again fall parallel to these lines and lie in the expected sequence (the highest friction factors associated with the highest values of n' at constant Re'). For suspension 2 (Figure 35) the laminar flow data are very scattered and are removed from the Poiseuille line. In general the turbulent flow data fall close to the positions predicted by Metzner and Reid for various values of n'. The data for the 54.4 percent suspension, however, is removed from the predicted position. From these data it can be concluded that neither suspension 1 nor suspension 2 behaved as a power-law pseudoplastic.

Figure 36 is a plot of the critical friction factor versus the power law expoent n'. The curve shown is that predicted by Ryan and Johnson (22) for power-law pseudoplastics.

The interpretations discussed in this section show that there are large deviations between the experimental and predicted data. These deviations are not necessarily due to the complexity of the rheological behavior. The following analysis of the sources of error in the experimental results is designed to indicate explanations for these deviations.

As stated previously (page 38) the pipeline, and associated pressure measuring equipment, were calibrated by pumping water through the equipment. Good agreement was obtained between the measured data, plotted as friction factor versus Reynolds number (Fig. 9) and the Karman-Nikuradse line. This indicated that the equipment was functioning satisfactorily and that the calibration data for the pressure

[illegible]

[illegible]

[illegible]

[illegible]

[illegible]

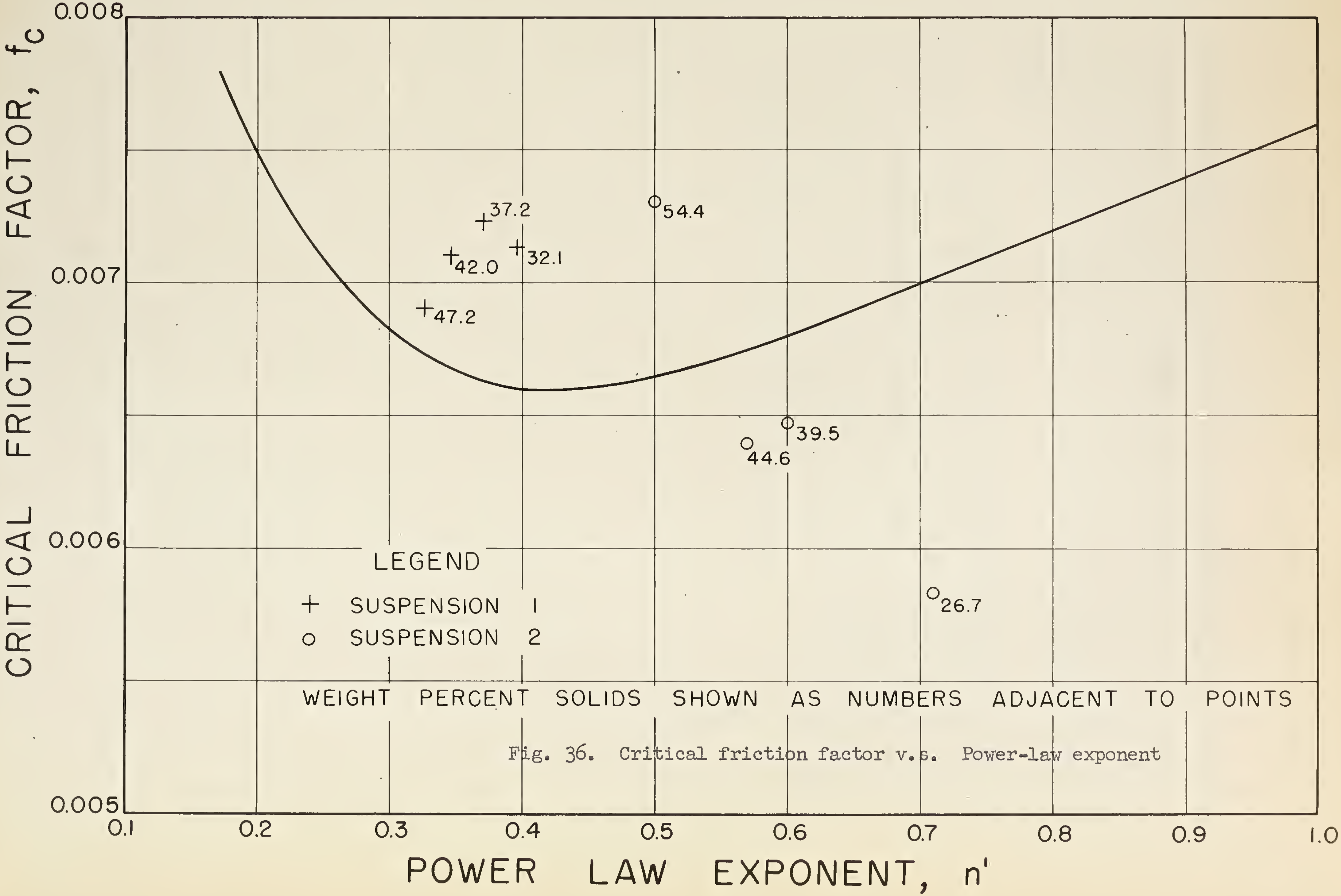

Fig. 36. Critical friction factor v.s. Power-law exponent

measuring system were accurate. The pressure drop data are, therefore, assumed to be accurate. This is substantiated by the good agreement between the experimental data, when plotted as friction factor versus modified Reynolds number (Fig. 10 through 17) and the Karman-Nikuradse line.

The possibility of errors in the rheological data, however, is much greater. A majority of these data were obtained in the low dial reading range of the Fann V-G meter where the calibration curve is no longer linear and small errors in the dial reading are magnified. Thus errors in T_y, η and n may be large. No method of determining the magnitude of these errors is available.

[illegible]

[illegible]

CONCLUSIONS

In the conclusions the two suspensions will be considered separately as their rheological behaviour is quite different.

1. Suspension 1

a) The rheological behaviour of this suspension, in the range of the pipeline tests, resembles that for a Bingham-plastic. Thus

i) Data obtained in the laminar flow region correlate approximately with that predicted for Bingham-plastics.

ii) Friction factors for the turbulent flow region are independent of the apparent Bingham yield number.

iii) Data obtained in the transition between laminar and turbulent flow follow a fairly well defined curve at constant values of the apparent Bingham yield number.

b) The rheological behaviour also resembles that for a power-law pseudoplastic. The agreement between experimental and predicted data is not however as close as that obtained when Bingham-plastic behaviour is assumed. Thus

i) The laminar flow data correlate approximately with the curve $f = 16/Re'$.

ii) The turbulent flow data do not follow the theoretical predictions.

c) This suspension behaves as a pseudoplastic, however, in the range of the experimental data, it can be treated as a

Bingham-plastic.

2. Suspension 2

a) The rheological behaviour of this suspension indicates that it is not a Bingham-plastic. Thus it is concluded that

i) The laminar flow data does not correlate as a Bingham-plastic at constant values of apparent Bingham yield number.

ii) Data obtained in the turbulent flow region still correlate approximately with the Karman-Nikuradse line as it is independent of the apparent Bingham yield number.

b) As indicated by the rheological data this suspension behaves as a pseudoplastic. However it is not a power-law pseudoplastic as

i) The laminar flow data do not correlate with the curve $f=16/Re'$.

ii) The turbulent flow data only correlate approximately with the theoretical predictions.

Nomenclature

A_1	Constant defined by Equation 41, dimensionless.
C , C ,	Constants defined by Equation 41, dimensionless.
dV/dr	Shear rate, $sec.^{-1}$ $(dV/dr)_{R1}$ refers to the shear rate at the wall of the inner cylinder of a rotational viscometer.
D	Diameter of tube, ft.
$\frac{D\Delta P}{4L}$	Shear stress at wall of a tube, $lb_F/ft.^2$
f	Fanning friction factor, dimensionless.
F	Shearing force, lb_F.
g_c	Dimensional conversion factor, 32.2 ft. lb_m $sec.^2$ lb_F.
H	Hedstrom number $\frac{T_y D^2 \rho g_c}{\eta^2}$, dimensionless.
k_1, k_2	Instrument constants defined by Equations 48 and 49, dimensionless.
K	Power-law constant defined by Equation 3 , $lb_F/sec.^{n'}/ft.^2$
L	Length of tube, ft.
n	Exponent defined by Equation 3 , dimensionless.
n'	Exponent defined by Equation 30, dimensionless.
n"	$\frac{d \ln t}{d \ln N}$, dimensionless.
N	Rotational speed, rev./sec.
P	Pressure, $lb_F/ft.^2$ dP_f refers to pressure loss due to friction.
Q	Volumetric rate of flow, $ft^3/sec.$

Re	Newtonian Reynolds number, dimensionless.
Re'	Power-law Reynolds number, dimensionless.
R_m	Bingham Reynolds number, dimensionless.
$R_1 R_2$	Radius of the inner and outer cylinder in a concentric cylinder viscometer, ft.
r	Radial distance from tube axis, ft. r_w is the radial distance to the tube wall.
s	Ratio R_1/R_2, dimensionless.
T	Shear stress, dynes/cm^2. T_w refers to the shear stress at the wall of a round tube, T_{R1} to the shear stress at the wall of the innder cylinder of a rotational viscometer, and T_y is the yield stress of a Bingham-plastic.
t	Torque on the spring of a rotational viscometer.
U_{max}	Maximum velocity of flow, ft/sec.
μ	Local axial velocity, ft/sec.
V	Mean velocity of flow, ft./sec.
V_*	Shear stress velocity, ft/sec.
8V/D	Shear rate at the wall of a tube for a Newtonian fluid in laminar flow, sec.$^{-1}$
v	Specific volume, ft^3/lb$_m$.
W	Flow function Q/ r_w^3 , sec.$^{-1}$
Y	Yield number $D\ T_y\ g_c/V \eta$, dimensionless.
Z	Criterion defined by Equation 36 . Z_{max} refers to maximum value of this criterion.

z	Elevation above a given datum, ft.
α	Constant in Equation 4, dimensionless.
γ	Denominator in power-law Reynolds number (Equation 34), $lb_m/ft\ sec.^{2-n'}$
δ	Pipe roughness, ft.
η	Coefficient of rigidity of a Bingham-plastic fluid, dynes sec./cm^2.
θ	Measurement of shear stress in a rotational viscometer, $sec.^{-1}$
θ', θ'', θ'''	Indicators of functional relationships.
μ	Viscosity of a Newtonian fluid, dynes sec./cm^2 (poise).
ρ	Fluid density, lb_m/ft^3.
ϕ (n)	Constant defined by Equation 39, dimensionless.
τ	Shear stress, dynes/cm^2. τ_W refers to the shear stress at the wall of a round tube, τ_{R_1} to the shear stress at the wall of the inner cylinder of a rotational viscometer, and τ_y is the yield stress of a Bingham-plastic.

BIBLIOGRAPHY

1. Alves, G.E., Boucher, D.F., and Pigford, R.L.,
Chem. Eng. Progr., 48, 385 (1952)

2. Barr, G.A.,
A Monograph on Viscometry, Oxford University Press, 1931.

3. Buckingham, E.,
Proc. Am. Inst. Chem. Engrs., 37, 237 (1941)

4. Christiansen, E.B., Ryan, N.W., and Stephens, W.E.,
A.I.Ch.E. Journal, 1, 543 (1955)

5. Dodge, D.W., and Metzner, A.B.,
A.I.Ch.E. Journal, 5, 189 (1959)

6. Govier, G.W., and Winning, M.D.,
Paper presented at Montreal Meeting, American Institute of Chemical Engineers (1948)

7. Govier, G.W., Shook, G.A., and Lilge, E.O.,
Trans. Can. Min. and Met. Soc., 60, 147 (1957)

8. Govier, G.W.
Chem. Eng., 66, No. 17, 142 (1959)

9. Govier, G.W.
Eng. Journal, 43, 85 (1960)

10. Green, H.,
"Industrial Rheology and Rheological Structures", J. Wiley and Sons, Inc., New York (1949)

11. Hahn, O.J.,
Report to the Department of Chemical Engineering, University of Alberta, Edmonton (1958)

12. Hedstrom, B.O.A.,
Ind. Eng. Chem., 44, 651 (1952)

13. Krieger, I.M., and Maron, S.H.
J. Appl. Phys., 25, 72 (1954)

14. Lindley, W.G.G.,
M.Sc. Thesis in Chemical Engineering, University of Alberta, Edmonton (1958)

15. Merrill, E.W.
J. Colloid Sci., 9, 7 (1954)

16. Metzner, A.B., and Reid, J.C.,
A.I.Ch.E. Journal, I, 434 (1955)

17. Metzner, A.B.,
"Non-Newtonian Technology". Contribution to "Advances in Chemical Engineering, Vol. 1", Academic Press, New York, 1956.

18. Mooney, M.,
J. Rheol., 2, 210 (1931)

19. Perkins, A., and Glick, J.J.,
B.Ch.E. Thesis, University of Delaware (1954)

20. Rabinowitsch, B.,
Z. Physik. Chem., A145, 1 (1929)

21. Reiner, M., and Riwlin, R.,
Kolloid - Z., 43, 1 (1927)

22. Ryan, N.W., and Johnson, M.M.,
A.I.Ch.E. Journal, 5, 433 (1959)

23. Shaver, R.G., and Merrill, E.W.,
A.I.Ch.E. Journal, 5, 181 (1959)

24. Streeter, V.L.
"Fluid Mechanics," 2nd Ed., McGraw-Hill, New York, 1958.

25. Weltmann, R.N.
Ind. Eng. Chem., Anal. Ed., 15, 424 (1943)

26. Weltmann, R.N.
Ind. Eng. Chem., 40, 272 (1948)

27. Weltmann, R.N.
Ind. Eng. Chem., 48, 387 (1956)

28. Winding, C.C., Baumann, G.P., and Kranich, W.L.,
Chem. Eng. Progr., 43, 527, 613 (1947)

29. Winning, M.D.,
M.Sc. Thesis in Chemical Engineering, University of Alberta, Edmonton, (1948)

APPENDIX A

Computation of the shear rate in the Viscometer

Supplementary Data

Stator radius $R_1 = 0.679$ inches

Rotor radius $R_2 = 0.724$ inches

$$\frac{R_2}{R_1} = 5 = 1.0663$$

The shear rate at the stator wall for a non-Newtonian fluid, is:

$$\left(\frac{dV}{dr}\right)_{R_1} = \frac{4\ \pi\ N}{1 - 1/S^2}\left[1 + k_1\left(\frac{1}{n''} - 1\right) + k_2\left(\frac{1}{n''} - 1\right)^2\right] \sec^{-1}$$

where $k_1 = \frac{S^2 - 1}{2S^2}\left(1 + \frac{2}{3}\ \ln S\right)$

$k_1 = 6.28 \times 10^{-2}$

and $k_2 = \frac{S - 1}{6\ S^2}\ \ln S$

$k_2 = 1.29 \times 10^{-3}$

If $\frac{4\ \pi}{1 - 1/S^2} = K_2$

then $K_2 = 104.3$

and $$\left(\frac{dV}{dr}\right)_{R_1} = 104.3\ N\left[1 + 6.28 \times 10^{-2}\left(\frac{1}{n''} - 1\right) + 1.29 \times 10^{3}\left(\frac{1}{n''} - 1\right)^2\right] \sec^{-1}$$

TABLE 1A

COMPUTATION OF SHEAR RATE IN THE VISCOMETER

(1)	(2)	(3)	(4)	(5)	(6)	(7)	(8)	(9)
Test Number	Percent Solids	Rotor Speed N r.p.s.	n"	a*	b**	1+a+b	K_2N	$(\frac{dV}{dr})_{R_1}$
1-1	32.1	1.67	0.318	0.1346	0.0059	1.1405	174.2	198.7
1-1	32.1	3.33	0.442	0.0791	0.0020	1.0811	347.3	375.5
1-1	32.1	5.0	0.518	0.0584	0.0011	1.0595	521.5	552.5
1-1	32.1	10.0	0.628	0.0373	0.0005	1.0378	1043.0	1082.4
1-2	37.2	0.56	0.168	0.3109	0.0316	1.3425	58.4	78.4
1-2	37.2	1.11	0.304	0.1438	0.0068	1.1506	115.8	133.2
1-2	37.2	1.67	0.377	0.1039	0.0035	1.1074	174.2	192.9
1-2	37.2	3.33	0.484	0.0672	0.0015	1.0687	347.3	371.2
1-2	37.2	5.00	0.542	0.0531	0.0009	1.0540	521.5	549.7
1-2	37.2	10.00	0.638	0.0357	0.0004	1.0361	1043.0	1080.7
1-3	42.0	0.56	0.143	0.3768	0.0464	1.4232	58.4	83.1
1-3	42.0	1.11	0.285	0.1576	0.0081	1.1657	115.8	135.0
1-3	42.0	1.67	0.362	0.1107	0.0040	1.1147	174.2	194.2
1-3	42.0	3.33	0.482	0.0675	0.0015	1.0690	347.3	371.3
1-3	42.0	5.00	0.548	0.0518	0.0004	1.0527	521.5	549.0
1-3	42.0	10.00	0.647	0.0342	0.0004	1.0346	1043.0	1079.1
1-4	47.2	0.56	0.162	0.3247	0.0345	1.3592	58.4	79.4
1-4	47.2	1.11	0.271	0.1689	0.0093	1.1782	115.8	136.4
1-4	47.2	1.67	0.340	0.1218	0.0049	1.1267	174.2	196.3
1-4	47.2	3.33	0.450	0.0767	0.0019	1.0786	347.3	374.6

* $a = k_1(\frac{1}{n''} - 1)$

** $b = k_2(\frac{1}{n''} - 1)^2$

(1)	(2)	(3)	(4)	(5)	(6)	(7)	(8)	(9)
1-4	47.2	5.00	0.505	0.0615	0.0012	1.0627	521.5	554.2
1-4	47.2	10.00	0.581	0.0452	0.0007	1.0459	1043.0	1090.9
2-2	39.5	1.67	0.223	0.2189	0.0156	1.2345	174.2	215.0
2-2	39.5	3.33	0.436	0.0813	0.0022	1.0835	347.7	376.7
2-2	39.5	5.00	0.575	0.0465	0.0007	1.0472	521.5	546.1
2-2	39.5	10.00	0.733	0.0229	0.0002	1.0231	1043.0	1067.0
2-3	44.6	1.67	0.310	0.1397	0.0064	1.1461	174.2	199.7
2-3	44.6	3.33	0.523	0.0573	0.0011	1.0584	347.7	368.0
2-3	44.6	5.00	0.640	0.0353	0.0004	1.0357	521.5	540.1
2-3	44.6	10.00	0.840	0.0119	0.0001	1.0120	1043.0	1056.0
2-4	54.4	0.37	0.180	0.2857	0.0267	1.3124	38.6	50.7
2-4	54.4	0.56	0.242	0.1966	0.0126	1.2092	58.4	70.6
2-4	54.4	1.11	0.367	0.1083	0.0038	1.1121	115.8	128.8
2-4	54.4	1.67	0.460	0.0738	0.0018	1.0756	174.2	187.4
2-4	54.4	3.33	0.640	0.0353	0.0004	1.0357	347.7	360.1
2-4	54.4	5.00	0.750	0.0210	0.0001	1.0211	521.5	532.5
2-4	54.4	10.00	0.925	0.0051	0.0000	1.0051	1043.0	1048.0
2-5	61.5	0.05	1.288	-0.0140	0.0001	0.9861	5.22	5.15
2-5	61.5	0.10	0.675	0.0302	0.0003	1.0305	10.43	10.75
2-5	61.5	0.185	0.370	0.1069	0.0037	1.1106	19.30	21.40
2-5	61.5	0.37	0.200	0.2512	0.0206	1.2718	38.60	49.1
2-5	61.5	0.56	0.196	0.2575	0.0217	1.2792	58.40	74.7
2-5	61.5	1.11	0.342	0.1209	0.0048	1.1257	115.8	130.4
2-5	61.5	1.67	0.467	0.0717	0.0017	1.0734	174.2	187.0
2-5	61.5	3.33	0.635	0.0361	0.0004	1.0365	347.7	360.4
2-5	61.5	5.00	0.730	0.0232	0.0002	1.0234	521.5	533.7
2-5	61.5	10.00	0.938	0.0041	0.0000	1.0041	1043.0	1047.0
2-6	68.7	0.05	1.375	-0.0171	0.0000	0.9829	5.22	5.13
2-6	68.7	0.10	0.813	0.0144	0.0000	1.0144	10.43	10.58
2-6	68.7	0.185	0.620	0.0385	0.0005	1.0390	19.3	20.10
2-6	68.7	0.37	0.515	0.0592	0.0012	1.0604	38.6	40.90

(1)	(2)	(3)	(4)	(5)	(6)	(7)	(8)	(9)
2-6	68.7	0.56	0.445	0.0784	0.0020	1.0804	58.4	63.1
2-6	68.7	1.11	0.332	0.1256	0.0052	1.1308	115.8	130.9
2-6	68.7	1.67	0.332	0.1256	0.0052	1.1308	174.2	197.0
2-6	68.7	3.33	0.495	0.0641	0.0014	1.0655	347.7	370.5
2-6	68.7	5.00	0.625	0.0377	0.0005	1.0382	521.5	541.4
2-6	68.7	10.00	0.806	0.0151	0.0000	1.0151	1043.0	1059.0

APPENDIX B

Viscometer experimental data

The shear stress at the stator wall is

$$T_{R_1} = K_1 \Theta \text{ dynes per cm}^2$$

or for a Newtonian fluid

$$T_{R_1} = \mu \left(\frac{dV}{dr}\right)_{R_1} \text{ dynes per cm}^2$$

where the viscosity μ is in poise.

It follows that

$$K_1\Theta = \mu \left(\frac{dV}{dr}\right)_{R_1}$$

However for a Newtonian fluid

$$\left(\frac{dV}{dr}\right)_{R_1} = K_2 N = 104.3 N$$

so $$K_1\Theta = \mu K_2 N$$

or $$K_1 = \frac{\mu K_2 N}{\Theta}$$

The value of K_1 determined by Lindley (14) AND Hahn (11) was 4.96

The correction curve for this calibration constant is shown in Figure 1B.

TABLE 1B

VISCOMETER EXPERIMENTAL DATA

(1) Test Number	(2) Percent Solids	(3) Deflection θ Scale Divisions	(4) Rotor Speed N r.p.s.	(5) Shear Rate $(\frac{dV}{dr})_{R_1}$ sec.$^{-1}$	(6) Correction to Calibration K_1	(7) Shear Stress dynes cm.$^{-2}$
1-1	32.1	3.0	1.67	198.7	0.810	12.05
1-1	32.1	3.9	3.33	375.5	0.855	16.54
1-1	32.1	4.7	5.0	552.5	0.880	20.51
1-1	32.1	7.0	10.0	1082.4	0.925	32.12
1-2	37.2	3.0	0.56	78.4	0.810	12.05
1-2	37.2	3.5	1.11	133.2	0.840	14.58
1-2	37.2	4.0	1.67	192.9	0.860	17.06
1-2	37.2	5.5	3.33	371.2	0.900	24.55
1-2	37.2	6.8	5.00	549.7	0.925	31.20
1-2	37.2	9.6	10.00	1080.7	0.960	43.80
1-3	42.0	3.8	0.56	83.1	0.850	16.01
1-3	42.0	4.4	1.11	135.0	0.875	19.09
1-3	42.0	5.0	1.67	194.2	0.890	22.07
1-3	42.0	6.8	3.33	371.3	0.925	31.20
1-3	42.0	8.5	5.00	549.0	0.945	39.84
1-3	42.0	12.5	10.00	1079.1	0.975	60.45
1-4	47.2	5.0	0.56	79.4	0.890	22.13
1-4	47.2	5.8	1.11	136.4	0.905	26.04
1-4	47.2	6.8	1.67	196.3	0.925	31.20
1-4	47.2	8.6	3.33	374.6	0.945	40.31
1-4	47.2	10.5	5.00	554.2	0.965	50.26
1-4	47.2	15.2	10.00	1090.9	0.985	74.26

(1)	(2)	(3)	(4)	(5)	(6)	(7)
2-2	39.5	2.5	1.67	215.0	0.765	9.49
2-2	39.5	3.0	3.33	376.7	0.810	12.05
2-2	39.5	4.0	5.00	546.1	0.860	17.06
2-2	39.5	6.0	10.00	1067.0	0.910	27.08
2-3	44.6	3.0	1.67	199.7	0.810	12.05
2-3	44.6	4.0	3.33	368.0	0.860	17.06
2-3	44.6	5.0	5.00	540.1	0.890	22.07
2-3	44.6	8.5	10.00	1056.0	0.945	39.84
2-4	54.4	3.0	0.37	50.7	0.810	12.05
2-4	54.4	3.3	0.56	70.6	0.825	13.51
2-4	54.4	4.0	1.11	128.8	0.860	17.06
2-4	54.4	4.8	1.67	187.4	0.885	21.07
2-4	54.4	7.0	3.33	360.1	0.925	32.12
2-4	54.4	9.3	5.00	532.5	0.955	44.05
2-4	54.4	16.5	10.00	1048.0	0.985	80.61
2-5	61.5	2.0	0.05	5.15	0.700	6.94
2-5	61.5	4.0	0.10	10.75	0.860	17.06
2-5	61.5	5.2	0.185	21.40	0.895	23.08
2-5	61.5	6.3	0.37	49.1	0.920	28.75
2-5	61.5	7.0	0.56	74.7	0.925	32.12
2-5	61.5	8.2	1.11	130.4	0.945	38.44
2-5	61.5	10.0	1.67	187.0	0.960	47.62
2-5	61.5	14.0	3.33	360.4	0.980	68.05
2-5	61.5	20.0	5.00	533.7	1.000	99.20
2-5	61.5	33.0	10.00	1047.0	1.000	163.70
2-6	68.7	3.5	0.05	5.13	0.835	14.47
2-6	68.7	7.5	0.10	10.58	0.935	34.71
2-6	68.7	11.0	0.185	20.10	0.965	52.55
2-6	68.7	16.3	0.37	40.90	0.985	79.48
2-6	68.7	21.5	0.56	63.1	1.000	106.40
2-6	68.7	27.0	1.11	130.9	1.000	133.70
2-6	68.7	30.0	1.67	197.0	1.000	148.50
2-6	68.7	37.0	3.33	370.5	1.000	183.20
2-6	68.7	49.0	5.00	541.4	1.000	242.60
2-6	68.7	83.0	10.00	1059.0	1.000	410.90

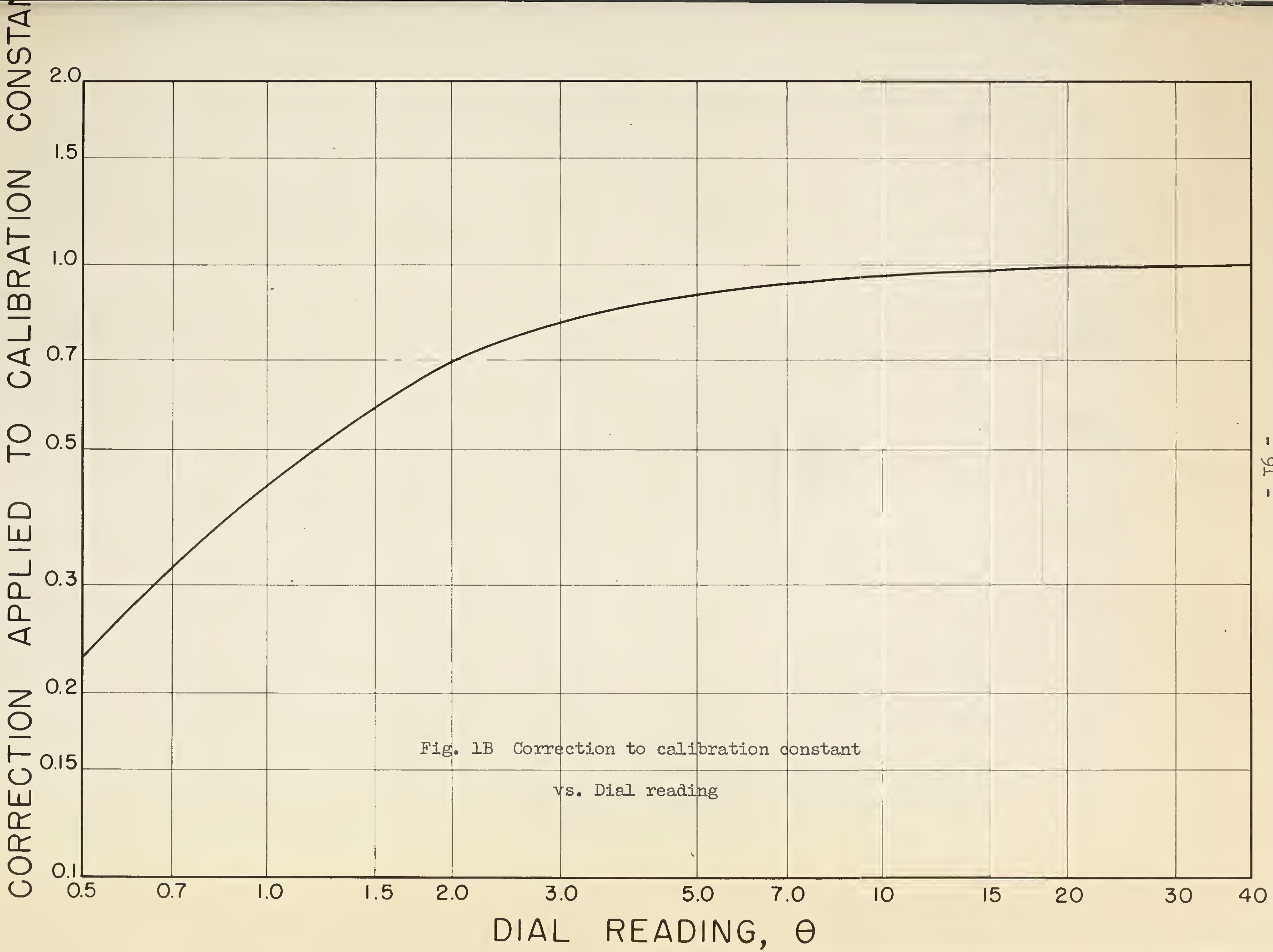

Fig. 1B Correction to calibration constant vs. Dial reading

APPENDIX C

PIPELINE EXPERIMENTAL DATA

TABLE 1C

PIPELINE EXPERIMENTAL DATA

(1) Test Number	(2) Percent Solids	(3) M.V.,F*	(4) Flow Rate lb./hr.	(5) M.V.,1**	(6) Pressure Drop per. 100 ft. Section 1	(7) M.V.,2***	(8) Pressure Drop per. 100 ft. Section 2	(9) Average Pressure Drop per. 100 ft.
0-1	0	2.59	4195	0.40	0.115	0.37	0.110	0.112
0-1	0	3.60	5017	0.46	0.157	0.44	0.162	0.159
0-1	0	5.11	6032	0.54	0.221	0.51	0.224	0.222
0-1	0	7.55	7374	0.70	0.309	0.68	0.309	0.309
0-1	0	10.53	8756	0.83	0.423	0.76	0.428	0.426
0-1	0	15.36	10637	1.06	0.604	0.96	0.593	0.598
0-1	0	21.28	12569	1.32	0.818	1.21	0.819	0.819
0-1	0	25.23	13710	1.48	0.939	1.34	0.934	0.937
0-1	0	29.75	14912	1.67	1.087	1.52	1.098	1.092
0-1	0	35.60	16341	1.91	1.270	1.73	1.280	1.275
0-1	0	40.07	17384	2.09	1.398	1.88	1.404	1.406
0-1	0	45.46	18502	2.32	1.590	2.09	1.581	1.585
0-1	0	50.12	19441	2.52	1.740	2.28	1.758	1.749
1-1	32.1	8.70	8683	1.25	0.684	1.12	0.657	0.671
1-1	32.1	12.70	10547	1.35	0.760	1.17	0.702	0.731
1-1	32.1	18.45	12765	1.55	0.917	1.52	1.008	0.962
1-1	32.1	20.25	13383	1.67	1.010	1.58	1.060	1.035
1-1	32.1	24.40	14706	1.85	1.149	1.72	1.182	1.165
1-1	32.1	29.10	16071	2.00	1.266	2.00	1.429	1.347

* D.P. cell output due to pressure drop across the venturi meter.
** D.P. cell output due to pressure drop across pipeline section 1.
*** D.P. cell output due to pressure drop across pipeline section 2.

(1)	(2)	(3)	(4)	(5)	(6)	(7)	(8)	(9)
1-1	32.1	30.30	16400	2.10	1.343	2.00	1.429	1.386
1-1	32.1	34.00	17383	2.30	1.499	2.20	1.603	1.551
1-1	32.1	35.25	17706	2.40	1.576	2.25	1.648	1.612
1-1	32.1	39.80	18818	2.65	1.771	2.35	1.735	1.753
1-1	32.1	41.10	19130	2.62	1.746	2.40	1.780	1.763
1-1	32.1	46.00	20259	2.95	2.002	2.65	1.999	2.000
1-1	32.1	47.30	20583	2.98	2.026	2.70	2.041	2.033
1-1	32.1	50.15	21406	3.10	2.119	2.78	2.114	2.116
1-1	32.1	51.85	22017	3.28	2.260	2.98	2.288	2.274
1-2	37.2	7.70	8318	1.33	0.745	1.12	0.657	0.700
1-2	37.2	12.70	10765	1.40	0.800	1.23	0.754	0.777
1-2	37.2	15.60	11959	1.40	0.800	1.33	0.841	0.820
1-2	37.2	17.80	12788	1.55	0.917	1.30	0.817	0.867
1-2	37.2	19.40	13365	1.60	0.955	1.40	0.904	0.925
1-2	37.2	24.40	15012	2.00	1.266	1.65	1.123	1.195
1-2	37.2	28.30	16177	2.10	1.343	1.92	1.359	1.351
1-2	37.2	31.25	17012	2.45	1.614	2.12	1.533	1.523
1-2	37.2	33.75	17677	2.60	1.731	2.05	1.474	1.602
1-2	37.2	35.60	18159	2.45	1.614	2.25	1.648	1.631
1-2	37.2	39.40	19112	2.60	1.731	2.40	1.780	1.756
1-2	37.2	42.70	19906	2.75	1.848	2.50	1.867	1.858
1-2	37.2	43.35	20047	2.82	1.903	2.55	1.912	1.908
1-2	37.2	45.60	20565	2.85	1.925	2.62	1.972	1.948
1-2	37.2	46.30	20747	2.98	2.026	2.75	2.086	2.056
1-2	37.2	47.80	21141	3.07	2.097	2.85	2.173	2.135
1-3	42.0	11.35	10300	1.50	0.878	1.35	0.859	0.869
1-3	42.0	11.90	10547	1.50	0.878	1.35	0.859	0.869
1-3	42.0	13.70	11341	1.50	0.878	1.33	0.841	0.860
1-3	42.0	14.20	11547	1.45	0.838	1.35	0.859	0.848
1-3	42.0	18.55	13230	1.50	0.878	1.37	0.876	0.877
1-3	42.0	18.70	13283	1.50	0.878	1.40	0.904	0.891
1-3	42.0	21.70	14330	1.55	0.917	1.45	0.945	0.931
1-3	42.0	23.95	15065	1.63	0.979	1.48	0.973	0.976
1-3	42.0	28.50	16447	1.85	1.149	1.67	1.140	1.145

(1)	(2)	(3)	(4)	(5)	(6)	(7)	(8)	(9)
1-3	42.0	29.80	16824	1.95	1.226	1.78	1.237	1.231
1-3	42.0	33.75	17906	2.25	1.460	2.05	1.474	1.467
1-3	42.0	39.20	19312	2.60	1.731	2.45	1.822	1.776
1-3	42.0	43.10	20259	2.80	1.887	2.55	1.912	1.899
1-3	42.0	44.50	20583	2.90	1.964	2.68	2.024	1.994
1-3	42.0	45.90	20977	2.93	1.987	2.70	2.041	2.014
1-3	42.0	48.60	21641	3.05	2.081	2.85	2.173	2.127
1-4	47.2	13.30	11388	2.05	1.305	1.85	1.297	1.300
1-4	47.2	15.40	12271	2.10	1.343	1.80	1.254	1.299
1-4	47.2	18.70	13541	2.10	1.343	1.92	1.359	1.351
1-4	47.2	21.85	14653	2.15	1.382	1.85	1.297	1.340
1-4	47.2	25.50	15847	2.28	1.484	2.00	1.429	1.456
1-4	47.2	27.60	16494	2.20	1.420	2.10	1.516	1.468
1-4	47.2	29.00	16912	2.40	1.576	2.15	1.561	1.569
1-4	47.2	32.00	17771	2.40	1.576	2.18	1.586	1.581
1-4	47.2	33.75	18253	2.48	1.638	2.30	1.693	1.666
1-4	47.2	35.70	18783	2.60	1.731	2.28	1.675	1.703
1-4	47.2	41.80	20324	2.70	1.808	2.57	1.929	1.868
1-4	47.2	44.00	20865	3.02	2.057	2.75	2.086	2.072
1-4	47.2	49.20	22230	3.40	2.353	2.98	2.288	2.320
1-4	47.2	5.75	23188	3.50	2.430	3.10	2.392	2.411
2-1	26.7	9.30	8835	1.50	0.878	1.37	0.876	0.877
2-1	26.7	14.10	10941	1.55	0.917	1.45	0.945	0.931
2-1	26.7	17.30	12141	1.60	0.955	1.50	0.991	0.973
2-1	26.7	20.20	13141	1.65	0.994	1.52	1.008	1.001
2-1	26.7	22.70	13941	1.70	1.031	1.58	1.060	1.045
2-1	26.7	24.55	14506	1.75	1.072	1.63	1.105	1.089
2-1	26.7	28.75	15706	1.92	1.203	1.75	1.210	1.207
2-1	26.7	32.40	16682	2.10	1.343	1.90	1.342	1.342
2-1	26.7	36.70	17759	2.23	1.444	2.07	1.493	1.469
2-1	26.7	39.15	18353	2.30	1.499	2.15	1.561	1.530
2-1	26.7	43.30	19300	2.50	1.654	2.25	1.648	1.651
2-1	26.7	46.50	20030	2.62	1.746	2.40	1.780	1.763
2-1	26.7	50.80	21253	2.85	1.925	2.55	1.912	1.918
2-1	26.7	52.75	22147	3.05	2.081	2.75	2.086	2.083

(1)	(2)	(3)	(4)	(5)	(6)	(7)	(8)	(9)
2-2	39.5	7.55	8241	1.30	0.723	1.23	0.754	0.738
2-2	39.5	12.15	10535	1.45	0.838	1.35	0.859	0.848
2-2	39.5	17.90	12847	1.52	0.893	1.45	0.945	0.919
2-2	39.5	20.50	13759	1.60	0.955	1.50	0.991	0.973
2-2	39.5	23.50	14741	1.70	1.031	1.60	1.078	1.050
2-2	39.5	30.80	16906	2.10	1.343	1.95	1.380	1.361
2-2	39.5	35.60	17812	2.28	1.484	2.12	1.533	1.508
2-2	39.5	36.60	18430	2.32	1.515	2.18	1.586	1.550
2-2	39.5	40.50	19406	2.50	1.654	2.32	1.735	1.694
2-2	39.5	44.00	20235	2.65	1.771	2.45	1.822	1.796
2-2	39.5	47.80	21165	2.85	1.925	2.65	1.999	1.962
2-2	39.5	49.00	21500	3.00	2.042	2.70	2.041	2.041
2-2	39.5	49.20	21571	2.90	1.964	2.70	2.041	2.002
2-2	39.5	52.30	22735	3.28	2.260	2.95	2.260	2.260
2-3	44.6	16.00	12383	1.75	1.072	1.60	1.078	1.075
2-3	44.6	18.60	13371	1.65	0.995	1.52	1.008	1.001
2-3	44.6	19.70	13765	1.80	1.111	1.60	1.078	1.095
2-3	44.6	20.80	14153	1.70	1.031	1.60	1.078	1.055
2-3	44.6	23.50	15060	1.75	1.072	1.65	1.123	1.097
2-3	44.6	25.70	15747	1.78	1.096	1.67	1.140	1.118
2-3	44.6	26.30	15941	1.80	1.111	1.70	1.165	1.138
2-3	44.6	29.50	16888	1.90	1.188	1.80	1.254	1.221
2-3	44.6	31.70	17506	2.05	1.305	1.90	1.342	1.318
2-3	44.6	35.80	18612	2.30	1.499	2.12	1.533	1.516
2-3	44.6	36.40	18770	2.30	1.499	2.12	1.533	1.516
2-3	44.6	39.70	19606	2.50	1.654	2.32	1.710	1.682
2-3	44.6	42.90	20394	2.68	1.793	2.43	1.805	1.800
2-3	44.6	43.70	20582	2.70	1.808	2.50	1.867	1.838
2-3	44.6	45.00	20894	2.80	1.887	2.60	1.954	1.920
2-3	44.6	46.00	21124	2.80	1.887	2.60	1.954	1.920
2-3	44.6	46.30	21212	2.82	1.903	2.60	1.954	1.929
2-3	44.6	47.40	21500	2.90	1.964	2.62	1.972	1.968
2-3	44.6	48.90	21935	2.98	2.026	2.70	2.041	2.033
2-3	44.6	50.10	22306	3.00	2.042	2.80	2.131	2.087

(1)	(2)	(3)	(4)	(5)	(6)	(7)	(8)	(9)
2-4	54.4	13.50	11741	2.30	1.499	2.18	1.586	1.542
2-4	54.4	14.40	12135	2.35	1.537	2.12	1.533	1.535
2-4	54.4	18.80	13900	2.25	1.460	2.05	1.474	1.467
2-4	54.4	19.80	14270	2.30	1.499	2.10	1.516	1.508
2-4	54.4	23.80	15659	2.35	1.537	2.12	1.533	1.535
2-4	54.4	26.10	16406	2.32	1.515	2.18	1.586	1.550
2-4	54.4	29.50	17453	2.45	1.614	2.20	1.603	1.608
2-4	54.4	30.00	17606	2.50	1.654	2.25	1.648	1.651
2-4	54.4	35.00	19030	2.60	1.731	2.43	1.805	1.768
2-4	54.4	35.40	19118	2.72	1.823	2.55	1.912	1.867
2-4	54.4	39.20	20147	2.95	2.002	2.70	2.041	2.021
2-4	54.4	41.60	20753	3.17	2.174	2.95	2.260	2.217
2-4	54.4	43.40	21206	3.40	2.353	3.05	2.350	2.351
2-4	54.4	46.90	22094	3.60	2.507	3.50	2.743	2.625
2-4	54.4	50.50	23200	3.97	2.794	3.80	3.007	2.900
2-4	54.4	50.90	23365	4.10	2.895	4.05	3.226	3.060
2-4	54.4	52.40	24047	4.47	3.182	4.20	3.356	3.269
2-4	54.4	52.60	24177	4.45	3.166	4.25	3.401	3.283

TABLE 2C

INITIAL INTERPRETATION OF PIPELINE DATA

(1) Test Number	(2) Percent Solids	(3) Average Pressure Drop per. 100 ft.	(4) Flow Rate V ft. per.sec.	(5) V^2	(6) Friction Factor	(7) Reynolds Number* X 10^{-4}
0-1	0	0.112	0.975	0.951	0.00686	1.413
0-1	0	0.159	1.166	1.360	0.00681	1.689
0-1	0	0.222	1.402	1.966	0.00658	2.031
0-1	0	0.309	1.714	2.939	0.00611	2.483
0-1	0	0.426	2.036	4.143	0.00598	2.948
0-1	0	0.598	2.473	6.115	0.00569	3.582
0-1	0	0.819	2.922	8.538	0.00558	4.232
0-1	0	0.937	3.187	10.158	0.00536	4.617
0-1	0	1.092	3.467	12.017	0.00529	5.021
0-1	0	1.275	3.799	14.431	0.00514	5.503
0-1	0	1.406	4.041	16.332	0.00501	5.854
0-1	0	1.585	4.301	18.500	0.00499	6.230
0-1	0	1.749	4.519	20.425	0.00498	6.546
1-1	32.1	0.671	1.715	2.940	0.01130	2.924
1-1	32.1	0.731	2.083	4.340	0.00832	3.552
1-1	32.1	0.962	2.521	6.355	0.00748	4.300
1-1	32.1	1.035	2.643	6.985	0.00732	4.507
1-1	32.1	1.165	2.904	8.435	0.00683	4.952
1-1	32.1	1.347	3.174	10.080	0.00660	5.366
1-1	32.1	1.386	3.239	10.490	0.00653	5.523

* Based upon the density of the flowing fluid and the viscosity of water at the pipeline conditions.

(1)	(2)	(3)	(4)	(5)	(6)	(7)
1-1	32.1	1.551	3.433	11.780	0.00651	5.856
1-1	32.1	1.612	3.497	12.230	0.00651	5.963
1-1	32.1	1.753	3.716	13.810	0.00627	6.336
1-1	32.1	1.763	3.777	14.270	0.00611	6.440
1-1	32.1	2.000	4.001	16.010	0.00617	6.822
1-1	32.1	2.033	4.065	16.530	0.00607	6.931
1-1	32.1	2.116	4.228	17.875	0.00585	7.209
1-1	32.1	2.274	4.348	18.910	0.00594	7.414
1-2	37.2	0.700	1.577	2.496	0.01330	2.801
1-2	37.2	0.777	2.041	4.165	0.00885	3.625
1-2	37.2	0.820	2.267	5.140	0.00756	4.027
1-2	37.2	0.867	2.424	5.875	0.00700	4.306
1-2	37.2	0.925	2.533	6.415	0.00684	4.500
1-2	37.2	1.195	2.846	8.100	0.00700	5.055
1-2	37.2	1.351	3.067	9.405	0.00682	5.448
1-2	37.2	1.523	3.225	10.400	0.00695	5.729
1-2	37.2	1.602	3.351	11.230	0.00676	5.952
1-2	37.2	1.631	3.442	11.850	0.00653	6.114
1-2	37.2	1.756	3.623	13.130	0.00635	6.436
1-2	37.2	1.858	3.773	14.240	0.00619	6.702
1-2	37.2	1.908	3.800	14.440	0.00627	6.750
1-2	37.2	1.948	3.898	15.195	0.00608	6.924
1-2	37.2	2.056	3.933	15.470	0.00631	6.986
1-2	37.2	2.135	4.007	16.060	0.00631	7.118
1-3	42.0	0.869	1.902	3.617	0.01110	3.468
1-3	42.0	0.869	1.948	3.794	0.01060	3.552
1-3	42.0	0.860	2.095	4.390	0.00905	3.820
1-3	42.0	0.848	2.132	4.545	0.00862	3.887
1-3	42.0	0.877	2.443	5.970	0.00679	4.454
1-3	42.0	0.891	2.453	6.015	0.00684	4.473
1-3	42.0	0.931	2.646	7.000	0.00615	4.824
1-3	42.0	0.976	2.782	7.740	0.00583	5.072
1-3	42.0	1.145	3.037	9.225	0.00574	5.537
1-3	42.0	1.231	3.107	9.655	0.00589	5.665

(1)	(2)	(3)	(4)	(5)	(6)	(7)
1-3	42.0	1.467	3.307	10.920	0.00620	6.030
1-3	42.0	1.776	3.567	12.720	0.00645	6.504
1-3	42.0	1.899	3.741	13.995	0.00627	6.821
1-3	42.0	1.994	3.801	14.445	0.00638	6.930
1-3	42.0	2.014	3.874	15.010	0.00620	7.063
1-3	42.0	2.127	3.997	15.980	0.00615	7.288
1-4	47.2	1.300	2.024	4.098	0.01410	3.834
1-4	47.2	1.299	2.181	4.758	0.01210	4.132
1-4	47.2	1.351	2.407	5.795	0.01040	4.560
1-4	47.2	1.340	2.604	6.780	0.00879	4.933
1-4	47.2	1.456	2.817	7.935	0.00816	5.337
1-4	47.2	1.468	2.932	8.595	0.00760	5.555
1-4	47.2	1.569	3.006	9.035	0.00773	5.695
1-4	47.2	1.581	3.159	9.980	0.00705	5.985
1-4	47.2	1.666	3.244	10.525	0.00704	6.146
1-4	47.2	1.703	3.338	11.140	0.00680	6.324
1-4	47.2	1.868	3.612	13.045	0.00637	6.843
1-4	47.2	2.072	3.709	13.760	0.00670	7.027
1-4	47.2	2.320	3.951	15.610	0.00661	7.485
1-4	47.2	2.411	4.121	16.980	0.00632	7.807
2-1	26.7	0.877	1.805	3.257	0.01380	2.975
2-1	26.7	0.931	2.235	4.995	0.00953	3.684
2-1	26.7	0.973	2.480	6.150	0.00809	4.087
2-1	26.7	1.001	2.685	7.210	0.00709	4.425
2-1	26.7	1.045	2.848	8.110	0.00659	4.694
2-1	26.7	1.089	2.964	8.785	0.00634	4.885
2-1	26.7	1.207	3.209	10.300	0.00599	5.289
2-1	26.7	1.342	3.408	11.615	0.00591	5.617
2-1	26.7	1.469	3.628	13.165	0.00571	5.979
2-1	26.7	1.530	3.750	14.060	0.00556	6.180
2-1	26.7	1.651	3.943	15.550	0.00543	6.498
2-1	26.7	1.763	4.092	16.740	0.00539	6.744
2-1	26.7	1.918	4.342	18.850	0.00520	7.156
2-1	26.7	2.083	4.525	20.470	0.00520	7.458

(1)	(2)	(3)	(4)	(5)	(6)	(7)
2-2	39.5	0.738	1.558	2.426	0.01440	2.774
2-2	39.5	0.848	1.992	3.970	0.01010	3.547
2-2	39.5	0.919	2.429	5.900	0.00737	4.325
2-2	39.5	0.973	2.602	6.770	0.00680	4.633
2-2	39.5	1.050	2.788	7.775	0.00639	4.965
2-2	39.5	1.361	3.197	10.220	0.00630	5.693
2-2	39.5	1.508	3.368	11.340	0.00629	5.997
2-2	39.5	1.550	3.485	12.140	0.00604	6.205
2-2	39.5	1.694	3.670	13.465	0.00595	6.535
2-2	39.5	1.796	3.826	14.640	0.00581	6.813
2-2	39.5	1.962	4.002	16.020	0.00579	7.126
2-2	39.5	2.041	4.066	16.530	0.00584	7.240
2-2	39.5	2.002	4.079	16.640	0.00569	7.263
2-2	39.5	2.260	4.300	18.490	0.00578	7.657
2-3	44.6	1.075	2.246	5.045	0.00967	4.170
2-3	44.6	1.001	2.425	5.880	0.00773	4.502
2-3	44.6	1.095	2.497	6.235	0.00797	4.636
2-3	44.6	1.055	2.567	6.590	0.00727	4.766
2-3	44.6	1.097	2.731	7.460	0.00668	5.070
2-3	44.6	1.118	2.856	8.155	0.00622	5.302
2-3	44.6	1.138	2.891	8.360	0.00618	5.367
2-3	44.6	1.221	3.063	9.380	0.00591	5.686
2-3	44.6	1.318	3.175	10.085	0.00593	5.894
2-3	44.6	1.516	3.376	11.400	0.00604	6.268
2-3	44.6	1.516	3.404	11.590	0.00594	6.320
2-3	44.6	1.682	3.556	12.640	0.00604	6.602
2-3	44.6	1.800	3.699	13.680	0.00597	6.867
2-3	44.6	1.838	3.733	13.940	0.00600	6.930
2-3	44.6	1.920	3.790	14.360	0.00607	7.036
2-3	44.6	1.920	3.831	14.675	0.00594	7.112
2-3	44.6	1.929	3.847	14.800	0.00592	7.142
2-3	44.6	1.968	3.900	15.210	0.00587	7.240
2-3	44.6	2.033	3.978	15.820	0.00583	7.385
2-3	44.6	2.087	4.046	16.370	0.00578	7.511

(1)	(2)	(3)	(4)	(5)	(6)	(7)
2-4	54.4	1.542	1.992	3.970	0.01650	3.953
2-4	54.4	1.535	2.059	4.240	0.01540	4.086
2-4	54.4	1.467	2.358	5.560	0.01140	4.679
2-4	54.4	1.508	2.421	5.860	0.01090	4.804
2-4	54.4	1.535	2.657	7.060	0.00923	5.273
2-4	54.4	1.550	2.784	7.750	0.00849	5.525
2-4	54.4	1.608	2.961	8.770	0.00779	5.876
2-4	54.4	1.651	2.987	8.920	0.00786	5.928
2-4	54.4	1.768	3.229	10.425	0.00720	6.408
2-4	54.4	1.867	3.244	10.525	0.00753	6.438
2-4	54.4	2.021	3.418	11.680	0.00735	6.783
2-4	54.4	2.217	3.521	12.400	0.00774	6.987
2-4	54.4	2.351	3.598	12.940	0.00772	7.140
2-4	54.4	2.625	3.749	14.050	0.00793	7.440
2-4	54.4	2.900	3.936	15.500	0.00795	7.811
2-4	54.4	3.060	3.964	15.720	0.00827	7.867
2-4	54.4	2.369	4.080	16.650	0.00834	8.097
2-4	54.4	3.283	4.102	16.830	0.00828	8.140

APPENDIX D

INTERPRETATION OF THE PIPELINE DATA ASSUMING BINGHAM PLASTIC BEHAVIOUR

TABLE 1D

INTERPRETATION ASSUMING BINGHAM PLASTIC BEHAVIOUR

(Laminar Flow Data)

(1)	(2)	(3)	(4)	(5)	(6)	(7)	(8)
Test Number	Apparent Coefficient of Rigidity lb_m per. ft. sec.	Apparent Yield Stress lb_F per. $ft.^2$	Flow Rate V ft. per.sec.	Apparent Bingham Reynolds Number (R_m)	Friction Factor (f)	f x R_m	Apparent Bingham Yield Number
1-1	0.00198	0.0130	1.715	9918	0.01130	112.10	16.59
1-1	0.00198	0.0130	2.083	12050	0.00832	110.30	13.66
1-2	0.00255	0.0185	1.577	7377	0.01330	98.11	20.96
1-2	0.00255	0.0185	2.041	9548	0.00885	84.50	16.20
1-2	0.00255	0.0185	2.267	10610	0.00756	80.21	14.50
1-2	0.00255	0.0185	2.424	11340	0.00700	79.38	13.65
1-3	0.00333	0.0255	1.902	6994	0.01110	77.63	20.25
1-3	0.00333	0.0255	1.948	7163	0.01060	75.93	19.77
1-3	0.00333	0.0255	2.095	7703	0.00905	69.71	18.38
1-3	0.00333	0.0255	2.132	7839	0.00862	67.57	18.06
1-3	0.00333	0.0255	2.443	8983	0.00679	60.99	15.76
1-3	0.00333	0.0255	2.453	9020	0.00684	61.70	15.70
1-3	0.00333	0.0255	2.646	9729	0.00615	59.83	14.55
1-4	0.00450	0.0350	2.024	5724	0.01410	80.71	20.76
1-4	0.00450	0.0350	2.181	6168	0.01210	74.63	19.22
1-4	0.00450	0.0350	2.407	6807	0.01040	70.79	17.46
1-4	0.00450	0.0350	2.604	7364	0.00879	64.73	16.14
2-1	0.00116	0.0021	1.805	17220	0.01380	237.60	5.05
2-1	0.00116	0.0021	2.235	21320	0.00953	203.20	4.08

(1)	(2)	(3)	(4)	(5)	(6)	(7)	(8)
2-1	0.00116	0.0021	2.480	23660	0.00809	191.40	3.67
2-1	0.00116	0.0021	2.685	25620	0.00709	181.60	3.39
2-1	0.00116	0.0021	2.848	27170	0.00659	179.10	3.20
2-2	0.00188	0.0050	1.558	9910	0.01440	142.70	8.50
2-2	0.00188	0.0050	1.992	12670	0.01010	128.00	6.71
2-2	0.00188	0.0050	2.429	15450	0.00737	113.90	5.50
2-2	0.00188	0.0050	2.602	16550	0.00680	112.50	5.14
2-3	0.00252	0.0071	2.246	11113	0.00967	107.46	6.31
2-3	0.00252	0.0071	2.425	12000	0.00773	92.76	5.84
2-3	0.00252	0.0071	2.497	12355	0.00797	98.47	5.67
2-3	0.00252	0.0071	2.567	12701	0.00727	92.34	5.52
2-3	0.00252	0.0071	2.731	13513	0.00668	90.27	5.19
2-3	0.00252	0.0071	2.856	14131	0.00622	87.89	4.96
2-3	0.00252	0.0071	2.891	14304	0.00618	88.39	4.90
2-4	0.00522	0.0158	1.992	5086	0.01650	83.92	7.64
2-4	0.00522	0.0158	2.059	5257	0.01540	80.96	7.39
2-4	0.00522	0.0158	2.358	6020	0.01140	68.63	6.45
2-4	0.00522	0.0158	2.421	6181	0.01090	67.37	6.29
2-4	0.00522	0.0158	2.657	6784	0.00923	62.62	5.73
2-4	0.00522	0.0158	2.784	7108	0.00849	60.35	5.47
2-4	0.00522	0.0158	2.961	7560	0.00779	58.89	5.14
2-4	0.00522	0.0158	2.987	7626	0.00786	59.94	5.09

TABLE 2D

INTERPRETATION ASSUMING BINGHAM PLASTIC BEHAVIOUR

(Turbulent Flow Data)

(1) Test Number	(2) Apparent Coefficient of Rigidity lb_m per. ft. sec.	(3) Apparent Yield Stress lb_F per. ft^2.	(4) Flow Rate V ft. per.sec.	(5) Apparent Bingham Reynolds Number	(6) Friction Factor	(7) Apparent Bingham Yield Number
1-1	0.00191	0.0209	2.521	14580	0.00748	11.28
1-1	0.00191	0.0209	2.643	15280	0.00732	10.76
1-1	0.00191	0.0209	2.904	16790	0.00683	9.79
1-1	0.00191	0.0209	3.174	18360	0.00660	8.96
1-1	0.00191	0.0209	3.239	18730	0.00653	8.77
1-1	0.00191	0.0209	3.433	19850	0.00651	8.28
1-1	0.00191	0.0209	3.497	20220	0.00651	8.13
1-1	0.00191	0.0209	3.716	21490	0.00627	7.65
1-1	0.00191	0.0209	3.777	21840	0.00611	7.52
1-1	0.00191	0.0209	4.001	23140	0.00617	7.11
1-1	0.00191	0.0209	4.065	23510	0.00607	7.00
1-1	0.00191	0.0209	4.228	24450	0.00585	6.73
1-1	0.00191	0.0209	4.348	25140	0.00594	6.53
1-2	0.00272	0.0246	2.533	11850	0.00684	13.00
1-2	0.00272	0.0246	2.846	13310	0.00700	11.61
1-2	0.00272	0.0246	3.067	14350	0.00682	10.78
1-2	0.00272	0.0246	3.225	15090	0.00695	10.25
1-2	0.00272	0.0246	3.351	15680	0.00676	9.83
1-2	0.00272	0.0246	3.442	16100	0.00653	9.60
1-2	0.00272	0.0246	3.623	16950	0.00635	9.12

(1)	(2)	(3)	(4)	(5)	(6)	(7)
1-2	0.00272	0.0246	3.773	17650	0.00619	8.76
1-2	0.00272	0.0246	3.800	17780	0.00627	8.70
1-2	0.00272	0.0246	3.898	18230	0.00608	8.48
1-2	0.00272	0.0246	3.933	18400	0.00631	8.41
1-2	0.00272	0.0246	4.007	18740	0.00631	8.25
1-3	0.00363	0.0301	2.782	10230	0.00583	13.84
1-3	0.00363	0.0301	3.037	11170	0.00574	12.68
1-3	0.00363	0.0301	3.107	11420	0.00589	12.39
1-3	0.00363	0.0301	3.307	12160	0.00620	11.64
1-3	0.00363	0.0301	3.567	13120	0.00645	10.79
1-3	0.00363	0.0301	3.741	13760	0.00627	10.29
1-3	0.00363	0.0301	3.801	13980	0.00638	10.13
1-3	0.00363	0.0301	3.874	14240	0.00620	9.94
1-3	0.00363	0.0301	3.997	14700	0.00615	9.63
1-4	0.00432	0.0427	2.817	7966	0.00816	14.92
1-4	0.00432	0.0427	2.932	8292	0.00760	14.33
1-4	0.00432	0.0427	3.006	8501	0.00773	13.97
1-4	0.00432	0.0427	3.159	8934	0.00705	13.29
1-4	0.00432	0.0427	3.244	9174	0.00704	12.95
1-4	0.00432	0.0427	3.338	9440	0.00680	12.59
1-4	0.00432	0.0427	3.612	10210	0.00637	11.63
1-4	0.00432	0.0427	3.709	10490	0.00670	11.33
1-4	0.00432	0.0427	3.951	11170	0.00661	10.63
1-4	0.00432	0.0427	4.121	11650	0.00632	10.21
2-1	0.00116	0.0021	2.964	28280	0.00634	3.07
2-1	0.00116	0.0021	3.209	30620	0.00599	2.83
2-1	0.00116	0.0021	3.408	32520	0.00591	2.67
2-1	0.00116	0.0021	3.628	34610	0.00571	2.51
2-1	0.00116	0.0021	3.750	35780	0.00556	2.42
2-1	0.00116	0.0021	3.943	37620	0.00543	2.31
2-1	0.00116	0.0021	4.092	39040	0.00539	2.22
2-1	0.00116	0.0021	4.342	41430	0.00520	2.09
2-1	0.00116	0.0021	4.532	43240	0.00520	2.01

(1)	(2)	(3)	(4)	(5)	(6)	(7)
2-2	0.00188	0.0050	2.788	17730	0.00639	4.79
2-2	0.00188	0.0050	3.197	20340	0.00630	4.18
2-2	0.00188	0.0050	3.368	21420	0.00629	3.97
2-2	0.00188	0.0050	3.485	22170	0.00604	3.83
2-2	0.00188	0.0050	3.670	23340	0.00595	3.64
2-2	0.00188	0.0050	3.826	24340	0.00581	3.49
2-2	0.00188	0.0050	4.002	25460	0.00579	3.34
2-2	0.00188	0.0050	4.066	25860	0.00584	3.29
2-2	0.00188	0.0050	4.079	25950	0.00569	3.28
2-2	0.00188	0.0050	4.300	27350	0.00578	3.11
2-3	0.00252	0.0071	3.063	15160	0.00591	4.62
2-3	0.00252	0.0071	3.175	15710	0.00593	4.46
2-3	0.00252	0.0071	3.376	16700	0.00604	4.20
2-3	0.00252	0.0071	3.404	16840	0.00594	4.16
2-3	0.00252	0.0071	3.556	17590	0.00604	3.98
2-3	0.00252	0.0071	3.699	18300	0.00597	3.83
2-3	0.00252	0.0071	3.733	18470	0.00600	3.79
2-3	0.00252	0.0071	3.790	18750	0.00607	3.74
2-3	0.00252	0.0071	3.831	18960	0.00596	3.70
2-3	0.00252	0.0071	3.847	19030	0.00592	3.68
2-3	0.00252	0.0071	3.900	19300	0.00587	3.63
2-3	0.00252	0.0071	3.978	19680	0.00583	3.56
2-3	0.00252	0.0071	4.046	20020	0.00578	3.50
2-4	0.00522	0.0158	3.229	8244	0.00720	4.71
2-4	0.00522	0.0158	3.244	8283	0.00753	4.69
2-4	0.00522	0.0158	3.418	8727	0.00735	4.45
2-4	0.00522	0.0158	3.521	8990	0.00774	4.32
2-4	0.00522	0.0158	3.598	9186	0.00772	4.23
2-4	0.00522	0.0158	3.749	9572	0.00793	4.06
2-4	0.00522	0.0158	3.936	10050	0.00795	3.86
2-4	0.00522	0.0158	3.964	10120	0.00827	3.84
2-4	0.00522	0.0158	4.080	10420	0.00836	3.73
2-4	0.00522	0.0158	4.102	10470	0.00828	3.71

APPENDIX E

INTERPRETATION OF THE PIPELINE DATA ASSUMING POWER-LAW PSEUDOPLASTIC BEHAVIOUR

TABLE 1E

INTERPRETATION ASSUMING POWER LAW PSEUDOPLASTIC BEHAVIOUR

(1) Test Number	(2) Power Law Exponent n'	(3) Power Law Constant K	(4) K'	(5) γ	(6) Flow Rate V ft. per.sec.	(7) $V^{2-n'}$	(8) Power Law Reynolds Number	(9) Friction Factor
1-1	0.397	3.42×10^{-3}	3.89×10^{-3}	3.58×10^{-2}	1.715	2.375	2319	0.01130
1-1	0.397	3.42×10^{-3}	3.89×10^{-3}	3.58×10^{-2}	2.083	3.250	3174	0.00832
1-1	0.397	3.42×10^{-3}	3.89×10^{-3}	3.58×10^{-2}	2.521	4.410	4306	0.00748
1-1	0.397	3.42×10^{-3}	3.89×10^{-3}	3.58×10^{-2}	2.643	4.760	4648	0.00732
1-1	0.397	3.42×10^{-3}	3.89×10^{-3}	3.58×10^{-2}	2.904	5.540	5410	0.00683
1-1	0.397	3.42×10^{-3}	3.89×10^{-3}	3.58×10^{-2}	3.174	6.400	6250	0.00660
1-1	0.397	3.42×10^{-3}	3.89×10^{-3}	3.58×10^{-2}	3.239	6.580	6425	0.00653
1-1	0.397	3.42×10^{-3}	3.89×10^{-3}	3.58×10^{-2}	3.433	7.210	7041	0.00651
1-1	0.397	3.42×10^{-3}	3.89×10^{-3}	3.58×10^{-2}	3.497	7.410	7236	0.00651
1-1	0.397	3.42×10^{-3}	3.89×10^{-3}	3.58×10^{-2}	3.716	8.200	8007	0.00627
1-1	0.397	3.42×10^{-3}	3.89×10^{-3}	3.58×10^{-2}	3.777	8.420	8222	0.00611
1-1	0.397	3.42×10^{-3}	3.89×10^{-3}	3.58×10^{-2}	4.001	9.250	9033	0.00617
1-1	0.397	3.42×10^{-3}	3.89×10^{-3}	3.58×10^{-2}	4.065	9.500	9277	0.00607
1-1	0.397	3.42×10^{-3}	3.89×10^{-3}	3.58×10^{-2}	4.228	10.100	9863	0.00585
1-1	0.397	3.42×10^{-3}	3.89×10^{-3}	3.58×10^{-2}	4.348	10.550	10300	0.00594
1-2	0.369	5.13×10^{-3}	5.85×10^{-3}	5.08×10^{-2}	1.577	2.102	1589	0.01330
1-2	0.369	5.13×10^{-3}	5.85×10^{-3}	5.08×10^{-2}	2.041	3.210	2427	0.00885
1-2	0.369	5.13×10^{-3}	5.85×10^{-3}	5.08×10^{-2}	2.267	3.810	2880	0.00756
1-2	0.369	5.13×10^{-3}	5.85×10^{-3}	5.08×10^{-2}	2.424	4.240	3205	0.00700
1-2	0.369	5.13×10^{-3}	5.85×10^{-3}	5.08×10^{-2}	2.533	4.550	3440	0.00684
1-2	0.369	5.13×10^{-3}	5.85×10^{-3}	5.08×10^{-2}	2.846	5.350	4045	0.00700
1-2	0.369	5.13×10^{-3}	5.85×10^{-3}	5.08×10^{-2}	3.067	6.230	4710	0.00682
1-2	0.369	5.13×10^{-3}	5.85×10^{-3}	5.08×10^{-2}	3.225	6.760	5111	0.00695
1-2	0.369	5.13×10^{-3}	5.85×10^{-3}	5.08×10^{-2}	3.351	6.920	5232	0.00676

(1)	(2)	(3)	(4)	(5)	(6)	(7)	(8)	(9)
1-2	0.369	5.13×10^{-3}	5.85×10^{-3}	5.08×10^{-2}	3.442	7.500	5670	0.00653
1-2	0.369	5.13×10^{-3}	5.85×10^{-3}	5.08×10^{-2}	3.623	8.180	6184	0.00635
1-2	0.369	5.13×10^{-3}	5.85×10^{-3}	5.08×10^{-2}	3.773	8.720	6592	0.00619
1-2	0.369	5.13×10^{-3}	5.85×10^{-3}	5.08×10^{-2}	3.800	8.820	6668	0.00627
1-2	0.369	5.13×10^{-3}	5.85×10^{-3}	5.08×10^{-2}	3.898	9.200	6955	0.00608
1-2	0.369	5.13×10^{-3}	5.85×10^{-3}	5.08×10^{-2}	3.933	9.320	7046	0.00631
1-2	0.369	5.13×10^{-3}	5.85×10^{-3}	5.08×10^{-2}	4.007	9.620	7273	0.00631
1-3	0.347	7.32×10^{-3}	8.38×10^{-3}	6.95×10^{-2}	1.902	2.900	1717	0.01110
1-3	0.347	7.32×10^{-3}	8.38×10^{-3}	6.95×10^{-2}	1.948	3.010	1782	0.01060
1-3	0.347	7.32×10^{-3}	8.38×10^{-3}	6.95×10^{-2}	2.095	3.400	2013	0.00905
1-3	0.347	7.32×10^{-3}	8.38×10^{-3}	6.95×10^{-2}	2.132	3.500	2072	0.00862
1-3	0.347	7.32×10^{-3}	8.38×10^{-3}	6.95×10^{-2}	2.443	4.380	2593	0.00679
1-3	0.347	7.32×10^{-3}	8.38×10^{-3}	6.95×10^{-2}	2.453	4.410	2611	0.00684
1-3	0.347	7.32×10^{-3}	8.38×10^{-3}	6.95×10^{-2}	2.646	5.000	2960	0.00615
1-3	0.347	7.32×10^{-3}	8.38×10^{-3}	6.95×10^{-2}	2.782	5.440	3220	0.00583
1-3	0.347	7.32×10^{-3}	8.38×10^{-3}	6.95×10^{-2}	3.037	6.270	3712	0.00574
1-3	0.347	7.32×10^{-3}	8.38×10^{-3}	6.95×10^{-2}	3.107	6.520	3860	0.00589
1-3	0.347	7.32×10^{-3}	8.38×10^{-3}	6.95×10^{-2}	3.307	7.230	4280	0.00620
1-3	0.347	7.32×10^{-3}	8.38×10^{-3}	6.95×10^{-2}	3.567	8.200	4854	0.00645
1-3	0.347	7.32×10^{-3}	8.38×10^{-3}	6.95×10^{-2}	3.741	8.820	5221	0.00627
1-3	0.347	7.32×10^{-3}	8.38×10^{-3}	6.95×10^{-2}	3.801	9.100	5387	0.00638
1-3	0.347	7.32×10^{-3}	8.38×10^{-3}	6.95×10^{-2}	3.874	9.400	5565	0.00620
1-3	0.347	7.32×10^{-3}	8.38×10^{-3}	6.95×10^{-2}	3.997	9.910	5867	0.00615
1-4	0.327	1.045×10^{-2}	1.197×10^{-2}	9.52×10^{-2}	2.024	3.260	1519	0.01410
1-4	0.327	1.045×10^{-2}	1.197×10^{-2}	9.52×10^{-2}	2.181	3.690	1720	0.01210
1-4	0.327	1.045×10^{-2}	1.197×10^{-2}	9.52×10^{-2}	2.407	4.360	2032	0.01040
1-4	0.327	1.045×10^{-2}	1.197×10^{-2}	9.52×10^{-2}	2.604	4.960	2312	0.00879
1-4	0.327	1.045×10^{-2}	1.197×10^{-2}	9.52×10^{-2}	2.817	5.650	2633	0.00816
1-4	0.327	1.045×10^{-2}	1.197×10^{-2}	9.52×10^{-2}	2.932	6.050	2820	0.00760
1-4	0.327	1.045×10^{-2}	1.197×10^{-2}	9.52×10^{-2}	3.006	6.310	2941	0.00773
1-4	0.327	1.045×10^{-2}	1.197×10^{-2}	9.52×10^{-2}	3.159	6.870	3202	0.00705
1-4	0.327	1.045×10^{-2}	1.197×10^{-2}	9.52×10^{-2}	3.244	7.180	3347	0.00704
1-4	0.327	1.045×10^{-2}	1.197×10^{-2}	9.52×10^{-2}	3.338	7.500	3496	0.00680
1-4	0.327	1.045×10^{-2}	1.197×10^{-2}	9.52×10^{-2}	3.612	8.600	4008	0.00637
1-4	0.327	1.045×10^{-2}	1.197×10^{-2}	9.52×10^{-2}	3.709	9.000	4195	0.00670

(1)	(2)	(3)	(4)	(5)	(6)	(7)	(8)	(9)
1-4	0.327	1.045×10^{-2}	1.197×10^{-2}	9.52×10^{-2}	3.951	9.980	4652	0.00661
1-4	0.327	1.045×10^{-2}	1.197×10^{-2}	9.52×10^{-2}	4.121	10.700	4987	0.00632
2-1	0.708	0.365×10^{-3}	3.92×10^{-4}	6.88×10^{-3}	1.805	2.145	5918	0.01380
2-1	0.708	0.365×10^{-3}	3.92×10^{-4}	6.88×10^{-3}	2.235	2.822	7786	0.00953
2-1	0.708	0.365×10^{-3}	3.92×10^{-4}	6.88×10^{-3}	2.480	3.240	8929	0.00809
2-1	0.708	0.365×10^{-3}	3.92×10^{-4}	6.88×10^{-3}	2.685	3.580	9877	0.00709
2-1	0.708	0.365×10^{-3}	3.92×10^{-4}	6.88×10^{-3}	2.848	3.860	10650	0.00659
2-1	0.708	0.365×10^{-3}	3.92×10^{-4}	6.88×10^{-3}	2.964	4.070	11230	0.00634
2-1	0.708	0.365×10^{-3}	3.92×10^{-4}	6.88×10^{-3}	3.209	4.520	12470	0.00599
2-1	0.708	0.365×10^{-3}	3.92×10^{-4}	6.88×10^{-3}	3.408	4.900	13520	0.00591
2-1	0.708	0.365×10^{-3}	3.92×10^{-4}	6.88×10^{-3}	3.628	5.290	14600	0.00571
2-1	0.708	0.365×10^{-3}	3.92×10^{-4}	6.88×10^{-3}	3.750	5.510	15200	0.00556
2-1	0.708	0.365×10^{-3}	3.92×10^{-4}	6.88×10^{-3}	3.943	5.880	16220	0.00543
2-1	0.708	0.365×10^{-3}	3.92×10^{-4}	6.88×10^{-3}	4.092	6.180	17050	0.00539
2-1	0.708	0.365×10^{-3}	3.92×10^{-4}	6.88×10^{-3}	4.343	6.670	18400	0.00520
2-1	0.708	0.365×10^{-3}	3.92×10^{-4}	6.88×10^{-3}	4.532	7.050	19450	0.00520
2-2	0.602	1.00×10^{-3}	1.10×10^{-3}	1.55×10^{-2}	1.558	1.860	3004	0.01440
2-2	0.602	1.00×10^{-3}	1.10×10^{-3}	1.55×10^{-2}	1.992	2.620	4231	0.01010
2-2	0.602	1.00×10^{-3}	1.10×10^{-3}	1.55×10^{-2}	2.429	3.460	5588	0.00737
2-2	0.602	1.00×10^{-3}	1.10×10^{-3}	1.55×10^{-2}	2.602	3.810	6153	0.00680
2-2	0.602	1.00×10^{-3}	1.10×10^{-3}	1.55×10^{-2}	2.788	4.190	6767	0.00639
2-2	0.602	1.00×10^{-3}	1.10×10^{-3}	1.55×10^{-2}	3.197	5.080	8204	0.00630
2-2	0.602	1.00×10^{-3}	1.10×10^{-3}	1.55×10^{-2}	3.368	5.470	8834	0.00629
2-2	0.602	1.00×10^{-3}	1.10×10^{-3}	1.55×10^{-2}	3.485	5.730	9254	0.00604
2-2	0.602	1.00×10^{-3}	1.10×10^{-3}	1.55×10^{-2}	3.670	6.180	9981	0.00595
2-2	0.602	1.00×10^{-3}	1.10×10^{-3}	1.55×10^{-2}	3.826	6.520	10530	0.00581
2-2	0.602	1.00×10^{-3}	1.10×10^{-3}	1.55×10^{-2}	4.002	6.950	11220	0.00579
2-2	0.602	1.00×10^{-3}	1.10×10^{-3}	1.55×10^{-2}	4.066	7.120	11500	0.00584
2-2	0.602	1.00×10^{-3}	1.10×10^{-3}	1.55×10^{-2}	4.079	7.150	11550	0.00569
2-2	0.602	1.00×10^{-3}	1.10×10^{-3}	1.55×10^{-2}	4.300	7.690	12420	0.00578
2-3	0.573	1.45×10^{-3}	1.60×10^{-3}	2.12×10^{-2}	3.847	6.840	8885	0.00592
2-3	0.573	1.45×10^{-3}	1.60×10^{-3}	2.12×10^{-2}	3.900	6.980	9067	0.00587

(1)	(2)	(3)	(4)	(5)	(6)	(7)	(8)	(9)
2-3	0.573	1.45×10^{-3}	1.60×10^{-3}	2.12×10^{-2}	3.978	7.170	9314	0.00583
2-3	0.573	1.45×10^{-3}	1.60×10^{-3}	2.12×10^{-2}	4.046	7.340	9535	0.00578
2-3	0.573	1.45×10^{-3}	1.60×10^{-3}	2.12×10^{-2}	2.246	3.175	4124	0.00967
2-3	0.573	1.45×10^{-3}	1.60×10^{-3}	2.12×10^{-2}	2.425	3.540	4598	0.00773
2-3	0.573	1.45×10^{-3}	1.60×10^{-3}	2.12×10^{-2}	2.497	3.690	4793	0.00797
2-3	0.573	1.45×10^{-3}	1.60×10^{-3}	2.12×10^{-2}	2.567	3.840	4988	0.00727
2-3	0.573	1.45×10^{-3}	1.60×10^{-3}	2.12×10^{-2}	2.731	4.190	5443	0.00668
2-3	0.573	1.45×10^{-3}	1.60×10^{-3}	2.12×10^{-2}	2.856	4.460	5794	0.00622
2-3	0.573	1.45×10^{-3}	1.60×10^{-3}	2.12×10^{-2}	2.891	4.540	5497	0.00618
2-3	0.573	1.45×10^{-3}	1.60×10^{-3}	2.12×10^{-2}	3.063	4.940	6417	0.00591
2-3	0.573	1.45×10^{-3}	1.60×10^{-3}	2.12×10^{-2}	3.175	5.210	6768	0.00593
2-3	0.573	1.45×10^{-3}	1.60×10^{-3}	2.12×10^{-2}	3.376	5.670	7365	0.00604
2-3	0.573	1.45×10^{-3}	1.60×10^{-3}	2.12×10^{-2}	3.404	5.740	7456	0.00594
2-3	0.573	1.45×10^{-3}	1.60×10^{-3}	2.12×10^{-2}	3.556	6.110	7937	0.00604
2-3	0.573	1.45×10^{-3}	1.60×10^{-3}	2.12×10^{-2}	3.699	6.470	8405	0.00597
2-3	0.573	1.45×10^{-3}	1.60×10^{-3}	2.12×10^{-2}	3.733	6.550	8508	0.00600
2-3	0.573	1.45×10^{-3}	1.60×10^{-3}	2.12×10^{-2}	3.790	6.700	8703	0.00607
2-3	0.573	1.45×10^{-3}	1.60×10^{-3}	2.12×10^{-2}	3.831	6.790	8820	0.00594
2-4	0.502	3.56×10^{-3}	3.98×10^{-3}	4.55×10^{-2}	1.992	2.805	2072	0.01650
2-4	0.502	3.56×10^{-3}	3.98×10^{-3}	4.55×10^{-2}	2.059	2.945	2175	0.01540
2-4	0.502	3.56×10^{-3}	3.98×10^{-3}	4.55×10^{-2}	2.358	3.610	2666	0.01140
2-4	0.502	3.56×10^{-3}	3.98×10^{-3}	4.55×10^{-2}	2.421	3.760	2777	0.01090
2-4	0.502	3.56×10^{-3}	3.98×10^{-3}	4.55×10^{-2}	2.657	4.320	3191	0.00923
2-4	0.502	3.56×10^{-3}	3.98×10^{-3}	4.55×10^{-2}	2.784	4.640	3427	0.00849
2-4	0.502	3.56×10^{-3}	3.98×10^{-3}	4.55×10^{-2}	2.961	5.090	3759	0.00779
2-4	0.502	3.56×10^{-3}	3.98×10^{-3}	4.55×10^{-2}	2.987	5.160	3811	0.00786
2-4	0.502	3.56×10^{-3}	3.98×10^{-3}	4.55×10^{-2}	3.229	5.790	4276	0.00720
2-4	0.502	3.56×10^{-3}	3.98×10^{-3}	4.55×10^{-2}	3.244	5.830	4306	0.00753
2-4	0.502	3.56×10^{-3}	3.98×10^{-3}	4.55×10^{-2}	3.418	6.300	4653	0.00735
2-4	0.502	3.56×10^{-3}	3.98×10^{-3}	4.55×10^{-2}	3.521	6.600	4875	0.00774
2-4	0.502	3.56×10^{-3}	3.98×10^{-3}	4.55×10^{-2}	3.598	6.800	5022	0.00772
2-4	0.502	3.56×10^{-3}	3.98×10^{-3}	4.55×10^{-2}	3.749	7.240	5347	0.00793
2-4	0.502	3.56×10^{-3}	3.98×10^{-3}	4.55×10^{-2}	3.936	7.800	5761	0.00795
2-4	0.502	3.56×10^{-3}	3.98×10^{-3}	4.55×10^{-2}	3.964	7.900	5835	0.00837
2-4	0.502	3.56×10^{-3}	3.98×10^{-3}	4.55×10^{-2}	4.080	8.200	6057	0.00834
2-4	0.502	3.56×10^{-3}	3.98×10^{-3}	4.55×10^{-2}	4.102	8.290	6123	0.00828

APPENDIX F

TABLE 1F DENSITY AND SETTLING DATA

TABLE 2F PARTICLE SIZE DISTRIBUTION DATA

TABLE 1F

DENSITY AND SETTLING DATA

Test Number	Density of Suspension lb_m per.ft^3	Specific Gravity of Suspension	Initial Settling Rate cm. per. min.
1-1	73.29	1.177	0.820
1-2	76.35	1.226	0.180
1-3	78.37	1.259	0.054
1-4	81.43	1.308	0.030
2-1	70.84	1.137	5.40
2-2	76.54	1.229	2.40
2-3	79.80	1.282	1.00
2-4	85.30	1.370	0.30

TABLE 2F

PARTICLE SIZE DISTRIBUTION DATA

Suspension Number	Sieve - Size		Weight Retained gms.	Weight Percent Retained	Cumulative Percent Retained
	Tyler Mesh	Microns			
1	20	830	0.1	0.018	0.018
1	28	590-830	1.5	0.267	0.285
1	35	420-590	5.3	0.045	1.23
1	48	297-420	15.1	2.68	3.91
1	65	210-297	77.6	13.80	17.71
1	100	149-210	109.7	19.45	37.16
1	150	105-149	56.8	10.10	47.26
1	200	74-105	41.1	7.30	54.56
1	230	62- 74	25.5	4.52	59.08
1	270	53- 62	5.1	0.91	59.99
1	325	44- 53	17.2	3.05	63.04
1	400	37- 44	3.9	0.70	63.74
1	400	37	205.7	36.50	100.00
2	20	830	1.0	0.19	0.19
2	28	590-830	3.0	0.57	0.76
2	35	420-590	7.0	1.34	2.10
2	48	297-420	9.6	1.84	3.94
2	65	210-297	55.7	10.60	14.54
2	100	149-210	87.2	16.65	31.19
2	150	105-149	53.8	10.25	41.44
2	200	74-105	46.2	8.80	50.24
2	230	62- 74	35.1	6.69	56.93
2	270	53-62	11.1	2.01	58.94
2	325	44- 53	28.7	5.47	64.41
2	400	37- 44	5.2	0.99	65.40
2	400	37	181.4	34.60	100.00

TABLE 2F (cont'd)

PARTICLE SIZE DISTRIBUTION DATA

(Sulphur Flour)

Sieve -	Size	Weight % retained		Cumulative % retained	
Tyler Mesh	Microns	Roller	Sieve	Roller	Sieve
35	297-420		0.05		0.05
48	210-297		0.81		0.86
65	149-210		4.89		5.75
100	105-149		3.82		9.57
150	74-105		15.28		24.85
200	62- 74		10.00		35.85
	55- 74	6.63		31.48	
230	53- 62		2.30		38.15
270	44- 53		16.50		54.65
	40- 55	16.92		48.40	
325	37- 44		5.95		59.60
	28- 40	34.51		82.91	
	20-28	4.08		86.99	
	10- 20	10.26		97.25	
	0- 10	2.75			

APPENDIX G

CALIBRATION DATA

TABLE 1G

DIFFERENTIAL PRESSURE CELL CALIBRATION DATA

Manometer Reading Inches of Mercury		Total Pressure Inches of Mercury	Total Pressure lb_F per. $in.^2$	D.P. Cell Output m.v.
L.H.S.	R.H.S.			
+0.70	+0.70	0	0	0.180
+0.20	+1.12	0.92	0.452	1.631
-0.82	+2.06	2.88	1.415	4.313
-1.77	+3.00	4.77	2.343	6.958
-2.91	+4.05	6.96	3.418	10.013
-4.08	+5.22	9.30	4.568	13.423
-6.48	+7.50	13.98	6.866	19.810
-9.23	+10.22	19.45	9.553	27.470
-11.50	+12.48	23.98	11.778	33.840
-14.10	+15.10	29.20	14.342	41.130
-16.42	+17.49	34.11	16.753	47.680
-19.16	+20.20	39.36	19.332	52.190

These data are plotted as D.P. cell output (millivolts) versus pressure difference (lb_F per. $in.^2$) in Figure 1G.

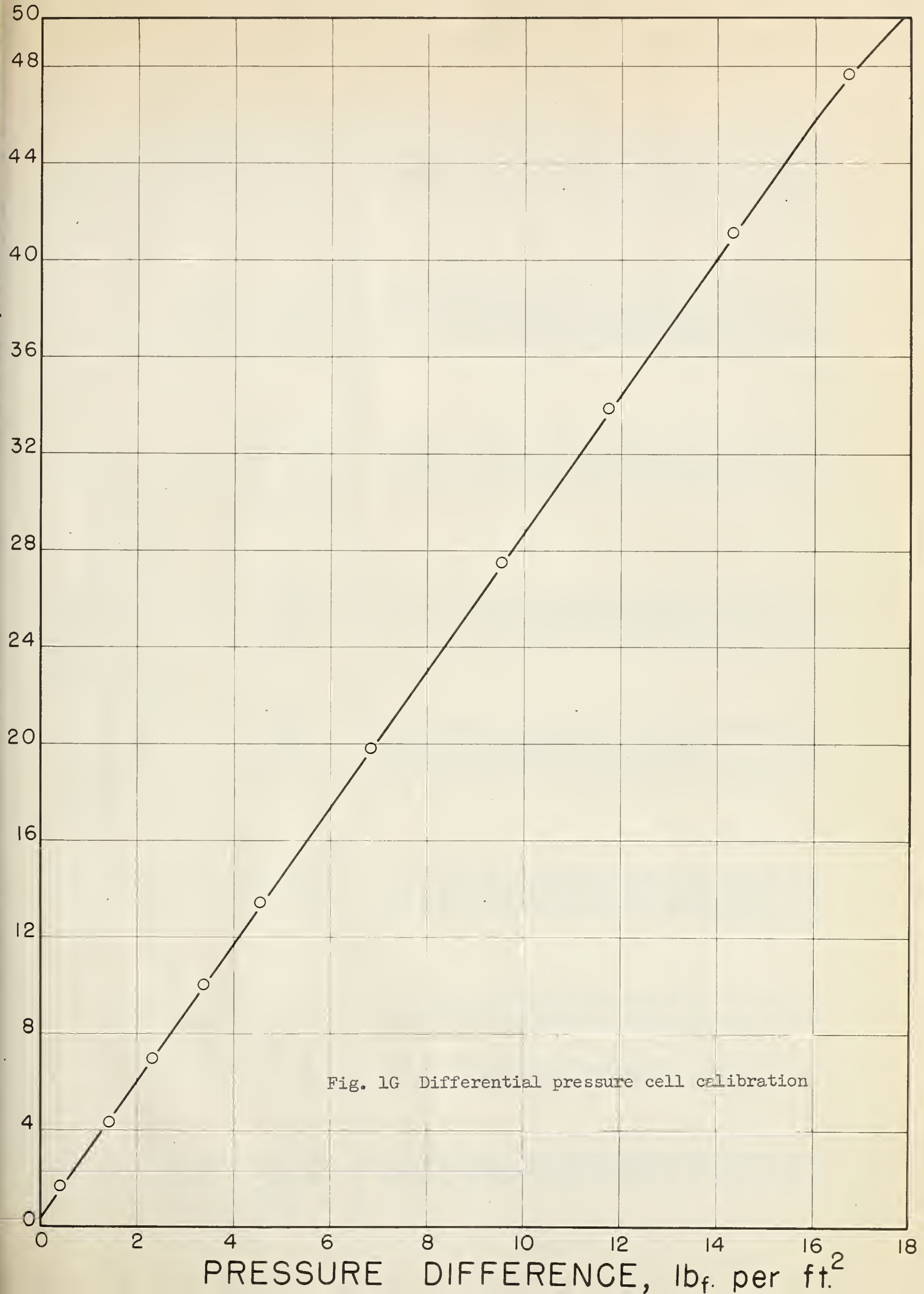

Fig. 1G Differential pressure cell calibration

TABLE 2G

VENTURE METER CALIBRATION DATA

(Obtained using water)

(1)	(2)		(3)	(4)	(5)	(6)	(7)	(8)
Weight of Water lb_m	Time min.	sec.	Flow Rate lb_m per. hr.	Density lb_m per. ft^3	D.P. Cell Output m.v.	Pressure Drop (ΔP) lb_F per. $in.^2$	$\Delta P.\rho$.	$\sqrt{\Delta P.\rho}$
200	4	2.2	2973	62.26	1.475	0.389	24.22	4.92
200	3	8.3	3824	62.26	2.274	0.670	41.71	6.46
400	5	5.0	4721	62.26	3.200	0.996	62.01	7.87
400	4	57.2	4845	62.26	3.400	1.067	66.43	8.15
400	4	14.8	5652	62.26	4.520	1.461	90.96	9.54
400	4	5.1	5875	62.26	4.860	1.581	98.43	9.92
400	3	52.6	6191	62.26	5.391	1.768	110.00	10.49
400	3	47.0	6344	62.26	5.700	1.876	116.80	10.81
400	3	38.4	6593	62.26	6.105	2.019	125.70	11.21
400	3	29.2	6883	62.26	6.690	2.225	138.50	11.77
400	3	14.4	7408	62.26	7.632	2.556	159.10	12.61
400	2	57.7	8104	62.26	9.058	3.058	190.40	13.80
400	2	53.2	8314	62.26	9.584	3.245	202.00	14.21
400	2	40.4	8978	62.26	11.018	3.748	233.40	15.27
400	2	33.4	9387	62.26	11.790	4.020	250.30	15.82
400	2	31.0	9536	62.26	12.326	4.209	262.10	16.19
400	2	23.5	10035	62.26	13.749	4.710	293.20	17.13
400	2	19.6	10315	62.26	14.320	4.911	305.80	17.48
400	2	17.1	10503	62.26	15.000	5.150	320.60	17.90
400	2	14.0	10746	62.26	15.889	5.463	340.10	18.44
400	2	8.7	11189	62.26	16.840	5.798	361.00	19.00
400	2	3.5	11660	62.26	18.425	6.356	395.70	19.90

(1)	(2)	(3)	(4)	(5)	(6)	(7)	(8)
400	1 45.7	13624	62.26	24.670	8.554	532.60	23.08
400	1 42.2	14090	62.26	26.510	9.202	572.90	23.94
400	1 37.0	14845	62.26	29.470	10.243	637.70	25.25
400	1 31.8	15686	62.26	32.980	11.479	714.70	26.73
400	1 28.3	16308	62.26	35.340	12.010	766.40	27.69
400	1 25.5	16842	62.26	38.000	13.246	824.70	28.72
400	1 22.9	17370	62.26	39.975	13.941	868.00	29.46
400	1 19.9	18023	62.26	43.245	15.092	939.60	30.65
400	1 17.7	18533	62.26	45.500	15.880	988.70	31.44
400	1 15.3	19124	62.26	48.480	17.120	1066.00	32.65
400	1 13.6	19565	62.26	50.660	18.250	1136.00	33.71
400	1 11.5	20140	62.26	52.500	19.600	1220.00	34.93

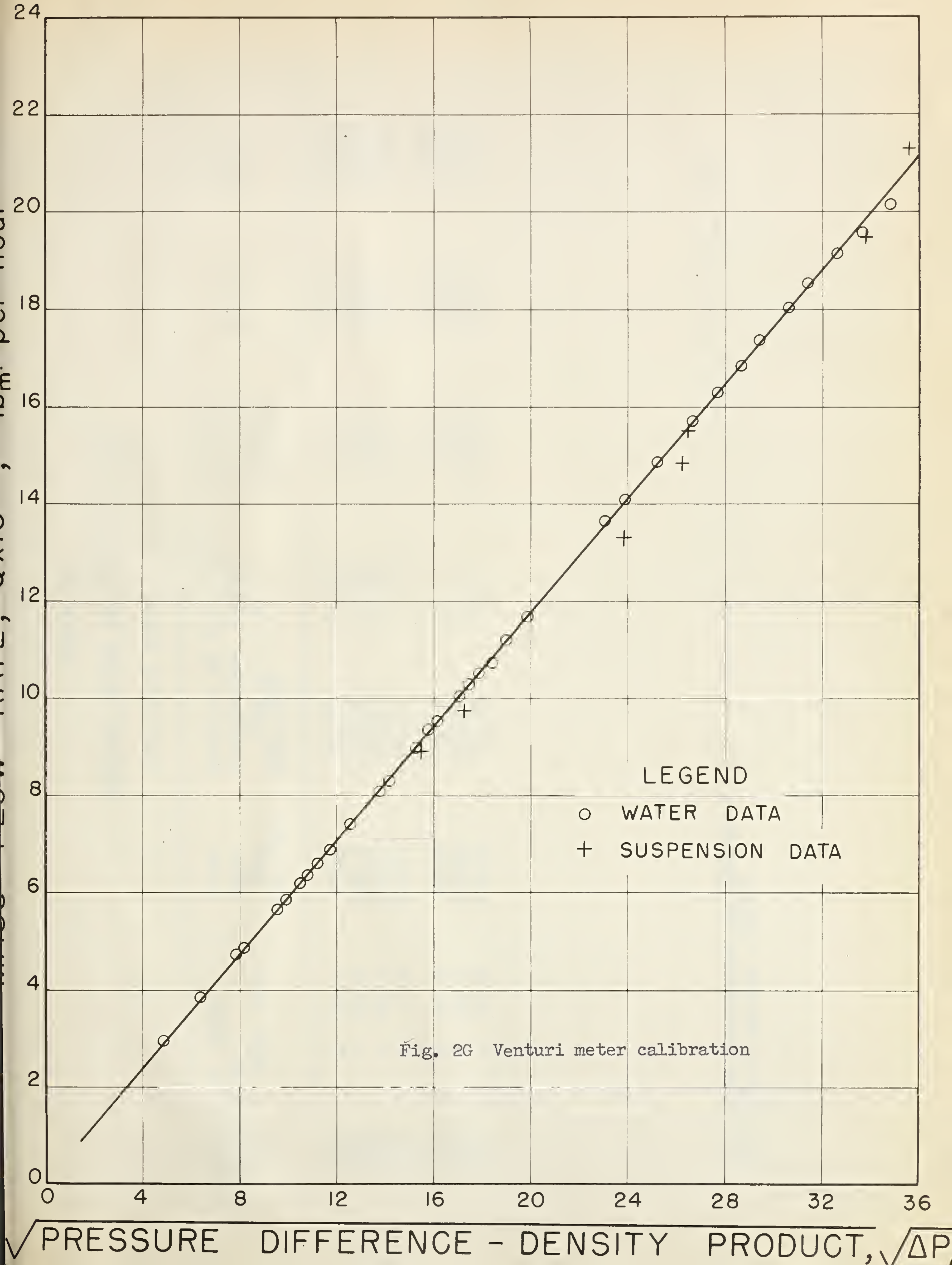

Fig. 2G Venturi meter calibration

TABLE 3G

VENTURI METER CALIBRATION DATA

(Obtained using suspension)

Weight of Suspension lb_m	Time min.	sec.	Flow Rate lb_m per. hr.	Density of Suspension lb_m per. ft^3	D.P. Cell Output m.v.	Pressure Drop (ΔP) lb_F per. in^2	$\Delta P.\rho.$	$\sqrt{\Delta P.\rho.}$
400	2	28.4	9705	78.99	11.15	3.795	299.8	17.30
200	-	48.6	148.5	78.99	25.30	8.776	693.2	26.32
200	-	46.5	15483	78.99	25.60	8.881	701.5	26.49
400	1	7.6	21295	78.99	46.00	16.080	1270	35.64
200	1	20.8	8910	76.14	9.4	3.179	242.0	15.56
200	-	54.2	13284	76.14	21.7	7.508	571.7	23.91
200	-	37.0	19459	76.14	43.0	15.040	1143.0	33.80

The data tabulated in Tables 2G and 3G are shown plotted in Figure 2G as flow rate (lb./hr.) versus $\sqrt{\Delta P.\rho}$.

B29790